University of Denver
Digital Commons @ DU

Electronic Theses and Dissertations | Graduate Studies

1-1-2016

Photoassisted Generation of Complex N, O, S Polyheterocycles

Weston James Umstead
University of Denver

Follow this and additional works at: https://digitalcommons.du.edu/etd

 Part of the Organic Chemistry Commons

Recommended Citation

Umstead, Weston James, "Photoassisted Generation of Complex N, O, S Polyheterocycles" (2016). *Electronic Theses and Dissertations*. 1117.
https://digitalcommons.du.edu/etd/1117

This Dissertation is brought to you for free and open access by the Graduate Studies at Digital Commons @ DU. It has been accepted for inclusion in Electronic Theses and Dissertations by an authorized administrator of Digital Commons @ DU. For more information, please contact jennifer.cox@du.edu,dig-commons@du.edu.

Photoassisted Generation of Complex N, O, S Polyheterocycles

Abstract

This research set out to continue the exploration and diversification of excited state *o*-azaxylylene cycloadditions, utilizing both pre-photochemical and post-photochemical modifications.

Pre-photochemical modifications came through the addition of heteroatoms, namely nitrogen and oxygen, to the tether that links the unsaturated photopendant to the photogenerated *o*-azaxylylene. Photochemistry resulted in the formation of new, interesting N, O, S polyheterocycles.

Post-photochemical modifications took place through several different cycloaddition reactions, including a [4+2] hetero-Diels Alder reaction, a [4+2] Povarov cyclization, a [3+2] nitrile oxide addition, and a [3+2] nitrone cyclization. These reactions were applied first to a model system, and then to a new scaffold that contained the biologically relevant beta-lactam fragment.

A summation of engineering work is also included to detail the development and implementation of several new LED irradiators. These irradiators are key to the photochemistry that will be discussed, and their development will serve as a blueprint for future work and improvement.

Document Type

Dissertation

Degree Name

Ph.D.

Department

Chemistry and Biochemistry

First Advisor

Andrei Kutateladze, Ph.D.

Second Advisor

James Fogelman, Ph.D.

Third Advisor

Bryan Cowen

Keywords

Beta-lactams, Diversity oriented synthesis, Hydantoins, O-azaxylylenes, Photochemistry, Polyheterocycles

Subject Categories

Organic Chemistry

Publication Statement

Copyright is held by the author. User is responsible for all copyright compliance.

This dissertation is available at Digital Commons @ DU: https://digitalcommons.du.edu/etd/1117

Photoassisted Generation of Complex N, O, S, Polyheterocycles

A Dissertation

Presented to

the Faculty of Natural Sciences and Mathematics

University of Denver

In Partial Fulfillment

of the Requirements for the Degree

Doctor of Philosophy

by

Weston James Umstead

June 2016

Advisor: Andrei G. Kutateladze

©Copyright by Weston James Umstead 2016

All Rights Reserved

Author: Weston James Umstead
Title: Photoassisted Generation of Complex N, O, S Polyheterocycles
Advisor: Andrei G. Kutateladze
Degree Date: June 2016

Abstract

This research set out to continue the exploration and diversification of excited state *o*-azaxylylene cycloadditions, utilizing both pre-photochemical and post-photochemical modifications.

Pre-photochemical modifications came through the addition of heteroatoms, namely nitrogen and oxygen, to the tether that links the unsaturated photopendant to the photogenerated *o*-azaxylylene. Photochemistry resulted in the formation of new, interesting N, O, S polyheterocycles.

Post-photochemical modifications took place through several different cycloaddition reactions, including a [4+2] hetero-Diels Alder reaction, a [4+2] Povarov cyclization, a [3+2] nitrile oxide addition, and a [3+2] nitrone cyclization. These reactions were applied first to a model system, and then to a new scaffold that contained the biologically relevant β-lactam fragment.

A summation of engineering work is also included to detail the development and implementation of several new LED irradiators. These irradiators are key to the photochemistry that will be discussed, and their development will serve as a blueprint for future work and improvement.

Acknowledgements

A person's accomplishments in life are best represented by the people that influenced them. More important are the teachers and mentors that had the patience to impart wisdom and knowledge. As such, my life is filled with people that planted seeds and cultivated them into the fruit of a doctorate degree.

First and for most I would like to give all the glory to God for this accomplishment. He has blessed me all the days of my life and is the author of this amazing story. I can do all things through Christ who gives me strength – Philippians 4:13. I'm especially thankful for the amazing family He blessed me with.

I want to thank my loving wife, who has remained loyal and devoted to me throughout this process, even when times became tough. Regardless of the trials of the day, I always know I can come home to her and everything will be washed away. I love you with all of my heart now and forever!

Due to space constraints, I can't include anyone else on this page, however, please take time to read Appendix A, which contains the remaining acknowledgements.

This dissertation is dedicated in memory of my grandfather, Robert E. Loomis.

Table of Contents

List of Figures

List of Schemes

Chapter One: Introduction and Background

A Growing Need for Drug Discovery

With the increasing average age of our country's population, and with the modern advancements in disease diagnostics, there is an ever growing need for new and improved pharmaceuticals.[1] As will be demonstrated in the following chapters, *o*-azaxylylene photochemistry will hopefully aid in this search.

In the United States, 44.7 million people were age 65 or older in the year 2014, which represents 14.1% of the population. By 2060, this number is estimated to reach 98 million people, or 21.7% of the population.[2] As people age, they are more susceptible to the formation of such diseases as atherosclerosis, other cardiovascular diseases, arthritis, cancer, osteoporosis, type 2 diabetes, and Alzheimer's disease.[3] Although there are some effective treatments for these conditions, some, like Alzheimer's disease, still remain mostly untreatable. These seven diseases alone account for nearly 70% of the deaths in the US population of 65 years and older,[4] so new more effective treatments should be a focus.

There is another group of diseases, called "orphan" or rare diseases, which currently do not have any effective treatments. There are an estimated 7,000 such orphan diseases that have been diagnosed,[5] having been defined by the Rare Disease Act of 2002

as “any disease or condition that affects fewer than 200,000 people in the United States.”.[7] These diseases are estimated to currently affect about 30 million Americans, or about 10% of the population. Although there has been an increase in funding for these diseases as a result of the Rare Disease Act of 2002, there are only an estimated 98 current studies on going, 13 cures developed, and 452 compounds in trials for approval.[7]

Another area of need is the growing number of antibiotic-resistant bacterial infections, caused by bacteria that have built up a resistance to current generations of treatments.[8] In the United States alone, it is estimated that 2 million people a year are diagnosed with an infection caused by a resistant strain of bacteria, leading to 23,000 deaths annually, with this number being much higher in less developed countries.[9]

For these reasons, and more it is critical for research to continue to find new and more effective small molecule drug candidates for the better health and wellbeing of our population. The synthesis and diversification of small libraries of *o*-azaxylylene-derived small molecules will help in this search, as will be presented in the following pages.

_o_-azaxylylenes

It would be most appropriate to begin the discussion of *o*-azaxylylenes with a historical overview. *o*-azaxylylenes are reactive, unstable heterodiene intermediates (**1.1’**) capable of undergoing [4+2] cycloaddition reactions with a limited number of dienophiles. Although they had been known for many years, their formation traditionally required harsh reaction conditions or exotic reagents, which rendered these species useless for many drug discovery applications. Their generation could be grouped into six

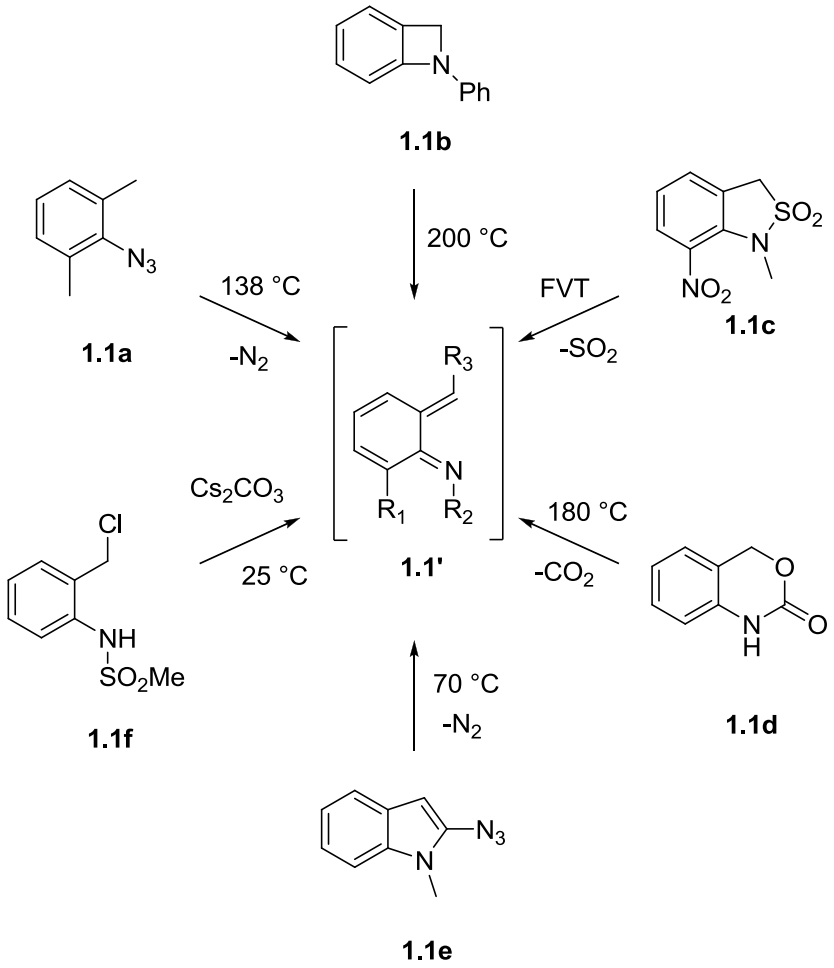

Scheme 1.1

unique reaction types (**Scheme 1.1**):[10] nitrene formation followed by a [1,4]-hydrogen shift (1.1a), electrocyclic ring opening of strained benzoazetines (1.1b), thermal cheleotropic extrusion of SO_2 (1.1c) elimination of CO_2 by a [4 + 2] cycloreversion (1.1d), ring-opening of heterocyclic systems (1.1e), and base-assisted elimination of HCl (1.1f). The latter, which encompasses work put forth by Corey and Steinhagen in 1999, represented the first straightforward method of the generation for *o*-azaxylylenes (**1.1f** and **Scheme 1.5**).[11] With the assistance of an external base, the elimination of HCl yielded the desired *o*-azaxylylene intermediate, pictured center of **Scheme 1.2**, which was

trapped by the tethered unsaturated alkene tail. The resulting scaffolds were obtained in moderate to good yields, and in the example of **Scheme 1.2**, allowed for quick access to

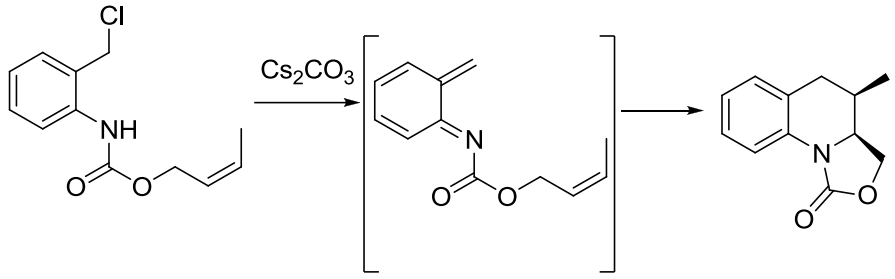

Scheme 1.2

the structural core of the antiviral drug virantmycin.[12]. Although on the surface this method appeared to be simple, there were some steps in the procedure that made it a bit challenging. In particular, the formation of the precursors required the use of phosgene to generate a chlorocarbamate intermediate that was then coupled to the aniline of choice. Phosgene is extremely toxic if inhaled, causing a wide range of symptoms from drowsiness to death by suffocation.[13] Precise temperature control is also required for precursor formation, in some cases -78°C was to be maintained for 24 hours for proper formation.[11] Additionally, syringe pump addition of Cs_2CO_3 over the course of 48 hours was required in some cases. Although this procedure represented a huge improvement over previous methods, and even though it was used several times in successful syntheses, there was still something left to be desired.

Photogenerated *o*-azaxylylenes

In 2011, the Kutateladze group published the seminal work on the *in situ* photochemical generation of *o*-azaxylylenes through an Excited State Intramolecular Proton Transfer (ESIPT).[14] The ESIPT process was previously described, however the

utilization in a synthetic application was completely new. The back-proton transfer historically occurred too quickly for trapping, but with the addition of a tethered, unsaturated pendant, the intermediate could be captured forming new complex N, O, S, polyheterocycles. This new method was preparatively simpler than Corey and Steinhagen's method, as it did not require any additional additives for azaxylylene formation. The key features of the method include: (i) modular assembly of the photoprecursors; (ii) rapid growth of complexity during the photochemical step, and (iii) possibility of post-photochemical modifications.

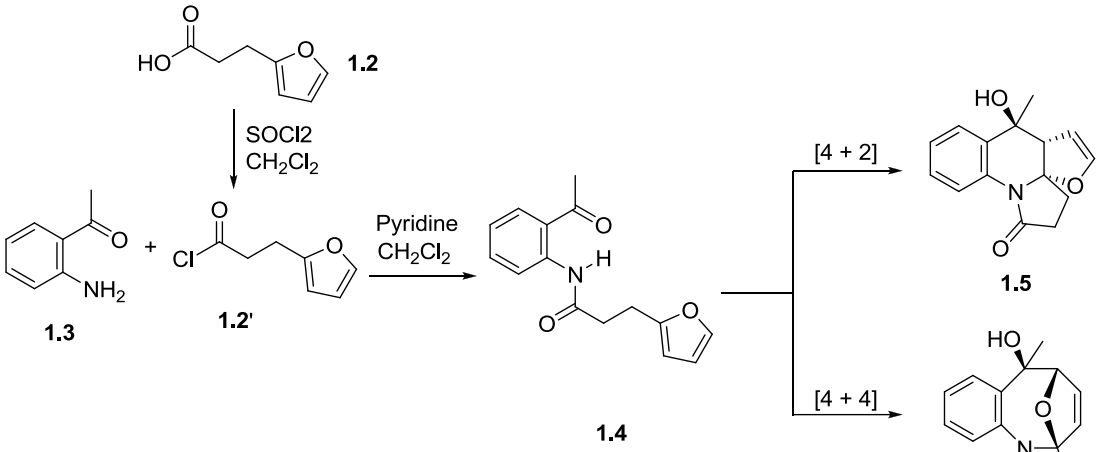

Scheme 1.3

The synthesis of the starting materials is straightforward, and in many cases involves only a simple acid chloride coupling sequence (**Scheme 1.3**). Starting from the commercially available 3-(2-furyl)propanoic acid (**1.2**), the acid chloride **1.2'** is generated cleanly *in situ* upon treatment with thionyl chloride ($SOCl_2$), and upon the addition to commercially available 2'-aminoacetophenone (**1.3**), yields the azaxylylene precursor (**1.4**) in two easy steps. The precursor is purified by flash chromatography, and

upon irradiation at 350 nm (*vide infra*) produces a [4+2] scaffold (**1.5**) and [4+4] scaffold (**1.6**).[14] The photoproducts are also easily purified by flash chromatography, with good to high yields ranging from 60-89%. The stereochemical control of these reactions is quite reliable, with the compounds shown being the major diastereomers. In most cases, the structures were elucidated with X-ray crystallography, showing that [4+2] favors the *anti* diastereomer (**1.5**) and [4+4] favors the *syn* diastereomer (**1.6**). Stereochemistry is assigned based on the relationship of the hydroxyl group and the bridged heteroatom, where *anti* puts these groups on opposite faces and *syn* puts them on the same face.

The photoprecursors generally have a UV absorbance maximum between 340-350 nm, and are typically irradiated using a 365 nm LED Engin or a Rayonet photoreactor fitted with broad UV source lamps ranging from 300-420 nm (emission maximum at 350 nm). The newest generations of irradiators will be discussed in detail in Chapter 5. Solvents for irradiation require optimization depending upon the system, but methanol,

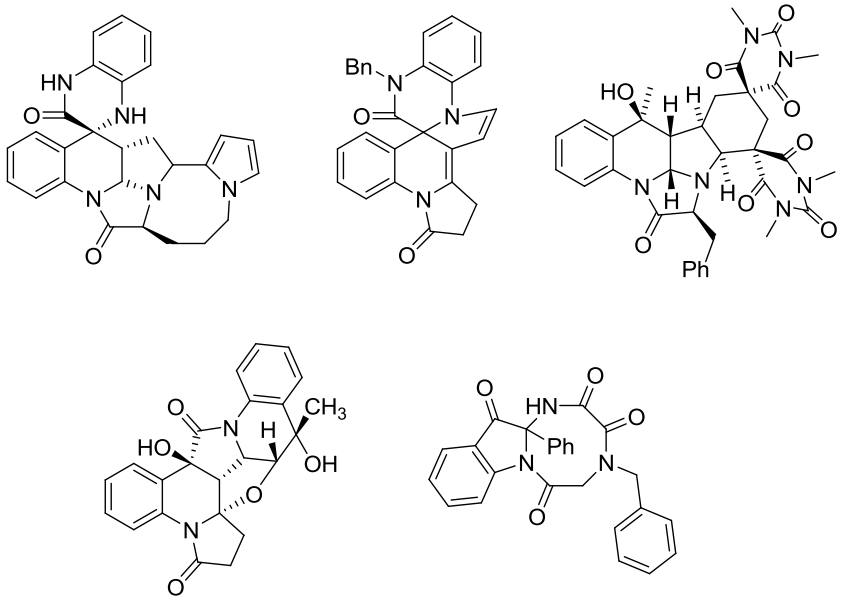

Figure 1.1

acetonitrile, DMSO, toluene, and acetone have all been used with much success. The Kutateladze group's method for azaxylylene generation has allowed for an impressively diverse number of small molecule scaffolds to be produced (**Figure 1.1**). This is important as diversity is key in new drug discovery.

Chemical Diversity and Complexity

Small molecules play an important role in drug discovery, as they themselves can be potential new drug candidates, or serve as building blocks for the assembly of larger molecules.[15] When the structure of a protein target is unknown, the goal of drug discovery is to synthesize as many small molecules as possible that cover a large scope of chemical diversity. This theoretically yields the highest probability of finding new drug candidates, since it allows for the probing of different regions of chemical space.

Chemical space is a set of descriptors that helps define the physical and chemical properties of a compound, which aids in the comparison of a compound to others.[1] Although the number of descriptors is virtually limitless, medicinal chemists have traditionally focused on the following six descriptors, as they have proven to be the most reliable at describing successful candidates. They are molecular weight (MW), number of rotatable bonds (RBs), hydrogen-bond acceptors (HBAs), hydrogen-bond donors (HBDs), topological polar surface area (TPSA), and the octanol/water partition coefficient (S log P).[16] These descriptors and their well-defined range of values were developed, in part, by work put forward by Christopher Lipinski in 1997.[17] His Rule of 5 arose from his work at Pfizer, which showed most successful oral drug candidates had a

MW less than 500 Daltons (Da), 5 or less HBAs and 10 or less HBDs, the S log P was less than or equal to 5, the TPSA was less than or equal to 140 square angstroms, and the total number of RBs was less than or equal to 10. While many potential candidates have been synthesized using these descriptors, it should be noted that many candidates have been found that lie outside of these desired ranges. For instance, the newly approved pharmaceutical Linzess®, which is used for the treatment of irritable bowel syndrome, violates every rule (**Figure 1.2)**. So while they have been useful to a point, at times they

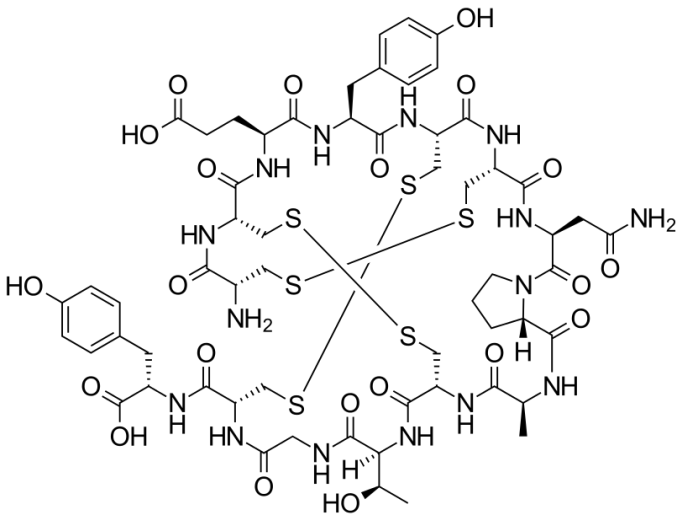

Figure 1.2: Linzess ®

have narrowed the scope too much. As new targets emerge, a shift in the space often follows, and guidelines are revised to reflect these new discoveries.[15]

Despite the large amount of effort put forward in synthesizing libraries of new small molecules, the approval of new drug candidates has still been extremely slow. There have been many specific reasons suggested as to why this is the case, but many agree that simply the wrong kinds of compounds are being synthesized.[18] An analysis of the Chemical Abstracts Service (CAS), a registry of over 109 million small molecules,

most organic compounds, has shown that nearly half of the registered compounds can be represented by 143 framework shapes.[19] And of those 143 framework shapes, the top 50 most abundant are present in 48-52% of the approved pharmaceuticals.[20] This is likely due to the biases of the chemists synthesizing more drug-like compounds instead of lead-like compounds.[21] Drug-like compounds are defined as those that have a high bioavailability, and can be used as is for biological testing. Usually inspired by previously synthesized or approved molecules, they sometimes narrow the chemical space too quickly. Lead-like compounds are those that are designed to fit to a specific target, but might require further optimization to increase bioavailability or druglikeness. While they might resemble natural products, their effectiveness lies in the fact that they can be optimized.

When evaluating a small library of compounds, it is not enough to simply say they are diverse, a statistical analyses based on Tanimoto coefficients can be used.[22] Using a binary string of 1's and 0's, the presence (1) or absence (0) of a set of structural and physical descriptors of a compound is determined. The same is done for a second compound, and the coefficient is determined (**Figure 1.3**).[23] The coefficient is equal to

$$T(a,b) = \frac{N_c}{N_a + N_b - N_c}$$

Figure 1.3

the sum of the similarities (N_c) divided by the sum of the presence of each descriptor for each compound (N_a and N_b) minus the sum of the similarities (N_c). A coefficient equal to 1 therefore means the compounds are identical, and a coefficient of 0 means the compounds are completely unique. A large matrix can be created, comparing all of the

compounds to one another and giving the chemists a numerical representation of how diverse their libraries are (for an example, see chapter 3).

Modern Approaches to Drug Discovery

With the understanding that new drug candidates should be diverse, it is imperative to cover the three methods commonly used by synthetic chemists to make such compounds. The first approach is called Target-Oriented Synthesis (TOS), and is used to synthesis one particular compound. Researchers start by isolating and attempting to characterize a new, interesting NP and then test it for biological activity. If some activity is observed, chemists then try to use traditional synthetic approaches to make the target in reasonable quantities. This has been very successful in the synthesis of several important drug candidates, for instance Taxol®, an anti-cancer drug, and Artemisinin, an anti-malarial drug (**Figure 1.4)**. The total synthesis of a specific target can usually be laid

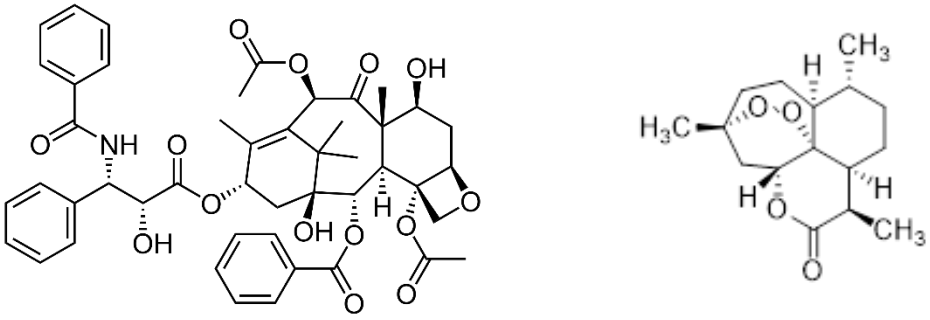

Figure 1.4: Taxol (left) and Artemisinin (right)

out quite easily by working backwards from the final product, and breaking bonds to form simpler subunits, a technique called retrosynthetic analysis. This allows for the development of a clear roadmap forward to the final product. TOS does have its disadvantages however, namely only one compound is synthesized for biological testing.

It results in a very pin point probing of the chemical space (**Scheme 1.4**) and often does

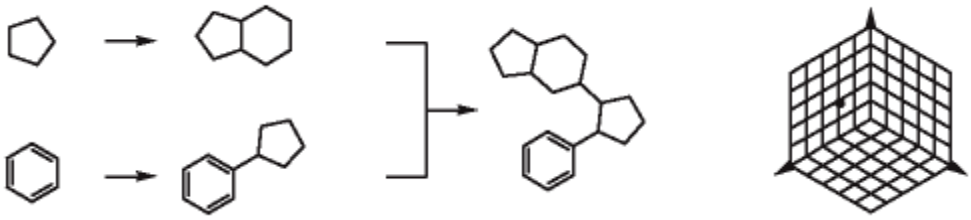

Scheme 1.4: Target-Oriented Synthesis[16]

not allow for the possibility of major structural modifications. If the target proves to be inactive in later-stage testing, there isn't much information given about what changes need to be made for improvement.

The second approach used by chemists is called combinatorial chemistry (**Scheme 1.5**).[2] Combinatorial chemistry is defined as "a rapid synthesis and screening of large

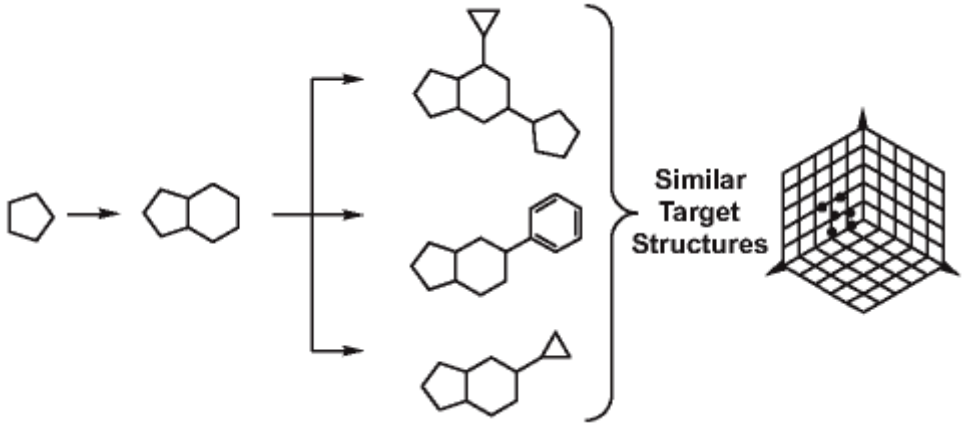

Scheme 1.5: Combinatorial Chemistry[16]

numbers of different but related chemical compounds generated from a mixture of known building blocks in order to recover new substances optimally suited for a specific function." [24] This approach uses a core scaffold of interest that contains several built-in

diversity inputs. These points are decorated with different functional groups, allowing for a slightly wider probing of the chemical space as compared to TOS (**Scheme 1.4**). It is however still restrictive to a specific region due to the similarity of the core. This means, if the resulting compounds don't show any desired biological activity, some conclusions can potentially be made about which modifications are better than others, but it's difficult to determine if the core scaffold is the issue.

The third approach used by chemists, which yields the most diverse library of compounds, is Diversity-Oriented Synthesis (DOS) (**Scheme 1.6**).[16] This approach, like

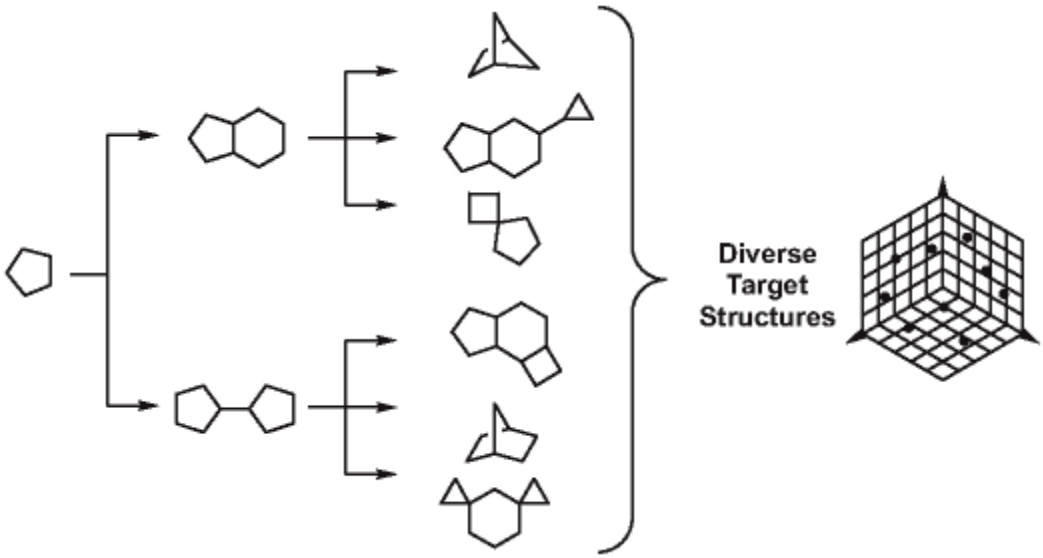

Scheme 1.6: Diversity Oriented Synthesis[16]

combinatorial chemistry, starts with one core scaffold, but rather than just adding functional groups to the core, DOS rapidly grows the complexity of the new compounds by changing the structure of the core as well. This allows for a more diverse library of compounds to be synthesized, and a much greater probing of the chemical space. Not only are insights gained about the nature of the modifications, but the overall scaffolds

are also very different as a result of the series of modifications, that insight is gained there as well.[16] The photochemical generation of *o*-azaxylylenes is a perfect example of DOS. As can be seen in **Scheme 1.7**, the rapid growth of complexity and inclusion of

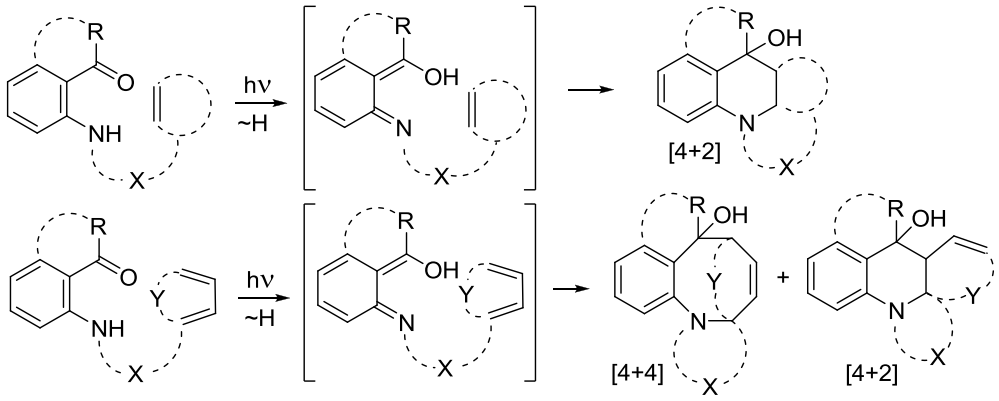

Scheme 1.7

several diversity inputs allows for the very unique scaffold synthesis. The tethered photopendant, as shown can either be an alkene[14] or an aromatic heterocycle (Y) such furan,[14] thiophene,[25] or pyrrole,[26] and in some cases, a benzoidal aromatic. The tether (X) can contain heteroatoms such as nitrogen and oxygen, and can vary in length from two to four atoms, yielding photoproducts with new 4, 5, or 6-membered heterocycles. And the azaxylylene fragment (R) can be diversified as an aldehyde, ketone, cyclic ketone, or imine, all of which can contain their own separate variable fragments for cross-coupling reactions.[27] The resulting N, O, S, polyheterocycles contain very important biologically relevant fragments that can used in a specific type of DOS called Fragment-Based Drug Discovery.

Fragment-Based Drug Discovery

Using DOS and computational methods together, there have been multiple new techniques developed by which a user can analyze compounds.[28] While some focus on the discovery of a complete molecule, a particularly successful approach that looks to optimize smaller pieces of a molecule is called Fragment-Based Drug Discovery (FBDD). This method was first proposed by William Jencks in 1981,[29] when he suggested that a binding event between a molecule and a protein could be viewed in one of two ways: one single event with one large change in energy, or as several smaller "fragment" bind events with their own individual changes in energy. Viewing the binding as separate events allows for an optimization of each fragment, which can then be chemically linked afterwards to create a larger drug candidate. This theoretical discussion was put into practice in a high-impact Science paper from Abbott Laboratories in 1996.[30]

Using the advancements in Nuclear Magnetic Resonance (NMR) spectroscopy, Abbott developed an effective method for analyzing the binding of organic fragments with a protein binding site of their interest. They dubbed this new method structure-activity relationship or "SAR by NMR". This method uses a 2D NMR technique called heteronuclear single quantum coherence (HSQC) which is used to observe the chemical shift of ^{1}H-amide and ^{15}N- in the protein target.[31] As different fragments are added to the protein, the binding causes a change in these chemical shifts. Analysis of these changes gives investigators an idea of how strong or weak the fragment is bound, and thus allows for optimization of the fragment. The greater a shift the stronger the binding. Proteins generally have several regions for interactions in the binding pockets, so each region is

probed and optimized with the relevant fragment. When fully optimized, all fragments are linked together forming one large candidate. The binding of the large molecule is then a sum of the individual binding energies, so even though typical screenings require millimolar (mM) concentrations of the fragments, the larger molecule can be administered at a more favorable micromolar (μM) concentration.[30]

As a result of this new FBDD method, in 2003, Astex Pharmaceticals published a new set of guidelines aimed specifically at successful characteristics of fragments.[32] Their new "Rule of 3" suggested fragments should have a MW less than 300 Da, less than 6 combined HBAs and HBDs, a S log P of less than 3, less than 3 RBs, and a TPSA of less than 60 square angstroms. These guidelines would serve to help keep the overall characteristics of the larger molecule in line with Lipinski's Rule of 5. These are of course just guidelines, and like Lipinski's Rule of 5, are constantly being revised. To date, it has been reported that somewhere around 20 new drug candidates have been identified using FBDD.[33] One notable example is Vemurafenib (**Figure 1.5)**, which was

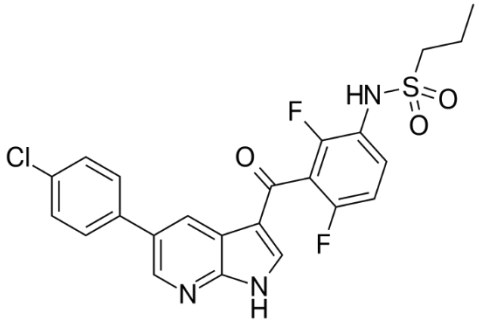

Figure 1.5

developed by Plexxikon in 2011.[34] It is used for the treatment of late-stage melanoma, and shows a 80% regression rate, which is a significant improvement over its predecessors.[35]

While the Kutateladze group does not use any specific computational techniques for the synthesis of *o*-azaxylylenes, the method could be included as a FBDD technique. As previously stated, the results of photochemistry incorporate new polyheterocycle fragments which are often found in biologically relevant small molecules, and currently approved pharmaceuticals.

In the following chapters, research will be presented that sets out to build upon the body of work previously put forth from the Kutateladze group. Particular attention will be given to how azaxylylene photochemistry can be used in FBDD, by incorporating fragments of interest both through pre-photochemical modifications as well as post-photochemical modifications. A new molecular scaffold will also be introduced, one that is of particular interest to the pharmaceutical industry. And as previously stated, the latest advancements in LED irradiator design will be shared to provide a blueprint for future work and improvements.

Chapter Two: Pre-photochemical Modifications

This particular project was exciting for me, because it was my first publication! There is something special in doing something new, and for me to be able to contribute to the chemistry community in this fashion with my first publication, was very gratifying. The research in this chapter was published in the European Journal of Organic Chemistry.[36]

Introduction

We have covered methods of drug discovery and why there is a need for more diverse scaffolds. As of April 2016, over 109 million compounds have been added to the (CAS) registry.[37] Of those, only 1513, as of 2011, have been approved by the U.S. Food and Drug Administration (FDA) for use as a pharmaceutical.[38] Of the 1513 approved for disease treatment, there were only 50 scaffolds represented in about 50% of the compounds, leading to the conclusions there is a large lack of diversity in these new drugs.[20]

The aim of the work presented in this chapter was to assemble photoprecursors through a DOS modular assembly approach and to test a few new post-photochemical modifications. These new techniques have led to the unlocking of unique complex scaffolds that are often overlooked by traditional synthetic methods. An overarching

theme of FBDD will emerge and be made clear during the synthesis of the post-photochemical modifications, and will be discussed when appropriate.

Results and Discussion – Pre-photochemical Modifications

The major focus of this work was on the introduction of additional heteroatoms into the tether that links the azaxylylene to the photo-active pendant (position X in **Scheme 1.7**). This would yield new heterocycles or polyheterocycles upon the irradiation of the starting materials. Three reactive carbonyl derivatives were chosen as a starting point, as they were either easily formed *in situ*, or were commercially available: furoyl isocyanate (**2.3'**), formed by reacting furoyl chloride (**2.3**) with sodium cyanate in the presence of tin (IV) chloride,[39] commercially available furfuryl isocyanate (**2.2**), and furfuryl chloroformate (**2.4'**), formed by the reaction of phosgene with furfuryl alcohol (**2.4**)[51] (**Scheme 2.1**). The *o*-amino ketones **2.1a-2.1c** were treated separately with these three electrophiles in one-step coupling reactions. The yields ranged from moderate to good, with products isolated by flash chromatography. When using benzaldehyde derivatives, such as **2.11**, a second oxidation step is required. Starting from amino alcohol

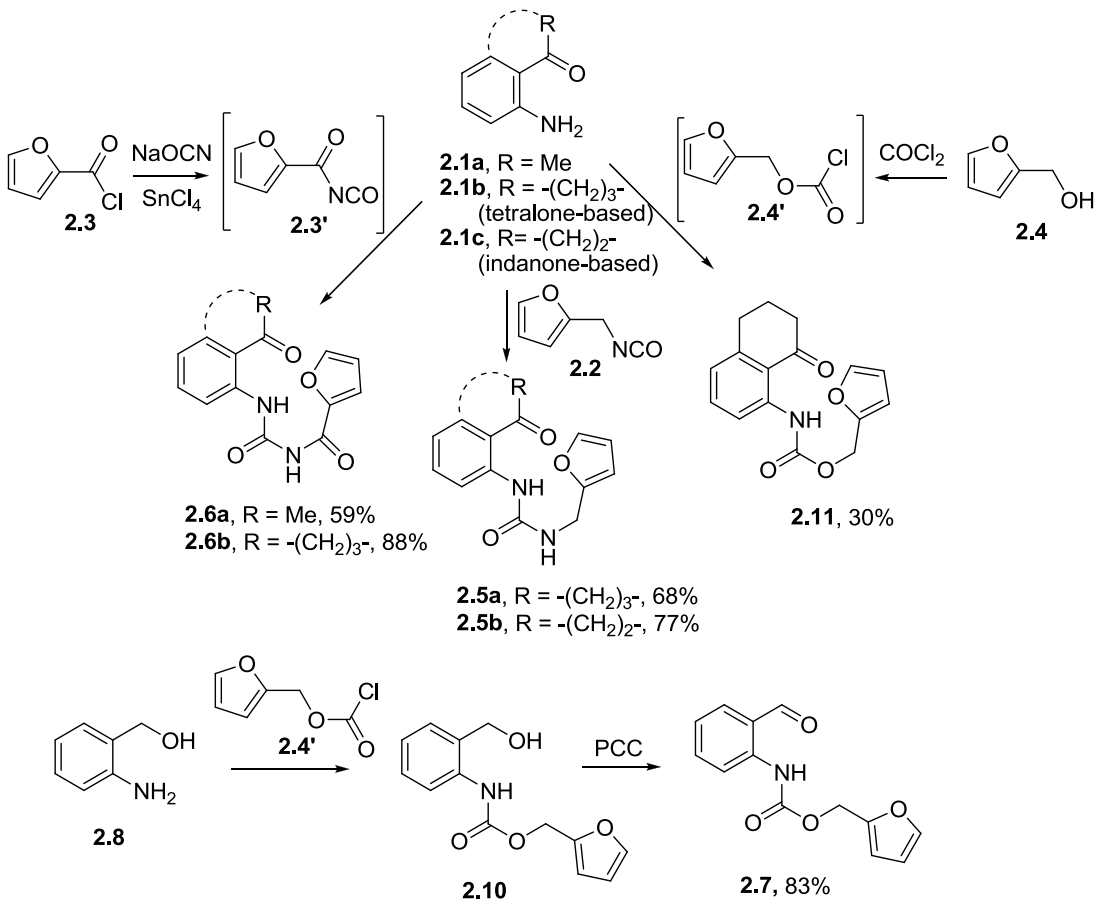

Scheme 2.1

2.8, coupling with furfuryl chloroformate (**2.4'**) yields benzyl alcohol (**2.10**) that is oxidized by pyridinium chlorochromate (PCC) into the photoactive amidobenzaldehyde.

The photoprecursors obtained in these reactions are characterized be a broad UV absorption from 330 nm to 380 nm, with a maximum around 360 nm. Therefore, they were irradiated in a Rayonet photoreactor equipped with RPR-3500 UV lamps to yield 9 new quinolinol and benzazacane scaffolds containing fused cyclic imidazolinones (**2.12b and 2.13b**), hydantoins (**2.14a, 2.14b, 2.15a, and 2.15b**), or cyclic carbamates (**2.16a, 2.16b, and 2.17a**) (**Scheme 2.2**). In this particular work, solvent optimization showed

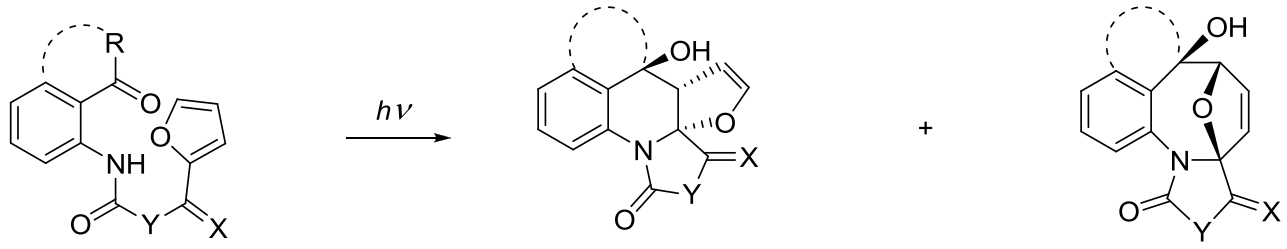

[4+2] [4+4]

2.5a, Y = N, X = H_2, R = -$(CH_2)_3$-
2.5b, Y = N, X = H_2, R = -$(CH_2)_2$-
2.6a, Y = N, X = O, R = Me
2.6b, Y = N, X = O, R = -$(CH_2)_3$-
2.7, Y = O, X = H_2, R = H
2.11, Y = O, X = H_2, R = -$(CH_2)_3$-

2.12a, Y = N, X = H_2, R = -$(CH_2)_3$-
2.13a, Y = N, X = H_2, R = -$(CH_2)_2$-, --
2.14a, Y = N, X = O, R = Me, 19%
2.15a, Y = N, X = O, R = -$(CH_2)_3$-, 19%
2.16a, Y = O, X = H_2, R = H, 58%
2.17a, Y = O, X = H_2, R = -$(CH_2)_3$-, 63%

2.12b, Y = N, X = H_2, R = -$(CH_2)_3$-, 54%
2.13b, Y = N, X = H_2, R = -$(CH_2)_2$-, 26%
2.14b, Y = N, X = O, R = Me, 63%
2.15b, Y = N, X = O, R = -$(CH_2)_3$-, 43%
2.16b, Y = O, X = H_2, R = H, 29%
2.17b, Y = O, X = H_2, R = -$(CH_2)_3$-, --

Scheme 2.2

that in methanol, the reaction proceeded cleanly and rapidly. After irradiation was complete as monitored by ^{1}H NMR, the reaction mixtures were purified by flash chromatography to yield the pure photoproducts (**Scheme 2.2**). Comparing all cases, the ratio of the [4+4] and [4+2] photoproducts was noticeably affected by the structure of the linker. In compounds **2.12a/b and 2.13a/b**, the [4+4] product was formed preferentially, with no evidence of any [4+2] formation. However in the case of **2.17a/b**, only the [4+2] cycloaddition product was present. In the other cases, both isomers formed, although their ratios varied. We propose some intermolecular or intramolecular hydrogen bond is the cause, which is reasonable given the number of HBDs and HBAs that were present, but we have no experimental evidence to support this claim. As with previous works, the photochemistry preferentially yielded the *syn* [4+4] diastereomer and the *anti* [4+2] diastereomer as confirmed by NMR spectroscopy.[14] Additionally, structures from

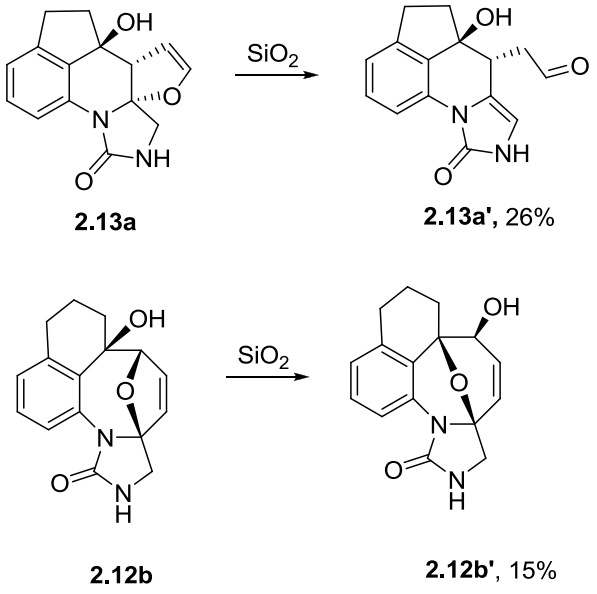

Scheme 2.3

compounds **2.14b, 2.15b, and 2.16b** were solved unambiguously with X-ray crystallography (see experimental for the ORTEP diagrams).

Two interesting observations were made upon the purification of compounds **2.13a** and **2.12b** (**Scheme 2.3).** The indanone-based [4+2] photoproduct **2.13a**, which is detectable by NMR before purification, undergoes an eliminative opening of the N, O-ketal to afford product **2.13a'** upon chromatography on slightly acidic silica media. The [4+4] adduct **2.12b** is also affected by the slightly acidic silica media, undergoing a bicyclo [4.2.1] nonadiene→bicyclo [3.3.1] nonadiene rearrangement of its 2,5-epoxyazacane core to yield the oxabicyclo [3.3.1] nonene scaffold **2.12b'.**[40] These rearrangements account for some loss in yield and lack of the primary photoproducts after purification.

Results and Discussion – Post-photochemical Modifications

This work also set out to establish that experimentally simple and straightforward post-photochemical modifications could be performed, adding diversity to these scaffolds via a modular assembly DOS approach. Previous post-photochemical modifications had been performed in the group by Cronk et al., via a palladium catalyzed Suzuki coupling.[27] This work added several interesting heterocycles to the azaxylylene fragment both before and after photochemistry. Additionally, Nandurkar et al., were successful in the dihydroxylation of the [4+4] product.[41] These new post-photochemical modifications, however, sought to change the core structure of the photoproducts through a straightforward, simple, widely applicable protocol. The reactions were specifically

aimed at additions to the newly formed double-bond fragment that results from the photochemistry.

Rather than exploring these post-photochemical modifications on the new, more complex scaffolds, it was decided that a simpler model system should be used. This would allow for easier monitoring of these reactions since they would be performed on a well-characterized system. As such, **2.18** and **2.19** (**Scheme 2.4**), were synthesized as previously reported, [14] and utilized for these post-photochemical modifications. A straightforward [3+2] cycloaddition was chosen utilizing bromonitrile oxide, which is generated *in situ* from dibromoformaldoxime and potassium bicarbonate.[45] In the reactions with both **2.18** and **2.19**, the addition occurred from the more sterically favored *exo* face, placing the newly formed 4,5-dihydro-1,2-oxazole *syn* to the oxo-bridge.

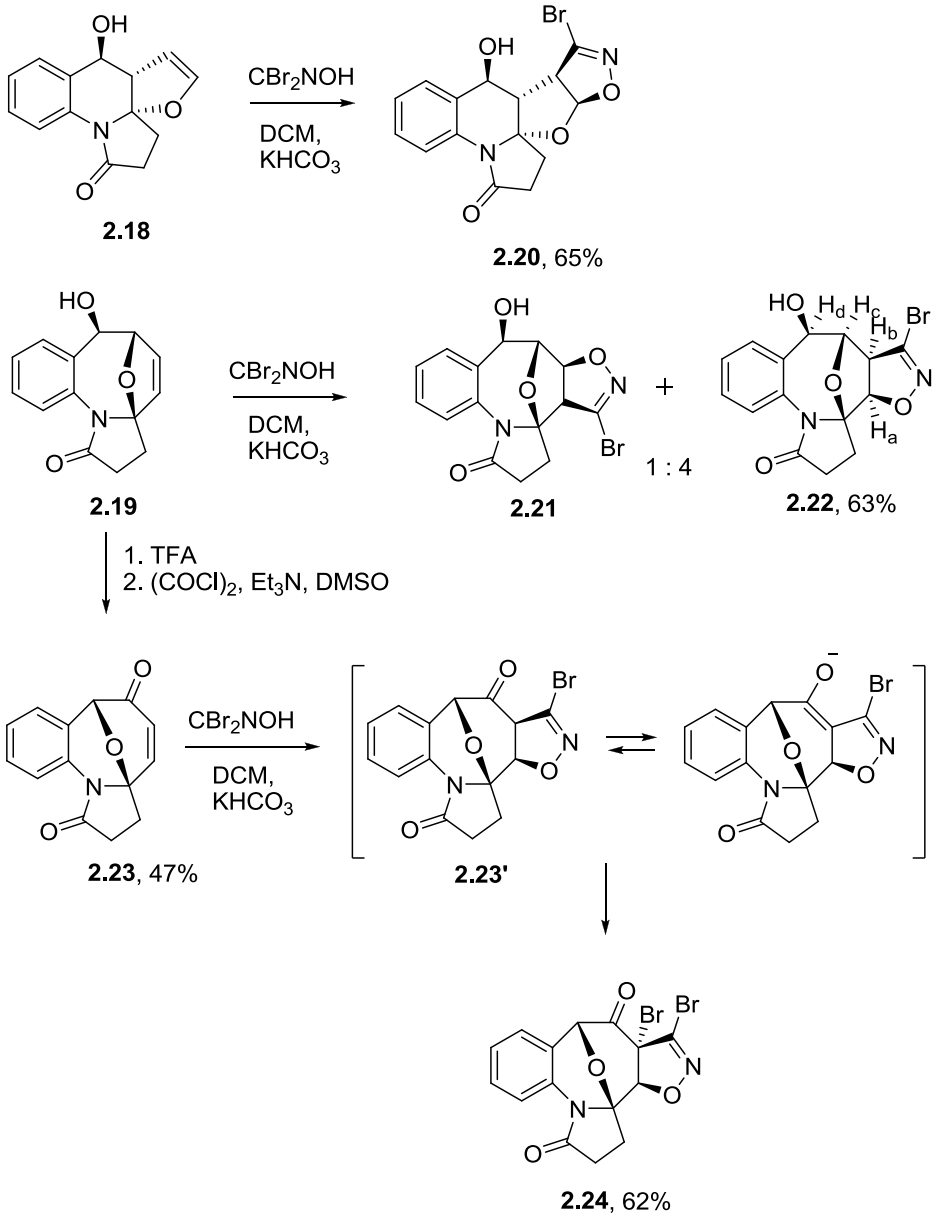

Scheme 2.4

Interestingly, the [4+2] photoproduct showed complete regiospecificity yielding only compound **2.20**, and no product with bromine pointing "south".

In the case of the [4+4] scaffold **2.19**, only weak regiocontrol is seen. The addition to either terminus of the double bond is electronically equivalent, so presumably

steric hindrance guides the process. The incoming substituent of the nitrile oxide will be in close proximity to the methylene group of the linker for the minor regioisomer **2.21**, whereas the major regioisomer **2.22** minimizes this interaction. As a result, the observed ratio was 4:1 in favor of the bromine being in the less sterically hindered position. As of note, **2.21** was only observable by NMR, and was not isolated or characterized. The regiochemistry of the major product **2.22**, which was isolated and characterized, was determined by the analysis of its spin–spin coupling constants and a series of NOEDIFF experiments.

In the NMR spectrum of compound **2.22**, proton H_a is a doublet at $\delta = 4.71$ ppm with $^3J = 8.7$ Hz, and H_b is a doublet of doublets at $\delta = 3.75$ ppm with $^3J = 8.7$ and 1.0 Hz (the second constant reflects the interaction with H_c). Upon irradiation of the proton at $\delta = 3.75$ ppm, a NOE of 4.6% is observed for the doublet of doublets at $\delta = 4.64$ ppm belonging to H_d, indicating H_b and H_d are on the same face. Further evidence obtained through DFT calculations showed the major isomer, **2.22**, to be 2 kcal/mol lower in energy than **2.21**, most likely due to the previously mentioned unfavorable steric interaction of the bromine with the methylene group in the linker.

An additional scaffold can be formed by the bicyclo [4.2.1] nonadienee→ bicyclo [3.3.1] nonadiene rearrangement of **2.19**, which is induced by the addition of trifluoroacetic acid (TFA). The resulting rearranged vinyl alcohol is oxidized under Swern oxidation conditions, affording α,β unsaturated ketone **2.23**. When this compound is reacted under the same bromonitrile oxide conditions, instead of the expected **2.23'**, dibrominated **2.24** is observed (**Scheme 2.4**). It is postulated there is an equilibrium

between the enolate and keto tautomer from the excess potassium bicarbonate present. The enolate can add a second atom of bromine, which comes from the excess of dibromoformaldoxime that is required. The dibrominated product **2.24** was isolated after flash chromatography and its structure solved unambiguously by X-ray crystallography (see experimental).

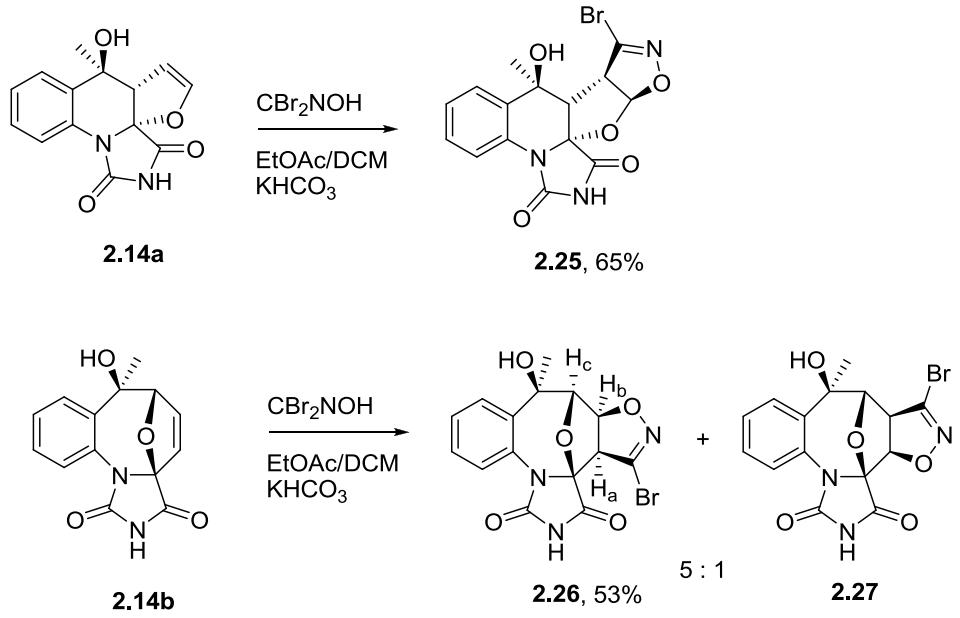

Scheme 2.5

This new post-photochemical modification was then applied to some new scaffolds, namely the hydantoins **2.14a** and **2.14b**. These photoproducts were chosen because hydantoins are a fragment of interest for FBDD programs. It can be found in several approved pharmaceutical including the anticonvulsants phenyltoin[46] and fosphenyltoin,[47] as well as iprodione,[48] a popular fungicide. Not surprisingly *exo* stereochemistry was again observed for the nitrile oxide addition (**Scheme 2.5**). The [4+2] photoproduct **2.14a** gave only one regioisomer **2.25**, whose stereochemistry was solved by X-ray crystallography. The [4+4] photoproduct **2.14b** gave two regioisomers,

however the ratio was reversed 5:1 in favor of the more sterically crowded **2.26**. As of note, the minor isomer, **2.27**, was only observed by NMR. The regiochemistry of the major isomer **2.26** was determined by NOEDIFF experiments. The compound has two doublets with a common spin–spin coupling constant of J = 8.8 Hz at δ = 4.92 and 3.85 ppm, where H_b is at 4.92 ppm and H_a is at 3.85 ppm. Upon irradiation of the methyl group, which is a singlet at δ = 1.71 ppm, only the proton at δ = 4.92 ppm was affected with a NOE of 2.4%, placing the methyl and H_b proton on the same face. Although H_a is also on the same face, it's possible it was simply too far away to experience any NOE. It was then postulated that, in this case, the electrostatic attraction of the lone-pairs from the carbonyl oxygen in the linker on the incoming bromine, overrides the stereochemical preferences as seen in **2.22**. This is supported further with DFT calculations. According to B3LYP/6-31G(d) calculations performed by others, major regioisomer **2.26** is about 0.75 kcal/mol lower in energy than minor regioisomer **2.27**. Provided that the transition state in these 1,3-dipolar cycloadditions is late, i.e. the vinyl ether double bond is already partially broken when the nitrile oxide adds, the relative product stability tracks the relative height of the activation barrier.

This first work has shown that it is possible to further diversify our group's [4+4] and [4+2] scaffolds through the simple pre-photochemical introduction of heteroatoms to the linker tethering the azaxylylene to the photo-active pendant. These new precursors undergo ESIPT upon irradiation at 350 nm, yielding new polyheterocyclic scaffolds that contain interesting fragments for FBDD research. Of special note are the hydantoins, as they are found in several approved pharmaceuticals. To add diversity, a new post-

photochemical modification was introduced that built upon the core scaffolds yielding even more interesting and complex products containing 3-bromooxazolines, another fragment of interest for FBDD research.

Experimental

Common solvents were purchased from Pharmco and used as is, except for THF, which was refluxed over and distilled from potassium benzophenone ketyl prior to use. Common reagents were purchased from Aldrich and used without additional purification, unless indicated otherwise. NMR spectra were recorded at 25°C on a Bruker Avance III 500 MHz in DMSO (unless noted otherwise). X-Ray structures were obtained with a Bruker APEX II instrument. High resolution mass spectra were obtained on the *MDS SCIEX/Applied Biosystems API QSTARTM Pulsar i Hybrid LC/MS/MS System* mass spectrometer by Dr. Jeremy Balsbaugh from the University of Colorado at Boulder. Flash column chromatography was performed using Teledyne Ultra Pure Silica Gel (230 – 400 mesh) on a Teledyne Isco Combiflash R_f using Hexanes/EtOAc or DCM/Methanol as an eluent.

Synthesis of photoprecursors

General procedure **I** for the synthesis of compounds **2.6a-2.6b**

1.3 eq of sodium cyanate was suspended in 2 ml of 1,2-dichlorobenzene. Under a nitrogen atmosphere 1 eq of 2-furoyl chloride and 0.05-0.15 eq of tin (IV) chloride were added. Upon complete addition the reaction mixture was refluxed for 3 hours, and then cooled to ambient temperature. 0.3-1.0 eq of the corresponding amine was then added. The reaction mixture was allowed to stir overnight, then filtered through a pad of

Celite®. Filter cake is washed with chloroform. The solvent was evaporated *in vacuo,* and the crude material was purified by flash chromatography.[39]

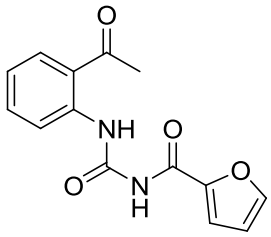

N-[(2-acetylphenyl)carbamoyl]furan-2-carboxamide (2.6a): General procedure **I** was followed. From 1.68 g of NaOCN (26.0 mmol, 1.3 eq) 2.0 ml of 2-furoyl chloride (20.0 mmol, 1 eq), 0.23 ml of $SnCl_4$ (2.0 mmol, 0.1 eq) and 2.0 ml of 2'-aminoacetophenone (16.5 mmol, 0.8 eq) 2.62 g (59%) of the title compound was obtained. ^{1}H NMR (500 MHz, DMSO) δ 12.35 (s, 1H), 10.86 (s, 1H), 8.40 (dd, *J* = 8.5, 1.2 Hz, 1H), 8.06 (dd, *J* = 1.8, 0.8 Hz, 1H), 8.03 (dd, *J* = 8.0, 1.6 Hz, 1H), 7.73 (dd, *J* = 3.6, 0.8 Hz, 1H), 7.62 (ddd, *J* = 8.5, 7.5, 1.6 Hz, 1H), 7.25 (ddd, *J* = 7.9, 7.5, 1.2 Hz, 1H), 6.75 (dd, *J* = 3.6, 1.7 Hz, 1H), 2.64 (s, 3H).^{13}C NMR (126 MHz, DMSO) δ 201.3, 158.0, 151.7, 148.3, 145.8, 138.2, 134.0, 131.8, 125. 9, 123.5, 122.5, 118.0, 112.9, 29.2. HRMS (ESI) calcd for $C_{14}H_{12}N_2NaO_4^+$ (MNa^+) 295.0695, found 295.0705

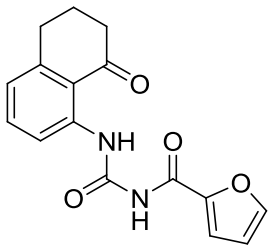

N-[(4-oxotetralin-5-yl)carbamoyl]furan-2-carboxamide (2.6b): General procedure **I** was followed. From 1.68 g of NaOCN (26.0 mmol, 1.3 eq), 2.0 ml of 2-furoyl chloride (20.0 mmol, 1 eq), 0.35 ml of $SnCl_4$ (3.0 mmol, 0.15 eq) and 0.60 g of 8-amino-tetralone (4.1 mmol, 0.3 eq) 0.98 g (88%) of the title compound was obtained. ^{1}H NMR (500 MHz, $CDCl_3$) δ 13.28 (s, 1H), 8.56 (d, *J*=8.4 Hz, 1H), 8.30 (s, 1H), 7.59 (dd, *J* = 1.8, 0.8 Hz,

1H), 7.49 (t, *J*=7.9 Hz, 1H), 7.46 (dd, *J* = 3.6, 0.8 Hz, 1H), 7.01 (dd, *J* = 7.5, 1.1 Hz, 1H), 6.63 (dd, *J* = 3.6, 1.7 Hz, 1H), 3.02 (t, *J* = 6.1 Hz, 2H), 2.77 (m, 2H), 2.12 (m, 2H). ^{13}C NMR (126 MHz, CDCl3) δ 201.4, 156.4, 150.6, 145.9, 145.9, 145.6, 140.1, 134.2, 123.7, 120.3, 119.6, 118.2, 113.2, 40.4, 31.1, 22.7 HRMS (ESI) calcd for $C_{16}H_{14}N_2NaO_4^+$ (MNa^+) 321.0851, found 321.0859

General procedure **II** for the synthesis of compounds **2.5a-2.5b**

1 eq of corresponding amine was dissolved in 20 ml of anh. DCM. To this was added dropwise 1 eq of furfuryl isocyanate dissolved in 5 ml of anh. DCM. The mixture was allowed to stir at ambient temperature for 8 hrs. The resulting mixture was diluted with DCM, washed with water, and then sat. brine. The organic layer was dried over Na_2SO_4 before concentrating *in vacuo* to yield the product which was used in the next step without further purification.

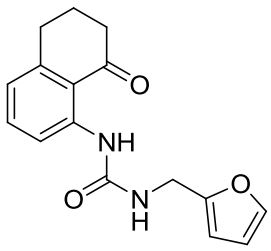

1-(2-furylmethyl)-3-(4-oxotetralin-5-yl)urea (2.5a): General procedure **II** was followed. From 0.65 g of 8-amino-tetralone (4.1 mmol, 1 eq) and 0.5g of furfuryl isocyanate (4.1 mmol, 1 eq), 0.79 g (68%) of the title compound was obtained. ^{1}H NMR (500 MHz, CDCl3) δ 11.68 (s, 1H), 8.46 (dd, *J* = 8.6, 1.1 Hz, 1H), 7.41 (dd, *J* = 8.6, 7.5 Hz, 1H), 7.37 (dd, *J* = 1.9, 0.8 Hz, 1H), 6.82 (dd, *J* = 7.5, 1.1 Hz, 1H), 6.33 (dd, *J* = 3.3, 1.9 Hz, 1H), 6.29 (m, 1H), 5.30 (t, *J* = 5.8 Hz, 1H), 4.49 (d, *J* = 5.7 Hz, 2H), 2.95 (t, *J* = 6.1 Hz,

2H), 2.66 (m, 2H), 2.07 (m, 2H). ^{13}C NMR (126 MHz, CDCl3) δ 203.5, 154.7, 151.8, 145.8, 143.8, 142.2, 135.1, 121.1, 117.5, 117.2, 110.4, 107.3, 40.7, 37.3, 31.0, 22.8 HRMS (ESI) calcd for $C_{16}H_{16}N_2O_3^+$ (MH^+) 285.1239, found 285.1248

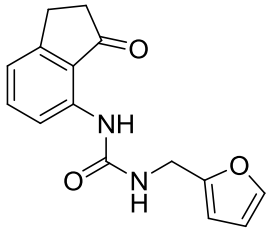

1-(2-furylmethyl)-3-(3-oxoindan-4-yl)urea (2.5b): General procedure **II** was followed. From 0.50 g of 7-amino-2,3-dihydro-1H-inden-1-one (3.4 mmol, 1 eq) and 0.42 g of furfuryl isocyanate (3.4 mmol, 1 eq), 0.71 g (77%) of the title compound was obtained.^{1}H NMR (500 MHz, DMSO) δ 9.51 (s, 1H), 8.19 (t, 1H), 8.16 (d, J=8.3 Hz, 1H), 7.60 (dd, *J* = 1.9, 0.9 Hz, 1H), 7.52 (t, *J*=7.8 Hz, 1H), 7.04 (dd, *J* = 7.5, 0.9 Hz, 1H), 6.41 (dd, *J* = 3.2, 1.8 Hz, 1H), 6.28 (dd, *J* = 3.2, 0.9 Hz, 1H), 4.28 (d, *J* = 5.5 Hz, 2H), 3.04 (m, 2H), 2.66 (m, 2H). ^{13}C NMR (126 MHz, DMSO) δ 208.5, 156.5, 154.8, 153.2, 142.6, 140.4, 136.7, 122.1, 118.7, 115.3, 110.9, 107.2, 36.6, 36.4, 25.4 HRMS (ESI) calcd for $C_{15}H_{14}N_2NaO_3^+$ (MNa^+) 293.0902, found 293.0909

General procedure **III** for the synthesis of compounds **2.7** and **2.11**

2 eq of a 15% wt phosgene solution in toluene was cooled to -78^{o}C under a N_2 atmosphere. To this was added dropwise 1 eq of furfuryl alcohol dissolved in 3 ml of anh. diethyl ether. Upon complete addition, the mixture was warmed to -15^{o}C and stirred for 3 hrs, followed by an additional 30 mins at 0^{o}C. The chlorocarbamate solution was added to a stirring solution of 0.5-1.0 eq of corresponding amine and 1.1-2.0 eq of dry pyridine,

dissolved in 10 ml of anh. DCM. The mixture was allowed to stir at ambient temperature overnight. The mixture was quenched with water and extracted with DCM. The organic layer was washed with sat. brine and dried over Na_2SO_4 before concentrating *in vacuo*. The crude product was further purified by flash chromatography.[11]

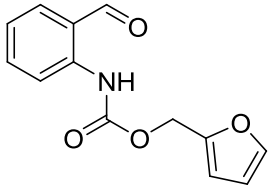

2-furylmethyl N-(2-formylphenyl)carbamate (2.7): General procedure **III** was followed. From 6.42 ml of 15% wt phosgene solution in toluene (9.0 mmol, 2 eq), 0.44 g of furfuryl alcohol (4.5 mmol, 1 eq), 0.55 g of 2-aminobenzyl alcohol **2.8** (4.5 mmol, 1 eq), and 0.41 ml of dry pyridine (5.1 mmol, 1.1 eq), 0.33 g (29%) of **2-furylmethyl N-(2-(hydroxymethyl)phenyl)carbamate (2.10)** was obtained. ^{1}H NMR (500 MHz, $CDCl_3$) δ 7.96 (s, 2H), 7.47 (dd, *J* = 1.9, 0.9 Hz, 1H), 7.35 (td, *J* = 7.8, 1.6 Hz, 1H), 7.18 (dd, *J* = 7.5, 1.6 Hz, 1H), 7.06 (td, *J* = 7.5, 1.2 Hz, 1H), 6.49 (dd, *J* = 3.2, 0.8 Hz, 1H), 6.41 (dd, *J* = 3.3, 1.8 Hz, 1H), 5.18 (s, 2H), 4.70 (s, 2H), 2.14 (s, 1H). ^{13}C NMR (126 MHz, CDCl3) δ 153.71, 149.67, 143.28, 137.40, 129.16, 129.11, 128.83, 123.61, 121.09, 110.77, 110.63, 64.02, 58.73. To 0.33 g of **2.10** (1.3 mmol, 1 eq) dissolved in 20 mL of anhydrous DCM was added 0.43 g of PCC (2.0 mmol, 1.5 eq). The mixture was stirred at ambient temperature overnight. The solution was filtered through a pad of silica gel and washed thoroughly with DCM. The resulting organic layer was concentrated *in vacuo* to yield 0.27 g (83%) of pale yellow solid **2.7**. ^{1}H NMR (500 MHz, CDCl3) δ 10.66 (s, 1H), 9.92 (d, *J* = 0.7 Hz, 1H), 8.50 (d, *J* = 8.5 Hz, 1H), 7.67 (dd, *J* = 7.7, 1.7 Hz, 1H), 7.63 (ddd, *J* = 8.8, 7.3, 1.7 Hz, 1H), 7.48 (dd, *J* = 1.9, 0.8 Hz, 1H), 7.21 (td, *J* = 7.5, 1.0 Hz,

1H), 6.50 (dd, *J* = 3.3, 0.7 Hz, 1H), 6.41 (dd, *J* = 3.3, 1.9 Hz, 1H), 5.21 (s, 2H). ^{13}C NMR (126 MHz, CDCl3) δ 195.0, 153.2, 149.4, 143.4, 141.1, 136.0, 122.1, 121.4, 118.4, 110.9, 110.6, 77.2, 58.8 HRMS (ESI) calcd for $C_{13}H_{11}NNaO_4^+$ (MNa^+) 268.0586, found 268.0594

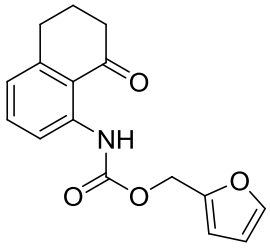

2-furylmethyl N-(4-oxotetralin-5-yl)carbamate (2.11): General procedure **III** was followed. From 6.42 mL of 15% wt phosgene solution in toluene (9.0 mmol, 2 eq), 0.44 g of furfuryl alcohol (4.5 mmol, 1 eq), 0.38 g of tetralone (4.5 mmol, 0.5 eq), and 0.9 mL of dry pyridine (5.1 mmol, 2.0 eq), 0.35 g (30%) of the title compound was obtained. ^{1}H NMR (500 MHz, CDCl3) δ 11.70 (s, 1H), 8.34 (dd, J = 8.6, 1.1 Hz, 1H), 7.45 (m, 1H), 7.43 (d, J = 8.0 Hz, 1H), 6.89 (dt, J = 7.4, 1.0 Hz, 1H), 6.48 (dd, *J* = 3.3, 0.8 Hz, 1H), 6.39 (dd, *J* = 3.2, 1.9 Hz, 1H), 5.17 (s, 2H), 2.96 (t, *J* = 6.1 Hz, 2H), 2.68 (dd, *J* = 7.3, 5.8 Hz, 2H), 2.07 (p, *J* = 6.4 Hz, 2H). 13C NMR (126 MHz, CDCl3) δ 202.7, 153.5, 149.8, 146.0, 143.2, 142.1, 134.9, 122.2, 118.2, 116.7, 110.6, 110.5, 58.6, 40.6, 31.0, 22.7. HRMS (ESI) calcd for $C_{16}H_{15}NO_4^+$ (MH^+) 286.1074, found 286.1079

Photochemical cycloaddition

General procedure IV for irradiation: Solutions with ca. 3.0 mM of the photo-precursors in methanol (except where noted) were degassed and irradiated in Pyrex or borosilicate glass reaction vessels in a Rayonet reactor equipped with RPR-3500 UV lamps (broadband 300-400 nm UV source with peak emission at 350 nm) until the

reaction was complete, as determined by ^{1}H NMR. The solution was concentrated and the mixture was purified by flash chromatography.

2.6a (0.20 g, 0.74 mmol) was irradiated following general procedure **IV** with acetonitrile as a solvent. Flash chromatography yielded 0.13 g (63%) of **12-hydroxy-12-methyl-16-oxa-3,5-diazatetracyclo[11.2.1.0^{1,5}.0^{6,11}]hexadeca-6(11),7,9,14-tetraene-2,4-dione (2.14b)** and 0.039 g (19%) of **11-hydroxy-11-methyl-7-oxa-2,4-diazatetracyclo[10.4.0.0^{2,6}.0^{6,10}]hexadeca-1(12),8,13,15-tetraene-3,5-dione (2.14a).**

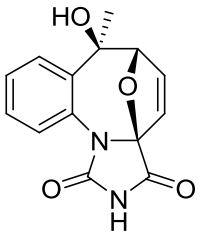

2.14b: ^{1}H NMR (500 MHz, DMSO) δ 11.58 (s, 1H), 7.58 (dd, *J* = 8.2, 1.5 Hz, 1H), 7.57 (dd, *J* = 8.1, 1.6 Hz, 1H), 7.28 (ddd, *J* = 8.3, 7.1, 1.5 Hz, 1H), 7.17 (ddd, *J* = 8.4, 7.2, 1.5 Hz, 1H), 6.65 (dd, *J* = 5.9, 1.7 Hz, 1H), 5.93 (dd, *J* = 5.9, 1.3 Hz, 1H), 5.53 (s, 1H), 4.78 (t, *J* = 1.5 Hz, 1H), 1.59 (s, 3H). ^{13}C NMR (126 MHz, DMSO) δ 169.4, 153.0, 137.7, 135.8, 132.2, 129.0, 127.81, 126.01, 125.61, 124.51, 97.31, 90.31, 78.51, 26.3. HRMS (ESI) calcd for $C_{14}H_{12}N_2NaO_4^+$ (MNa^+) 295.0695, found 295.0709

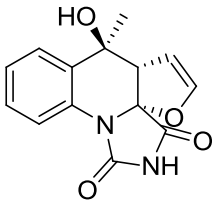

2.14a: ^{1}H NMR (500 MHz, DMSO) δ 11.59 (s, 1H), 7.37 (m, 3H), 7.28 (td, *J* = 7.2, 2.0 Hz, 1H), 6.52 (t, *J* = 2.8 Hz, 1H), 5.47 (s, 1H), 4.87 (dd, *J* = 2.9, 2.2 Hz, 1H), 3.88 (t, *J* = 2.5 Hz, 1H), 1.66 (s, 3H). ^{13}C NMR (126 MHz, DMSO) δ 171.6, 154. 5, 146.9, 136.4, 133.5, 128.0, 126.2, 125.5,

125.1, 100.3, 94.0, 69.0, 58.7, 24.2 HRMS (ESI) calcd for $C_{14}H_{12}N_2NaO_4^+$ (MNa^+) 295.0695, found 295.0703

2.6b (0.36 g, 1.2 mmol) was irradiated following general procedure **IV**. Flash chromatography yielded 0.15 g (43%) **1-hydroxyl-19-oxa-7,9-diazapentacyclo[8.7.1.1^{2,5}.0^{5,9}.0^{14,18}]nonadeca-3,10(18),11,13-tetraene-6,8-dione (2.15b)** and 0.072 g (19%) of **11-hydroxy-7-oxa-2,4-diazapentacyclo[9.7.1.0^{2,6}.0^{6,10}.0^{15,19}]nonadeca-1(19),8,15,17-tetraene-3,5-dione (2.15a)**

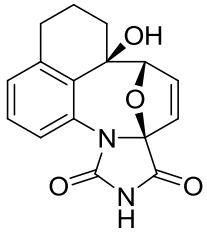

2.15b: ^{1}H NMR (500 MHz, DMSO) δ 11.52 (s, 1H), 7.33 (dd, *J* = 7.9, 1.2 Hz, 1H), 7.14 (t, *J* = 7.8 Hz, 1H), 6.95 (dd, *J* = 7.5, 1.4 Hz, 1H), 6.68 (dd, *J* = 5.9, 1.7 Hz, 1H), 5.90 (dd, *J* = 5.9, 1.2 Hz, 1H), 5.39 (d, *J* = 1.3 Hz, 1H), 4.62 (t, *J* = 1.5 Hz, 1H), 2.81 (m, 1H), 2.70 (ddd, *J* = 17.2, 12.9, 5.6 Hz, 1H), 2.01 (m, 1H), 1.87 (m, 1H), 1.69 (m, 2H). ^{13}C NMR (126 MHz, DMSO) δ 169.4, 153.0, 138.9, 137.9, 133.4, 132.3, 127.6, 127.3, 124.7, 124.3, 97.3, 89.0, 75.5, 35.7, 31.5, 17.4 HRMS (ESI) calcd for $C_{16}H_{14}N_2NaO_4^+$ (MNa^+) 321.0851, found 321.0856

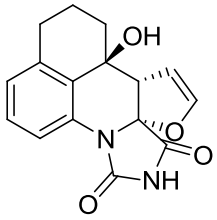

2.15a: ^{1}H NMR (500 MHz, DMSO) δ 11.59 (s, 1H), 7.25 (t, *J* = 7.7 Hz, 1H), 7.17 (dd, *J* = 7.6, 1.1 Hz, 1H), 7.05 (d, *J* = 8.0 Hz, 1H), 6.54 (t, *J* = 2.8 Hz, 1H), 5.45 (s, 1H), 4.95 (dd, *J* = 3.0, 2.2 Hz, 1H), 3.90 (t, *J*= 2.4 Hz, 1H), 2.72 (m, 1H), 2.60 (m, 1H), 1.90 (m, 3H), 1.72 (m, 1H). ^{13}C NMR (126 MHz, DMSO) δ 172.1, 155. 0, 147.2, 138.4, 133.9, 131.4, 127.8, 127.2, 123.4, 101.1, 94.5, 67.9, 57.9, 35.4, 29.5, 18.4 HRMS (ESI) calcd for $C_{16}H_{14}N_2O_4^-$ (MH^-) 297.0875, found 297.0886

2.5a (0.50 g, 1.8 mmol) was irradiated following general procedure **IV**. Flash chromatography yielded 0.27 g (54%) of **1-hydroxy-19-oxa-7,9-diazapentacyclo[8.7.1.1^{2,5}.0^{5,9}.0^{14,18}]nonadeca-3,10,12,14(18)tetraen-8-one (2.13b)** and 0.077 g (15%) of **2-hydroxy-19-oxa-7,9-diazapentacyclo[8.7.1.1^{1,5}.0^{5,9}.0^{14,18}]nonadeca-3,10,12,14(18)tetraen-8-one (2.13a)**.

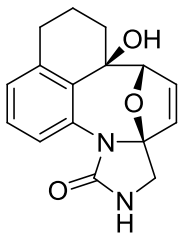

2.12b: ^{1}H NMR (500 MHz, DMSO) δ 7.21 (s, 1H), 7.09 (m, 2H), 6.87 (m, 1H), 6.53 (dd, *J* = 5.7, 1.8 Hz, 1H), 5.77 (dd, *J* = 5.7, 1.1 Hz, 1H), 4.46 (m, 1H), 3.80 (dd, *J* = 10.8, 1.1 Hz, 1H), 3.48 (dd, *J* = 10.7, 1.4 Hz, 1H), 2.79 (m, 1H), 2.68 (ddd, *J* = 17.4, 12.9, 5.5 1H), 2.00 (m, 1H), 1.84 (m, 1H), 1.68 (m, 3H). ^{13}C NMR (126 MHz, DMSO) δ 157.0, 138.3, 136.2, 135.1, 133.1, 128.1, 126.9, 126.6, 126.0, 99.6, 87.6, 75.5, 46.4, 36.0, 31.51, 17.7 HRMS (ESI) calcd for $C_{16}H_{16}N_2O_3^-$ (MH^-) 283.1083, found 283.1087

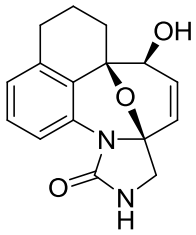

2.12b': ^{1}H NMR (500 MHz, $CDCl_3$) δ 7.64 (d, *J* = 8.1 Hz, 1H), 7.25 (t, *J* = 7.8 Hz, 1H), 6.92 (d, *J* = 7.6 Hz, 1H), 6.22 (dd, *J* = 9.7, 5.4 Hz, 1H), 5.93 (d, *J* = 9.7 Hz, 1H), 5.69 (s, 1H), 3.84 (d, *J* = 5.4 Hz, 1H), 3.68 (d, *J* = 1.1 Hz, 2H), 3.51 (s, 1H), 2.90 (m, 2H), 2.49 (ddd, *J* = 12.2, 6.8, 2.4 Hz, 1H), 2.11 (m, 2H), 1.96 (m, 1H), 1.56 (td, *J* = 12.3, 7.7 Hz, 1H). ^{13}C NMR (126 MHz, $CDCl_3$) δ 157.55, 136.1, 131.2, 130.0, 128.8, 127.9, 125.5, 123.8, 118.0, 84.3, 77.1, 64.3, 49.4, 29.1, 26.1, 15.9. HRMS (ESI) calcd for $C_{16}H_{16}N_2LiO_3^+$ (MLi^+) 291.1321, found 291.1328

2.5b (0.30 g, 1.1 mmol) was irradiated following general procedure **IV**. Flash chromatography yielded 0.15 g (52%) **1-hydroxyl-18-oxa-7,9-diazapentacyclo[8.6.1.1^{2,5}.0^{5,9}.0^{14,17}]octadeca-3,10,12,14(17)-tetraen-8-one (2.13b)** and 0.077 g (26%) **2-(8-hydroxy-3-oxo-2,4-diazatertacyclo[6.6.1.0^{2,6}.0^{11,15}]pentadeca-1(14),5,11(15),12-tetraen-7-yl)acetaldehyde (2.13b')**.

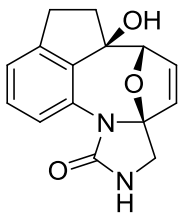

2.13b: ^{1}H NMR (500 MHz, DMSO) δ 7.33 (d, *J* = 8.1 Hz, 1H), 7.23 (s, 1H), 7.15 (dd, *J* = 8.1, 7.3 Hz, 1H), 6.96 (d, *J* = 7.3 Hz, 1H), 6.53 (dd, *J* = 5.8, 1.9 Hz, 1H), 5.80 (dd, *J* = 5.8, 1.2 Hz, 1H), 5.09 (s, 0H), 4.77 (t, *J* = 1.5 Hz, 1H), 3.80 (d, *J* = 10.6 Hz, 1H), 3.48 (dd, *J* = 10.7, 1.4 Hz, 1H), 3.11 (m, 1H), 2.75 (m, 1H), 1.93 (m, 2H). 13C NMR (126 MHz, DMSO) δ 156.73, 145.44, 136.75,

136.44, 132.62, 128.45, 128.24, 122.64, 120.73, 100.31, 89.03, 85.93, 47.15, 36.20, 30.37. HRMS (ESI) calcd for $C_{15}H_{14}N_2O_3^+$ (MH^+) 271.1083, found 271.1091

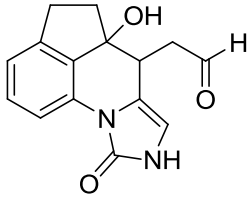

2.13b': ^{1}H NMR (500 MHz, DMSO) δ 10.03 (d, J = 2.4 Hz, 1H), 9.56 (d, J = 2.7 Hz, 1H), 7.90 (d, J = 8.0 Hz, 1H), 7.30 (t, J = 7.8 Hz, 1H), 7.03 (d, J = 7.5 Hz, 1H), 6.36 (d, J = 2.3 Hz, 1H), 5.24 (s, 1H), 3.67 (dd, J = 8.9, 5.7 Hz, 1H), 3.19 (m, 1H), 2.82 (dd, J = 15.8, 8.4 Hz, 1H), 2.59 (dd, J = 16.8, 5.7 Hz, 1H), 2.11 (m, 1H), 1.97 (m, 2H). ^{13}C NMR (126 MHz, DMSO) δ 202.24, 172.47, 151.90, 144.33, 132.09, 132.01, 130.28, 121.43, 120.34, 113.62, 107.15, 78.74, 46.23, 40.89, 39.54, 36.63, 36.36, 30.81, 21.52 HRMS (ESI) calcd for $C_{15}H_{14}N_2O_3^-$ (MH^-) 269.0926, found 269.0928

2.7 (0.26 g, 1.1 mmol) was irradiated following general procedure **IV**. Flash chromatography yielded 0.076 g (29%) **12-hydroxy-3,16-dioxa-5-azatetracyclo[11.2.1.0^{1,5}.0^{6,11}]hexadeca-6,8,10,14-tertaen-4-one (2.16b)** and 0.15 g (58%) **11-hydroxy-4,7-dioxa-2-azatetracyclo[10.4.0.0^{2,6}.0^{6,10}]hexadeca-1(16),8,12,14-tertaen-3-one (2.16a)** .

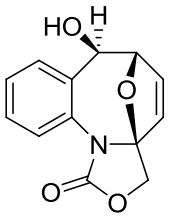

2.16b: ^{1}H NMR (500 MHz, DMSO) δ 7.71 (dt, *J* = 8.0, 1.4 Hz, 1H), 7.34 (m, 1H), 7.30 (tdd, *J* = 7.8, 1.8, 0.7 Hz, 1H), 7.25 (td, *J* = 7.5, 1.7 Hz, 1H), 6.55 (dd, *J* = 5.8, 1.8 Hz, 1H), 6.18 (d, *J* = 6.4 Hz, 1H), 5.95 (dd, *J* = 5.8, 1.0 Hz, 1H), 4.91 (dd, *J* = 6.4, 3.3 Hz, 1H), 4.85 (ddd, *J* = 3.2, 1.8, 1.0 Hz, 1H), 4.75 (d, *J* = 10.2 Hz, 1H), 4.49 (d, *J* = 10.2 Hz, 1H). ^{13}C NMR (126 MHz, CDCl3) δ 158.6, 142.0, 140.4, 136.2, 132.7, 132.3, 131.9, 131.3, 130.8, 104.2, 88.5, 79.4, 73.9 HRMS (ESI) calcd for $C_{13}H_{11}NNaO_4^+$ (MNa^+) 268.0586, found 268.0596

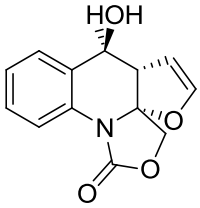

2.16a: ^{1}H NMR (500 MHz, DMSO) δ 7.50 (dd, *J* = 7.8, 1.3 Hz, 1H), 7.44 (dt, *J* = 7.4, 1.4 Hz, 1H), 7.31 (tdd, *J* = 7.7, 1.7, 0.9 Hz, 1H), 7.25 (td, *J* = 7.5, 1.3 Hz, 1H), 6.43 (t, *J* = 2.7 Hz, 1H), 5.97 (d, *J* = 5.5 Hz, 1H), 4.95 (t, *J* = 5.9 Hz, 1H), 4.84 (dd, *J* = 3.1, 2.2 Hz, 1H), 4.76 (d, *J* = 10.1 Hz, 1H), 4.62 (d, *J* = 10.1 Hz, 1H), 3.96 (dt, *J* = 6.2, 2.3 Hz, 1H). ^{13}C NMR (126 MHz, DMSO) δ 153.5, 146.6, 134.4, 131.9, 127.4, 125.9, 125.3, 120.9, 99.6, 98.0, 73.4, 65.8, 54.1 HRMS (ESI) calcd for $C_{13}H_{11}NNaO_4^+$ (MNa^+) 268.0586, found 268.0594

2.11 (0.10 g, 0.35 mmol) was irradiated following general procedure **IV**. Flash chromatography yielded 0.063 g (63%) **11-hydroxy-4,7-dioxa-2-azapentacyclo[9.7.1.0^{2,5}.0^{6,10}.0^{15,19}]nonadeca-1(18),8,15(19),16-tetraen-3-one (12b)**

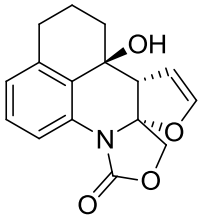

2.17a: ^{1}H NMR (500 MHz, $CDCl_3$) δ 8.00 (s, 1H), 7.56 (dt, *J* = 7.9, 1.1 Hz, 1H), 7.31 (t, *J* = 7.8 Hz, 1H), 7.02 (dq, *J* = 7.7, 1.0 Hz, 1H), 6.31 (t, *J* = 2.9 Hz, 1H), 4.73 (dd, *J* = 3.2, 2.3 Hz, 1H), 4.71 (d, *J* = 9.4 Hz, 1H), 4.60 (d, *J* = 9.5 Hz, 1H), 3.75 (t, *J* = 2.4 Hz, 1H), 2.97 (d, *J* = 0.4 Hz, 1H), 2.89 (d, *J* = 0.7 Hz, 1H), 2.82 (m, 1H), 2.72 (m, 1H), 2.21 (s, 1H), 2.07 (m, 1H), 1.92 (m, 1H). ^{13}C NMR (126 MHz, $CDCl_3$) δ 146.9, 138.0, 133.2, 128.8, 128.5, 126.7, 121.2, 99.1, 97.4, 77.2, 75.4, 69.3, 58.3, 35.4, 29.5, 18.5. HRMS (ESI) calcd for $C_{16}H_{15}NLiO_4^+$ (MLi^+) 292.1161, found 292.1169

Post-photochemical cycloadditions

The model system, an equimolar mixture of **4-hydroxy-2,3-benzo-8-oxa-1-azatricyclo[7.3.0.0^{5,9}]dodeca-2,6-dien-12-one (2.18)** and **2-hydroxy-3,4-benzo-12-oxa-5-aza-tricyclo[7.2.1.0^{5,9}]dodec-3,10-dien-6-one) (2.19),** was synthesized as previously described.[14]

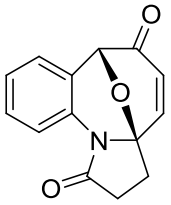

16-oxa-5-azatetracyclo[10.3.1.0^{1,5}.0^{6,11}]hexadeca-6(11),7,9,14-tetraen-4,13-dione (2.23): A 0.50 g mixture of **2.18** and **2.19 (**2.1 mmol, 1 eq), was dissolved in 40 ml of $CHCl_3$. To this was added 5 ml of TFA. The mixture stirred at room temperature overnight. The reaction was quenched with sat. $NaHCO_3$ solution, followed by washing of the organic layer with brine, drying over anhydr. Na_2SO_4, and concentration *in vacuo*. The resulting residue was purified by flash

chromatography to yield 0.19 g of **13-hydroxy-16-oxa-5-azatetracyclo[10.3.1.0^{1,5}.0^{6,11}]hexadeca-6(11),7,9,14-tetraen-4-one** (39%). ^{1}H NMR (500 MHz, $CDCl_3$) δ 8.38 (dd, *J* = 8.3, 1.2 Hz, 1H), 7.41 (dddd, *J* = 8.1, 7.4, 1.7, 0.5 Hz, 1H), 7.30 (m, 1H), 7.22 (td, *J* = 7.5, 1.2 Hz, 1H), 6.13 (d, *J* = 9.9 Hz, 1H), 6.07 (ddd, *J* = 9.8, 5.0, 1.2 Hz, 1H), 5.31 (s, 1H), 5.17 (dd, *J* = 5.0, 1.2 Hz, 1H), 2.77 (m, 2H), 2.45 (m, 2H). ^{13}C NMR (126 MHz, $CDCl_3$) δ 171.4, 133.6, 132.6, 129.3, 125.5, 124.6, 121.3, 120.9, 120.3, 85.8, 73.8, 71.0, 30.2, 29.7. 0.07 ml of oxalyl chloride (0.84 mmol, 1.1 eq) was dissolved in 0.9 ml of anhydrous DCM and cooled to -78^{o}C before 0.12 ml of dry DMSO (1.7 mmol, 2.2 eq) was slowly added. Upon complete addition, the mixture stirred for 2 mins while the evolution of gas stopped. Then, 0.19 g of the alcohol (0.77 mmol, 1 eq) dissolved in 1.5 ml of anhydrous DCM was added dropwise. After stirring for 15 mins, 0.54 ml of NEt_3 (3.9 mmol, 5 eq) was slowly added. Upon complete addition, the mixture was slowly warmed to RT at which it was stirred overnight. The reaction mixture was quenched with water, and extracted with DCM. The resulting organic layer was washed with brine, dried over Na_2SO_4, and concentrated *in vacuo* to yield 0.11 g of **2.23** (60%). The resulting solid was used in the next step without further purification. ^{1}H NMR (500 MHz, $CDCl_3$) δ 8.46 (dd, *J* = 8.4, 1.2 Hz, 1H), 7.41 (ddd, *J* = 8.6, 7.3, 1.6 Hz, 1H), 7.27 (dd, *J* = 7.8, 1.7 Hz, 1H), 7.19 (td, *J* = 7.5, 1.2 Hz, 1H), 6.79 (d, *J* = 10.0 Hz, 1H), 6.19 (dd, *J* = 10.1, 0.7 Hz, 1H), 5.22 (s, 1H), 2.79 (m, 2H), 2.55 (ddd, *J* = 13.5, 7.1, 4.5 Hz, 1H), 2.41 (dt, *J* = 13.5, 10.4 Hz, 1H). 13C NMR (126 MHz, CDCl3) δ 192.5, 170.9, 143.2, 132.3, 129.5, 126.3, 125.8, 125.0, 119.9, 119.3, 86.3, 78.7, 31.0, 29.7. HRMS (ESI) calcd for $C_{14}H_{11}NO_3^{+}$ $(MH)^{+}$ 242.0812 found 242.0816

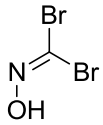

Synthesis of dibromoformaldoxime:[45] To a solution of 20.3 g of glyoxylic acid monohydrate (0.22 mol, 1 eq) in 160 ml of water (1.4M) was added 19.4 g of hydroxylamine hydrochloride (0.28 mmol, 1.3 eq). The mixture was stirred at ambient temperature for 24 hrs. 47.7 g of NaHCO3 (0.57 mmol, 2.58 eq) was slowly added, followed by 70 ml of DCM. Upon cooling the resulting mixture in the ice bath, 19.5 ml of Br_2 (0.38 mol, 1.7 eq) in 100 ml of DCM was slowly added maintaining the temperature at or below 10^{o}C. Upon complete addition, the mixture was stirred at room temperature for 3 hrs. The resulting mixture was diluted with 100 ml of water, extracted with 3x30 ml of DCM, dried over Na_2SO_4, and concentrated *in vacuo*. The resulting solid was recrystallized from hexanes to yield 12.5 g (28%) of a white crystalline solid. mp 65-66^{o}C (lit. 65-66^{o}C).[45]

General procedure V for nitrile oxide addition:[45] 1 eq of photoproduct(s) was dissolved in EtOAc or EtOAc/DCM mixture. To this was added 3 eq of dibromoformaldoxime and 6 eq of $KHCO_3$. An additional 3 eq of dibromoformaloxime and 6 eq of $KHCO_3$ were usually added after stirring for 12 hrs. The reaction was monitored by NMR until the starting materials were consumed. The resulting mixture was diluted with water, extracted with 3x20 ml of EtOAc or DCM, washed with brine, dried over Na_2SO_4, and concentrated *in vacuo*. The mixture was then purified by flash chromatography.

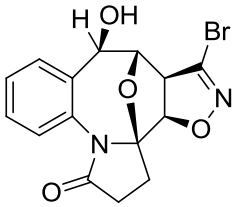

15-bromo-12-hydroxy-17,19-dioxa-5,16-diazapentacyclo[11.5.1.0^{1,5}.0^{6,11}.0^{14,18}]nonadeca-6(11),7,9,15-tetraen-4-one (2.22): General procedure **V** was followed using EtOAc. From 0.19 g of **2.19** (0.76 mmol, 1 eq), 0.46 g of dibromoformaloxime (2.3 mmol, 3 eq), and 0.46 g of $KHCO_3$ (4.6 mmol, 6 eq), 0.17 g (63%) of a 4:1 mixture of two regioisomers were obtained. ^{1}H NMR (500 MHz, DMSO) δ 7.39 (m, 3H), 7.27 (m, 1H), 5.53 (d, *J* = 5.8 Hz, 1H), 4.71 (d, *J* = 8.6 Hz, 1H), 4.64 (dd, *J* = 5.8, 4.3 Hz, 1H), 4.53 (d, *J* = 4.2 Hz, 1H), 3.75 (dd, *J* = 8.6, 1.1 Hz, 1H), 2.68 (ddd, *J* = 16.1, 9.9, 8.8 Hz, 1H), 2.55 (m, 1H), 2.46 (m, 1H), 2.07 (m, 1H). ^{13}C NMR (126 MHz, DMSO) δ 173.3, 140.0, 134.3, 134.2, 133.4, 128.9, 128.4, 126.9, 104.1, 88.1, 81.7, 76.4, 61.0, 29.5, 27.3. HRMS (ESI) calcd for $C_{15}H_{13}N_2LiO_4Br^+$ (MLi^+) 371.0219, found 371.0219

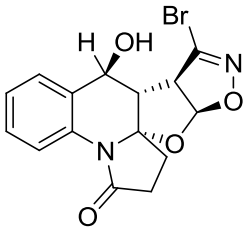

15-bromo-12-hydroxyl-17,19-dioxa-5,16-diazapentacyclo[11.6.0.0^{1,5}.0^{6,11}.0^{14,18}]nonadeca-6,8,10,15-tetraen-4-one (2.20): General procedure **V** was followed. From 0.20 g **2-Hydroxy-3,4-benzo-12-oxa-5-aza-tricyclo[7.2.1.0^{5,9}]dodec-3,10-dien-6-one (2.18)** (0.82 mmol, 1 eq), 1.0 g of dibromoformaloxime (4.9 mmol, 6 eq), and 1.0 g of $KHCO_3$ (9.8mmol, 12 eq), 0.19 g (65%) of the title compound was obtained. ^{1}H NMR (500 MHz, $CDCl_3$) δ 7.92 (d, *J* = 7.9 Hz, 1H), 7.49 (td, *J* = 7.8, 1.5 Hz, 1H), 7.37 (dd, *J* = 7.5, 1.5 Hz, 1H), 7.25 (td, *J* = 7.5, 1.2 Hz, 1H), 5.65 (d, *J* = 6.0 Hz, 1H), 4.79 (t, *J* = 2.9 Hz, 1H), 3.51 (s, 1H), 3.45 (dd, *J* = 6.0, 3.6 Hz, 1H), 3.37 (dd, *J* = 3.5, 2.9 Hz, 1H), 2.85 (ddd, *J* = 16.6, 9.9, 8.7 Hz, 1H),

2.48 (m, 3H). ^{13}C NMR (126 MHz, $CDCl_3$) δ 173.2, 140.8, 134.2, 130.8, 129.0, 128.7, 126.1, 123.7, 106.8, 101.2, 71.0, 61.6, 41.0, 34.2, 29.9. HRMS (ESI) calcd for $C_{15}H_{13}N_2O_4Br^+$ (MH^+) 366.0168, found 366.0181

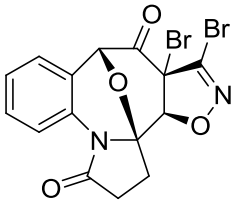

14,15-dibromo-17,19-dioxa-5,16-diazapentacyclo[10.6.1.0^{1,5}.0^{5,11}.0^{1,18}]nonadeca-6,8,10,15-tetraene-4,13-dione (2.24): General procedure **V** was followed using EtOAc/DCM mixture. From 0.11 g of **2.23**, 0.13 g of the title compound was obtained after flash chromatography (62%). ^{1}H NMR (500 MHz, CD_2Cl2) δ 8.44 (m, 1H), 7.49 (ddd, *J* = 8.4, 7.4, 1.8 Hz, 1H), 7.28 (m, 2H), 5.41 (s, 1H), 5.15 (s, 1H), 3.04 (ddd, *J* = 13.8, 8.1, 3.7 Hz, 1H), 2.74 (m, 2H), 2.30 (dt, *J* = 13.8, 10.1 Hz, 1H). ^{13}C NMR (126 MHz, CD_2Cl2) δ 191.8, 172.6, 141.4, 134.1, 131.0, 126.4, 126.0, 120.8, 118.1, 92.7, 90.1, 78.2, 57.7, 30.1, 28.8. HRMS (ESI) calcd for $C_{15}H_{10}Br_2N_2O_4Li$ (MLi^+) 448.9148, found 449.1726

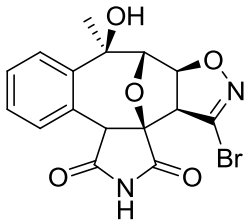

15-bromo-12-hydroxy-12-methyl-17,19-dioxa-3,5,16-triazapentacyclo[11.5.1.0^{1,5}.0^{6,11}.0^{14,18}]nondeca-6(11),7,9,15-tetraene-2,4-dione (2.26): General procedure **V** was followed. From 0.16 g of **2.14b** (0.58 mmol, 1 eq), 0.70 g of dibromoformaloxime (3.4 mmol, 6 eq), and 0.70 g of $KHCO_3$ (12.0 mmol, 12 eq), a 5:1 mixture of two regioisomers of the title compound was observed. After purification, 0.12 g (53%) of the major isomer was isolated. ^{1}H NMR (500 MHz, DMSO) δ 11.89 (s, 1H),

7.66 (dd, *J* = 8.1, 1.4 Hz, 1H), 7.54 (dd, *J* = 8.1, 1.5 Hz, 1H), 7.37 (m, 1H), 7.25 (ddd, *J* = 8.7, 7.3, 1.4 Hz, 1H), 5.44 (s, 1H), 4.92 (d, *J* = 8.7 Hz, 1H), 4.54 (d, *J* = 0.7 Hz, 1H), 3.85 (dd, *J* = 8.7, 0.7 Hz, 1H), 1.71 (s, 3H). ^{13}C NMR (126 MHz, DMSO) δ 166.5, 152.8, 136.2, 135.2, 133.4, 128.8, 128.3, 127.1, 126.5, 94. 9, 91.3, 88.5, 73.6, 63.5, 26.0. HRMS (ESI) calcd for $C_{15}H_{12}BrN_3LiO_5^+$ (MLi^+) 401.0132, found 401.0136

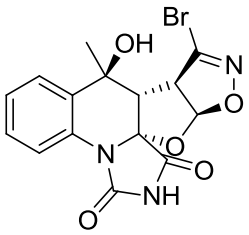

15-bromo-12-hydroxy-12-methyl-17,19-dioxa-3,5,16-triazapentacyclo[11.6.0.0^{1,5}.0^{6,11}.0^{14,18}]nonadeca-6(11),7,9,15-tetraene-2,4-dione (2.25): General procedure **V** was followed. From 0.15 g of **2.14a** (0.55 mmol, 1 eq), 0.66 g of dibromoformaloxime (3.2 mmol, 6 eq), and 0.66 g of $KHCO_3$ (6.6 mmol, 12 eq), 0.14 g (65%) of the title compound was obtained. ^{1}H NMR (500 MHz, DMSO) δ 11.68 (s, 1H), 7.49 (m, 2H), 7.38 (m, 2H), 5.71 (d, *J* = 6.0 Hz, 1H), 4.02 (dd, *J* = 6.0, 4.2 Hz, 1H), 3.20 (d, *J* = 4.2 Hz, 1H), 2.55 (s, 1H), 1.77 (s, 3H).^{13}C NMR (126 MHz, DMSO) δ 170.5, 154.7, 142.9, 135.0, 133.4, 129.0, 126.6, 126.0, 107.7, 93.9, 69.0, 59.6, 57.5, 30.6, 24.2. HRMS (ESI) calcd for $C_{15}H_{12}N_3LiO_5^+$ (MLi^+) 402.0102, found 402.0110

X-Ray Structures

X-Ray structures were obtained with a Bruker APEX II instrument and the structure was refined using XShell software. The goodness of fit "S" is listed after each entry. Structures have been deposited with the Cambridge Crystallographic Data Centre (CCDC).

1. **12-hydroxy-12-methyl-16-oxa-3,5-diazatetracyclo[11.2.1.$0^{1,5}$.$0^{6,11}$]hexadeca-6(11),7,9,14-tetraene-2,4-dione** S = 0.910

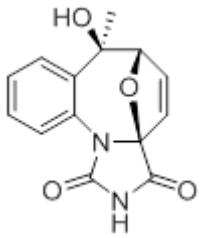

2. **1-hydroxyl-19-oxa-7,9-diazapentacyclo[8.7.1.1^{2,5}.$0^{5,9}$.$0^{14,18}$]nonadeca-3,10(18),11,13-tetraene-6,8-dione (2.15b)** S = 0.853

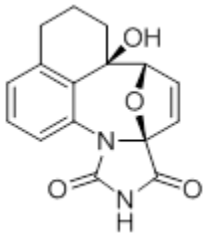

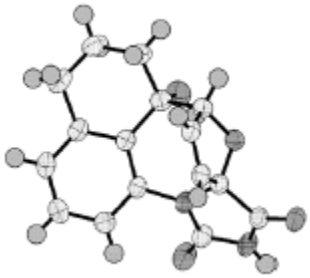

3. **12-hydroxy-3,16-dioxa-5-azatetracyclo[11.2.1.$0^{1,5}$.$0^{6,11}$]hexadeca-6,8,10,14-tertaen-4-one (2.16b)** S = 0.983

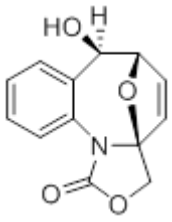

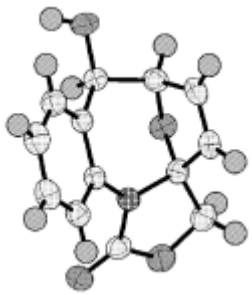

4. **15-bromo-12-hydroxyl-17,19-dioxa-5,16-diazapentacyclo[11.6.0.0^{1,5}.0^{6,11}.0^{14,18}]nonadeca-6,8,10,15-tetraen-4-one (2.20)**

   S = 1.019

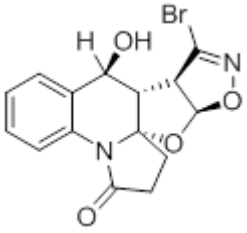

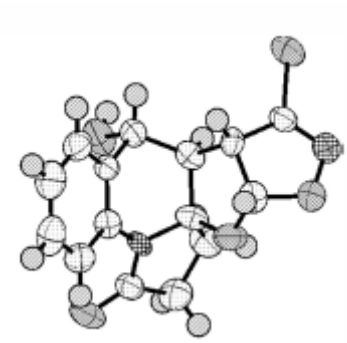

5. **15-bromo-12-hydroxy-12-methyl-17,19-dioxa-3,5,16-triazapentacyclo[11.6.0.0^{1,5}.0^{6,11}.0^{14,18}]nonadeca-6(11),7,9,15-tetraene-2,4-dione (2.25)** S = 1.032

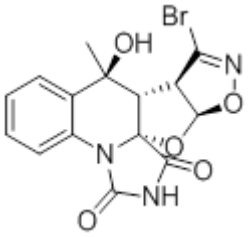

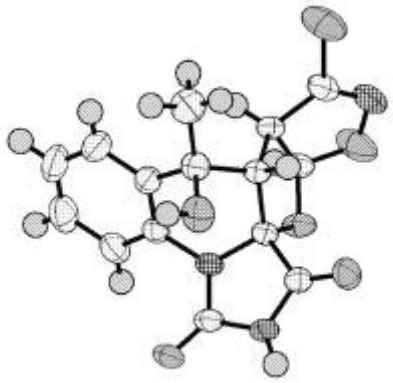

Chapter 3: Post-photochemical Modifications

The exciting result of several successful modifications opened the door to explore other reactions capable of a spectacular growth of complexity. The work in this chapter builds upon the simple, yet elegant nitrile oxide addition, with three new post-photochemical modifications. These modifications add to the diversity of our libraries and allows for a more effective probing of the chemical space. This work was published in the Australian Journal of Chemistry.[25]

Introduction

With the discovery that it is possible to perform post-photochemical modifications on our diverse azaxylylene scaffolds, effort was focused on finding additional reactions that would continue to increase complexity and probe the chemical space. A small sampling of previously synthesized compounds (**Figure 3.1**) shows that the cores themselves are very diverse, and they fit the criteria of Lipinski's Rule of 5 perfectly. The MWs are less than 500 Da, the S log Ps are less than 5, and the number of rotatable bonds are less than 5. An additional descriptor is included, the newly derived Lovering saturation coefficient, or fsp^3. This new descriptor has been developed to provide more information as to what makes a successful drug candidate, by comparing the number of

saturated sp^3 carbons to the total carbon count.[49] Lovering and co-workers found that most successful drug candidates in the Glaxo-Smith Kline BIO database had an fsp^3 on average around 0.47, and that later stage drug candidates showed a higher average fsp^3 than the early stage candidates.[49] As show in **Figure 3.1**, many of the scaffolds produced from azaxylylenes are near to or greater than Lovering's findings of 0.47. The closeness of our compound's fsp^3 values to what is known to be a successful drug candidate's fsp^3

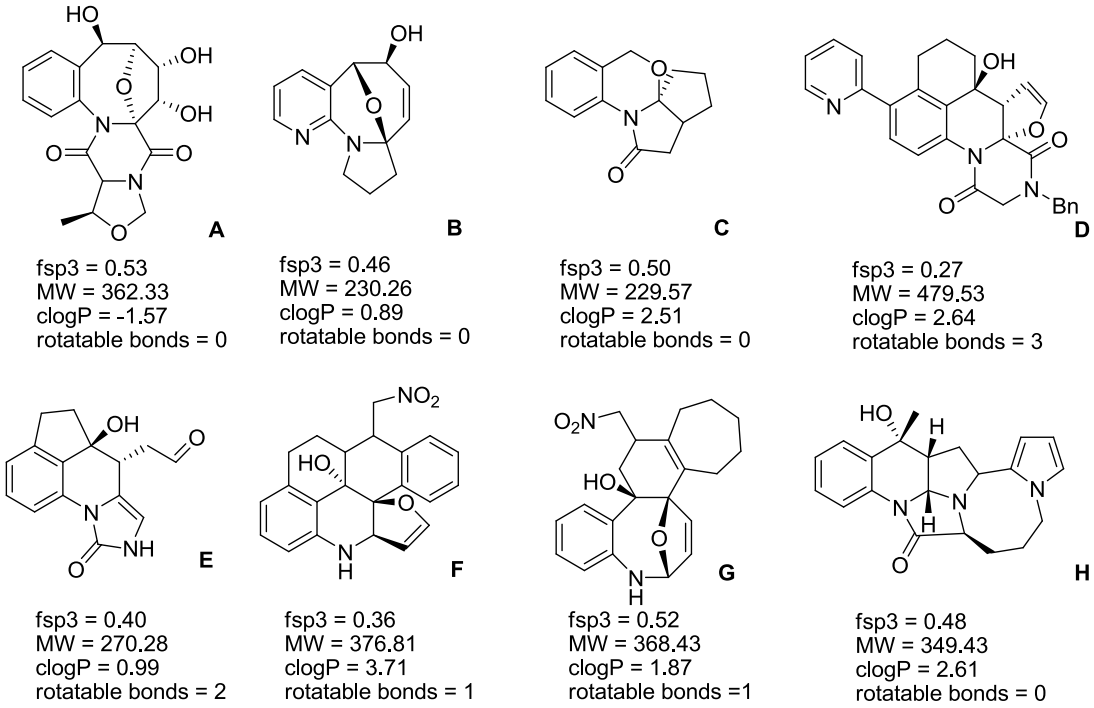

Figure 3.1

values is very promising for our compounds, and thus the development of new scaffolds from azaxylylenes should seek to match or improve upon this finding.

Results and Discussion – Synthesis of Starting Materials and Nitrile Oxide Addition

The previous successes of post-photochemical modifications were continued using the model system from the end of the last chapter (**Scheme 3.1**). Its simple assembly and high yields (89%) made it the best candidate for this exploration. The [3+2]

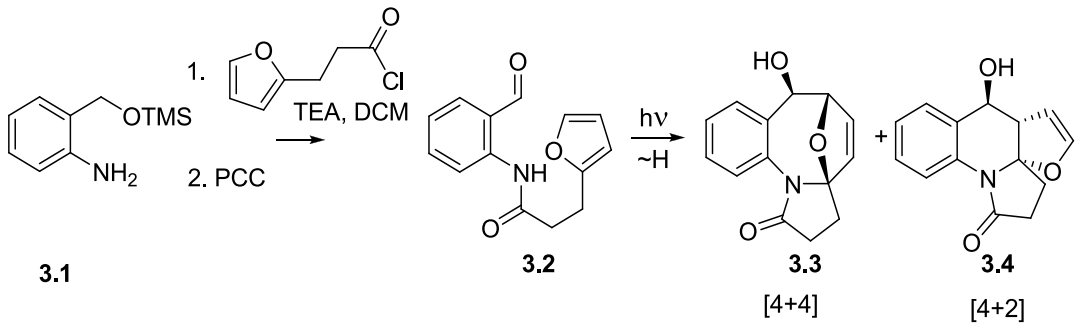

Scheme 3.1

nitrile oxide cycloaddition from the previous chapter was modified by addition of a phenyl group in replacement of bromine. As previously seen, the benzonitrile oxide addition occurs from the *exo* face (**Scheme 3.2**). From **3.4**, only one regioisomer, **3.5**, is seen due to the charge controlled intermediate. From **3.3**, two regioisomers **3.6** and **3.6'** form with a ratio of 3:1, of which **3.6** is the major. As reasoned previously, this structure is more energetically favored due to the steric strain from interaction of phenyl and the methylene bridge of the linker. As of note, **3.6'** was only observed in NMR and not isolated for characterization. The structure of **3.6** was determined by NMR and comparison to the previously synthesized analogs.

Results and Discussion – [3+2] Nitrone Cycloaddition

A new [3+2] cycloaddition was introduced, utilizing the addition of a nitrone.[50] Due to the high temperature required for the reaction, **3.4** decomposes, not allowing for

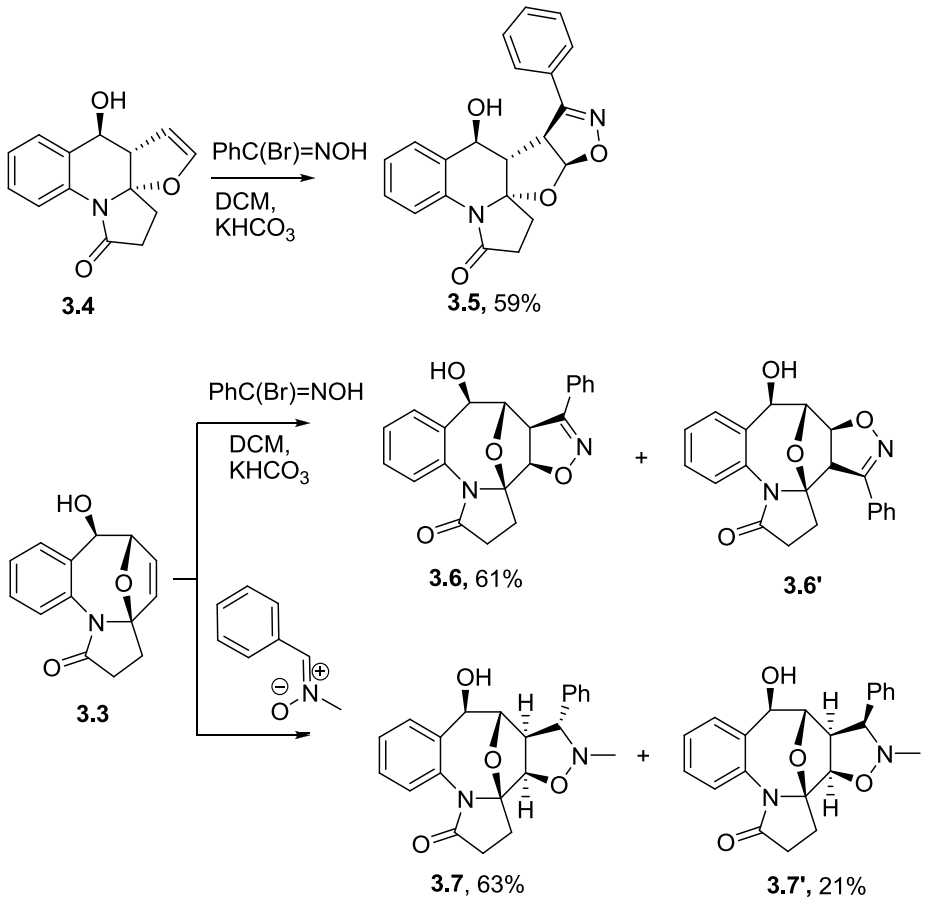

Scheme 3.2

any product isolation. However, upon addition to **3.3**, two regioisomers **3.7** and **3.7'** are formed in a 2:1 ratio, with **3.7** being the major isomer. The same argument can be made for this regiochemistry as was made for the nitrile oxide addition: steric strain favors the phenyl group being away from the methylene group in the linker. The addition also

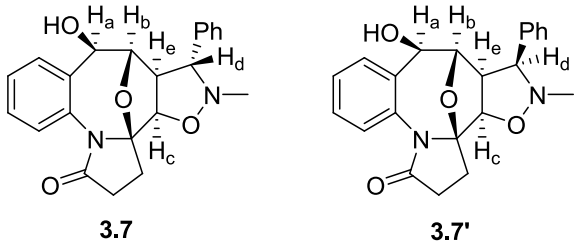

Figure 3.2

occurs on the *exo* face, similar to the nitrile oxide addition. The structure of major isomer

3.7 was unambiguously solved by X-ray crystallography. The structure of minor isomer **3.7'**, was assigned based on NOE experiments (**Figure 3.2**). The aliphatic regions of the ^{1}H NMR spectra of both stereoisomers **3.7** and **3.7'** possess two separate spin systems: H_a–H_b and H_c–H_d–H_e. The spin–spin coupling constant H_b–H_e is not observed experimentally. In both cases, H_e signal is a triplet at 2.73 (**3.7**) or 2.82 (**3.7'**) ppm. In **3.7**, upon irradiating the triplet H_e at 2.73 ppm, a NOE of 3% with H_a is observed, which is indicative of the regiochemistry shown, as well as a NOE of 13% on H_b and H_c. Of note, signals for protons H_b and H_c overlap, so their assignment was difficult; we assigned the H_a signal to the doublet in the lowest field. No signal from H_d is observed, which implies that protons H_d and H_e reside on the opposite faces of the isoxazoline ring. Similarly, in **3.7'**, upon irradiating the triplet H_e at 2.82 ppm, an observed NOE of 8% with protons H_a and H_b (signals overlap) again indicated that the phenyl group is located on the 'northern' side of the molecule, *syn* to the benzylic OH group and *anti* to the pyrrolidone moiety. Additionally, we see NOE on both H_c and H_d (13% and 11 %, respectively), suggesting that all three protons are *syn* to each other.

Results and Discussion – Chlorocarbene Addition

Throughout all of the post-photochemical modifications, it was clear that the standard [4+4] scaffold was recalcitrant towards several different conditions. Because of that the previously mentioned bicyclo [4.2.1] nonadiene→bicyclo [3.3.1] nonadiene rearrangement and oxidation (**Scheme 3.3**) was performed to yield the more reactive α,β unsaturated ketone (**3.9**).[36] The dichlorocarbene was generated *in sit*u from chloroform

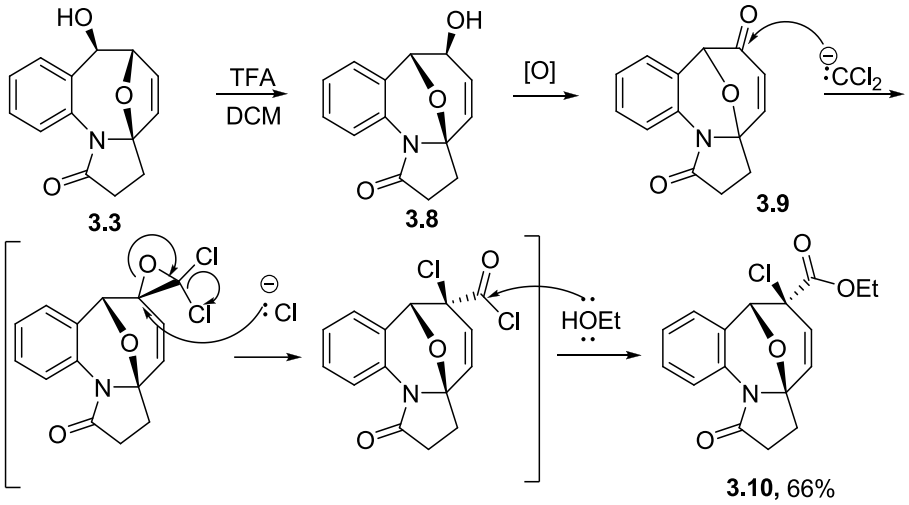

Scheme 3.3

and sodium hydroxide, but rather than the expected cyclopropanation, the carbene adds directly to the carbonyl yielding α-chloroester **3.10**, which is presumably formed as a result of Jocic–Reeve reaction.[51] We hypothesized that the carbene attacked from *exo*-side of the bicyclic benzoazacane ring, and the initially formed epoxide is ring-opened by the nucleophile (Cl^-) from the sterically accessible *exo*-side.

Results and Discussion – [4+2] hetero Diels-Alder and Povarov Cyclizations

Not surprisingly, the [4+4] scaffold was recalcitrant toward milder cycloaddition reactions such as [4+2] hetero Diels-Alder and Povarov cyclization. These reactions only proceeded on the [4+2] scaffold. The Povarov cyclization was conducted in 2,2,2-trifluoroethanol, as a solvent, at 40°C (**Scheme 3.4**).[52] As previously seen, the 2-azadiene attacks from the less hindered *exo*-face, yielding only product **3.11**, with the pyridine ring pointing down in the thermodynamically favored equatorial position. The structure of the product was supported by the NMR data (**Figure 3.3**). Among the aliphatic protons, H_c

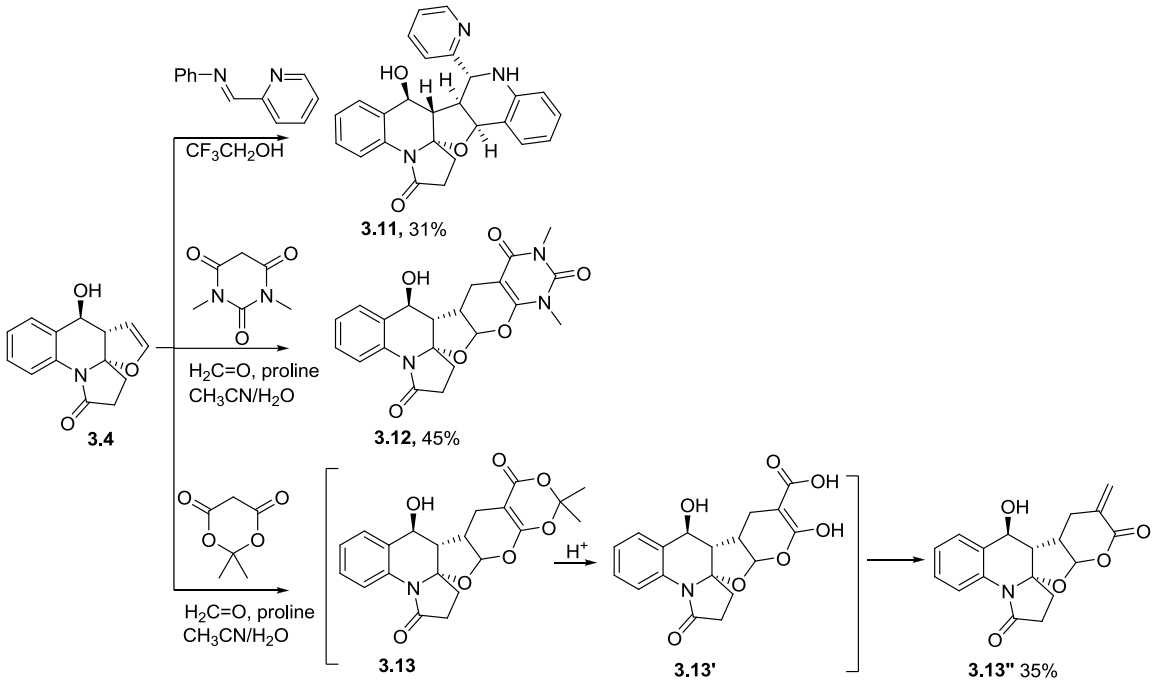

Scheme 3.4

has the highest chemical shift, observed at 5.25 ppm as a doublet, J = 7.7 Hz. H_b is characterized by a ddd at 2.54 ppm with the spin–spin coupling constants of 10.4 Hz (with H_a), 7.8 Hz (with H_c), and 2.9 Hz (with H_d). The value of the biggest constant corresponds to axial–axial interaction, which puts the pyridine ring in equatorial position.

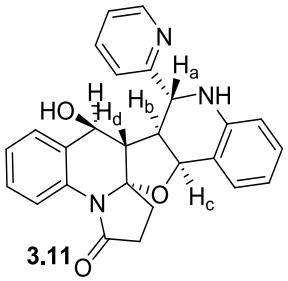

H_a-H_b = 10.4 Hz
H_b-H_c = 7.8 Hz
H_b-H_d = 2.6 Hz

Figure 3.3

Next, we tried several hetero-Diels–Alder reactions using oxabutadienes generated *in situ*

from 1,3-dicarbonyl compounds (Meldrum's acid and dimethylbarbituric acid). The reaction with both Meldrum's acid and 1,3-dimethylbarbituric acid proceeds smoothly. However, while the reaction of 1,3-dimethylbarbituric acid yields the expected *exo*-addition product **3.12**, the initially formed product from the reaction with Meldrum's acid reacts further, yielding the unexpected **3.13"**, whose structure was solved unambiguously by X-ray crystallography. We proposed that the initially formed **3.13** was unstable and underwent ketal hydrolysis giving intermediate **3.13'** (not isolated), followed by decarboxylation to give the isolated product **3.13"**.

To demonstrate the scope of the reaction, we also carried out the dimethylbarbituric acid hetero-Diels Alder reaction on the thiophene-based photoproduct (**3.14**).[54] The single isomer **3.15** (**Figure 3.4**) was formed as confirmed by ^{1}H NMR, and further supported by comparison of the experimental and predicted spin–spin coupling constants (SSCCs). For this, an in house density functional theory (DFT) relativistic force field method, developed by Kutateladze and Mukhina,[53] was used. The method is based on fast and accurate scaling of Fermi contacts.[53] Using this method, spin-spin coupling

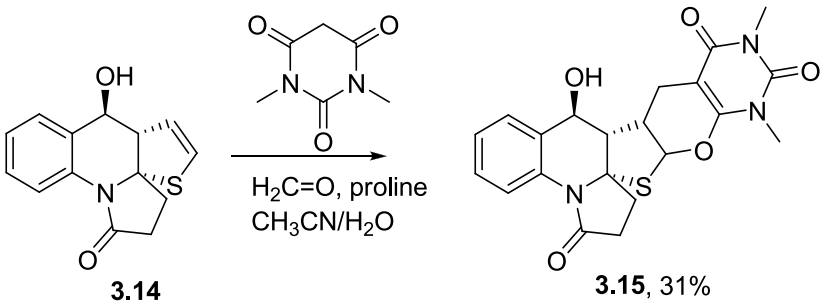

3.14 **3.15**, 31%

Figure 3.4

constants can be accurately predicted in under an hour for most conformationally rigid organic molecules.[53] As shown in **Figure 3.5**, the green experimental constants (top

number) match up exceptionally well with the pink predicted constants (bottom number) from this method, rendering support to our stereochemical assignments.

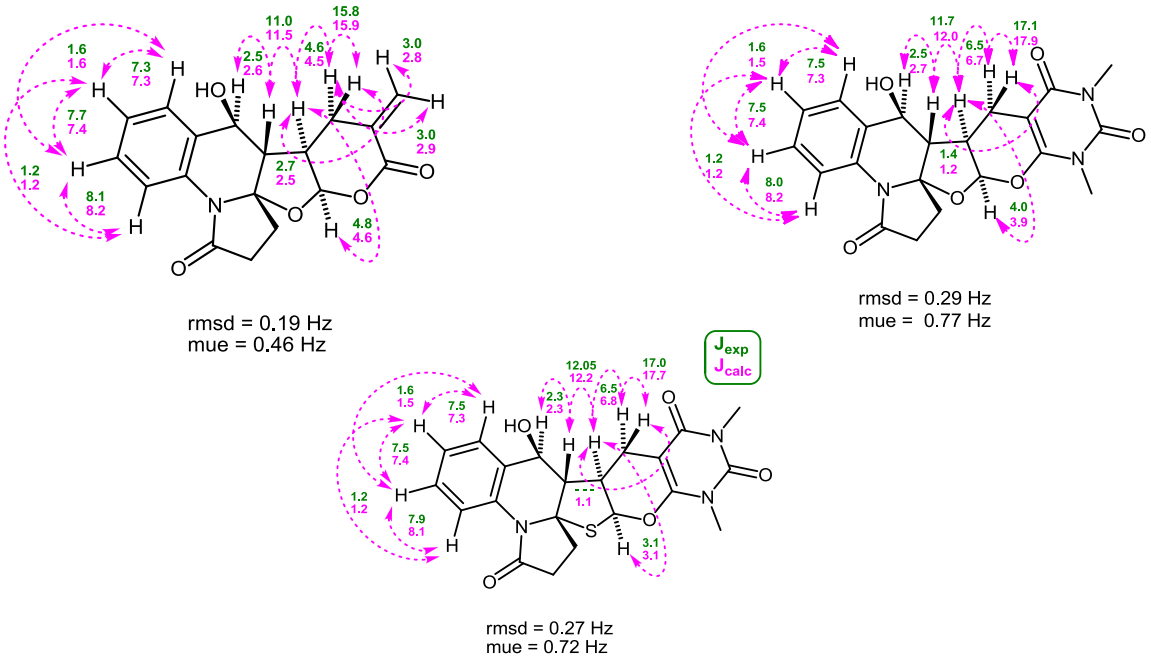

Figure 3.5

To continue to test the scope, we used the enantiopure phenylalanine derived pyrrole **3.16**, which was synthesized according to the previously published method.[54] The irradiation took place in DMSO, affording the pyrroline **3.17**, which is not isolated, but rather used directly in the hetero-Diels Alder reaction with dimethylbarbituric acid (**Scheme 3.5**). Rather than yielding the expected mono addition product **3.18**, the reaction continued further, producing the bis-spiro cycloadduct **3.19,** which was isolated after chromatography. This bis-spiro adduct was unexpected, and from our search, only one other such example exists in the literature.[55] We proposed that the initially formed mono adduct **3.18** exists in an equilibrium with its opened, zwitterionic form **3.18 +/-**, which is formed by the assistance of the lone-pairs on nitrogen and the added stability of the

formed iminium ion. The zwitterion **3.18 +/-** can then add to a second molecule of dimethylbarbituric acid, yielding the bis-spiro final product **3.19**.

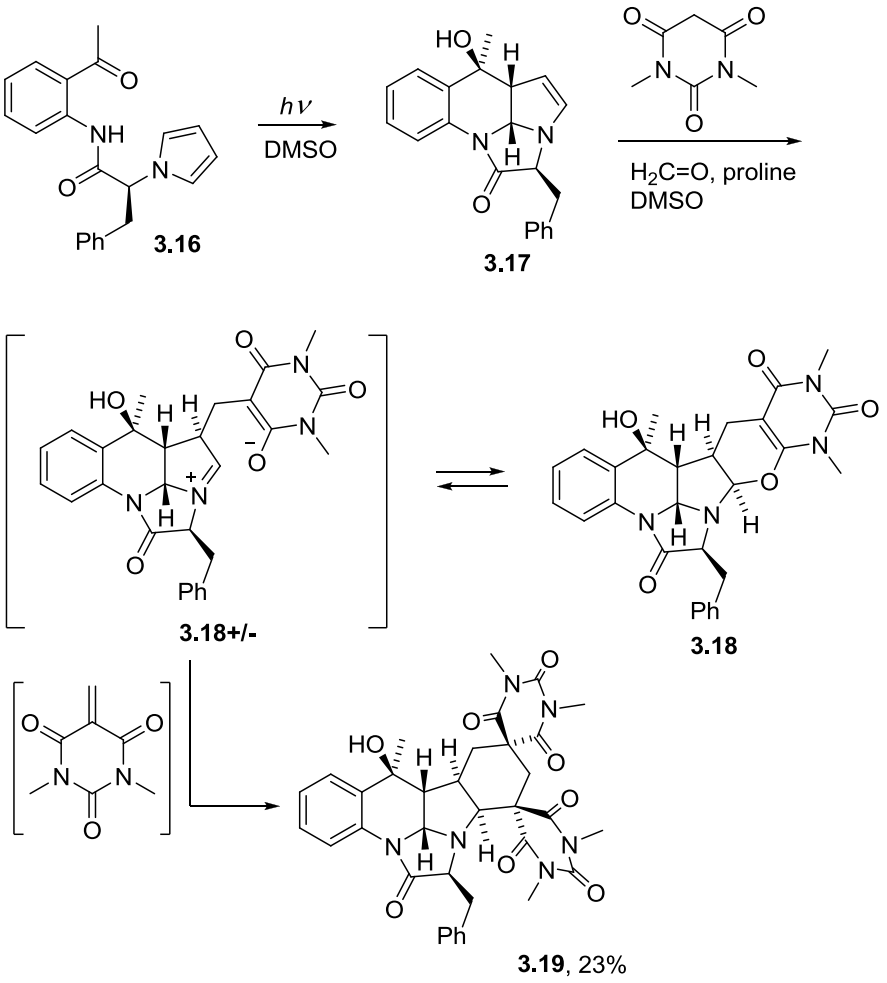

Scheme 3.5

The structure of **3.19** was supported by more advanced NMR experiments such as ^{13}C attached proton test (APT), heteronuclear multiple-bond correlation (HMBC), and heteronuclear multiple-quantum correlation (HMQC), as well as the previously mentioned RFF calculations. HMBC allows for the detection of long-range ^{13}C-^{1}H coupling constants that cannot be detected by other types of 2D experiments.

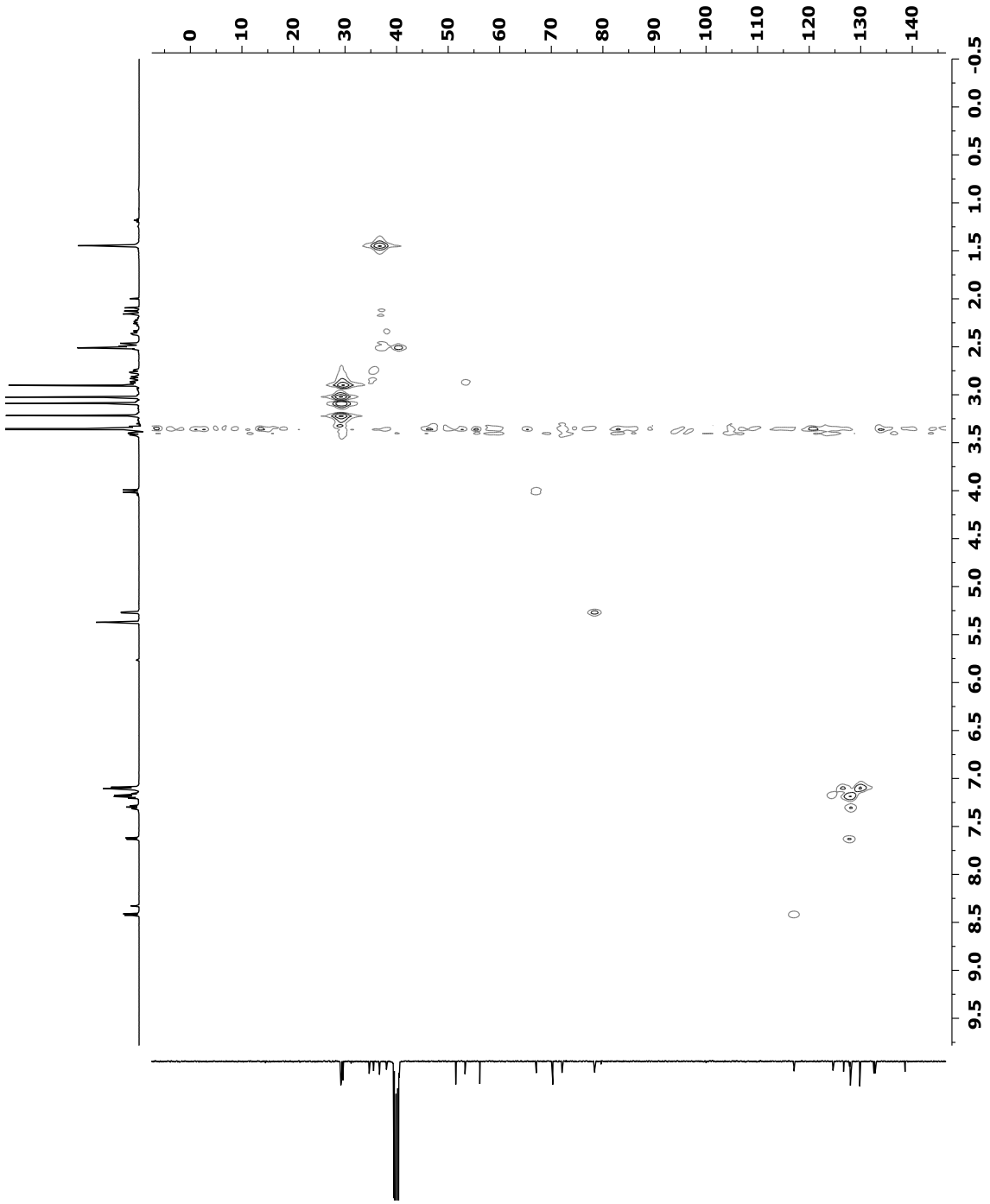

Figure 3.6 HMQC spectrum of 3.19

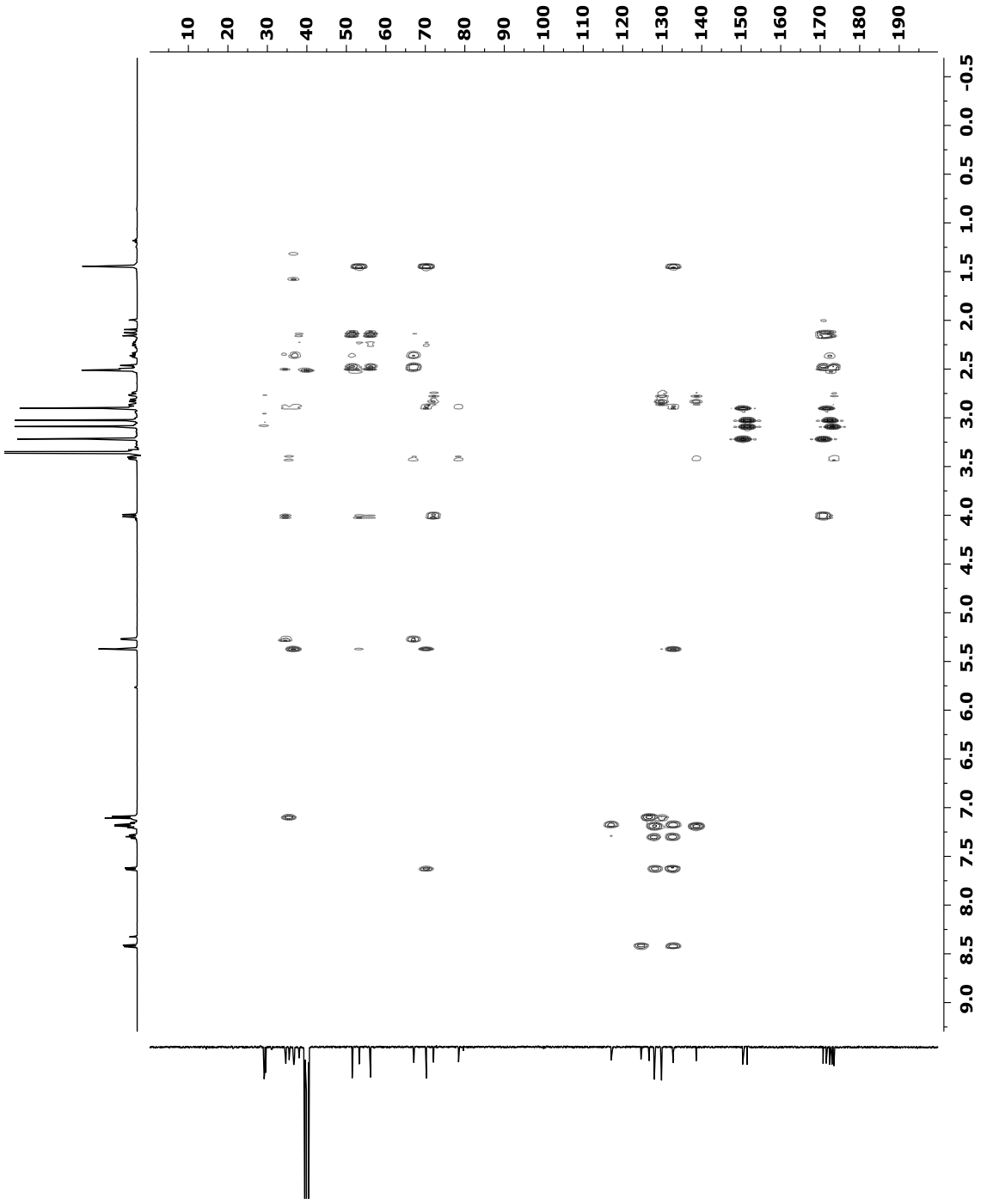

Figure 3.7 HMBC spectrum of 3.19

HMBC analysis for **3.19** revealed the pyrrolo-quinolinone skeleton, similar to **3.17**, remained unchanged in the final product (**Figure 3.7**). A characteristic feature of the spectrum are the two protons on C_d (**Figure 3.6**), which are represented by two doublets at 2.14 and 2.48 ppm with ^2J = 15.3 Hz. In the HMBC spectrum, these doublets exhibit cross-peaks with quaternary carbons C_c and C_e at 51.5 and 56.1 ppm. The peak at 56.1 ppm is attributed to carbon C_e judging by the cross-peaks with C_f–H and C_a–H. The peak at 51.5 ppm, which has a cross-peak with C_b–H, is attributed to carbon C_c. HMQC, which

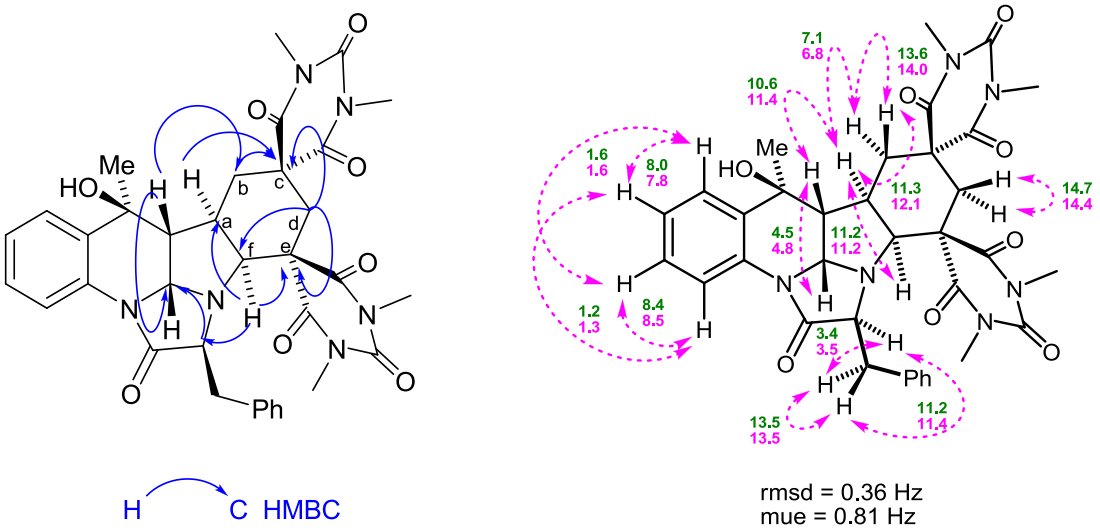

Figure 3.8

is also a 2D NMR technique, was then run to confirm this structure. Unlike HMBC, this technique only shows a correlation for protons and carbons that are directly attached to each other. The spectrum for this compound showed the proposed structure was in fact what was isolated (**Figure 3.6**). The structure was independently confirmed by calculation and comparison of spin–spin coupling constants. The calculated constants shown in green (top), agreed excellently with the experimentally obtained constants in pink (bottom) (**Figure 3.8**).

With these new compounds in hand, it is important to reflect back on the purpose of this chemistry: to synthesize new potential drug candidates that reflect good fit to the desired descriptors used by FBDD researchers. Several of the compounds synthesized in this work are included in **Figure 3.9**. As is demonstrated, these new compounds have very good fsp^3 values, even as high as 0.50 for the barbituric acid derivative **3.12**. The number of rotatable bonds is less than or equal to 5, as criterion of Lipinski's rule of 5, and all except for **3.19** have molecular weights less than 500 Da. And all excluding **3.19** fit or are close to Astex's Rule of 3 for fragments. So, whether using our azaxylylenes as drug candidates or as fragments, these new compounds show a range of diversity sought after by DOS and FBDD researchers.

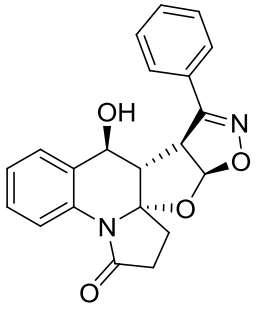

3.5
fsp^3 = 0.33
MW = 362.28
RBs = 0

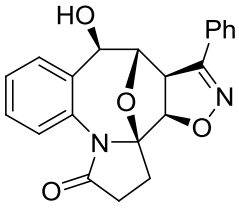

3.6
fsp^3 = 0.41
MW = 362.28
RBs = 0

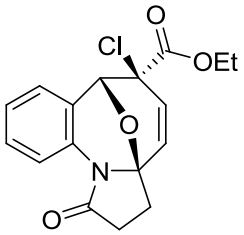

3.10
fsp^3 = 0.41
MW = 333.76
RBs = 2

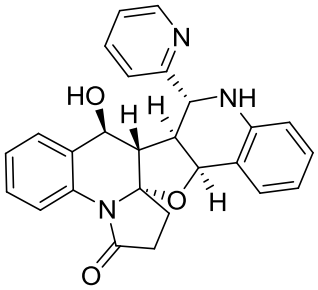

3.11
fsp^3 = 0.31
MW = 425.48
RBs = 0

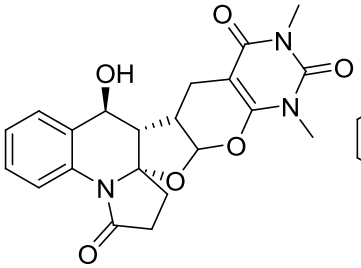

3.12
fsp^3 = 0.50
MW = 411.41
RBs = 2

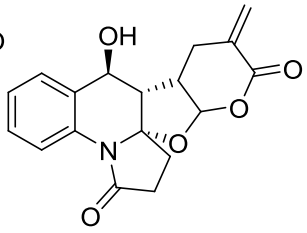

3.13"
fsp^3 = 0.44
MW = 327.33
RBs = 2

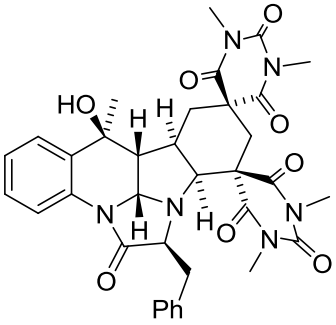

3.19
fsp^3 = 0.39
MW = 668.70
RBs = 5

Figure 3.9

Additionally, we tried to assess the diversity of the library generated using a table of Tanimoto coefficients. We supplemented this library with some previous examples from our group (**Figure 3.1**). The results show that the small library is quite diverse (**Figure 3.10**). Along the diagonal of the table the compounds are compared to each other, hence the coefficient of 1. But the off diagonals show coefficients less than 0.70, and in most cases less than 0.50, which is considered statistically non-similar.

So, to summarize, this chapter contains an elaboration of previous post-photochemical modifications, which were intended to add diversity to the azaxylylene scaffolds previously synthesized by the Kutateladze group. The rapid growth in complexity is representative of a DOS approach to drug discovery, and statistical analysis shows a much greater area of chemical space could be probed when testing for biological activity.

	A	B	C	D	E	F	G	H	3.5	3.6	3.7	3.10	3.11	3.12	3.13”	3.15	3.19
A	1	0.37	0.44	0.47	0.27	0.33	0.43	0.38	0.44	0.56	0.6	0.42	0.48	0.43	0.52	0.33	0.42
B	0.37	1	0.41	0.32	0.24	0.34	0.46	0.27	0.34	0.36	0.38	0.63	0.4	0.31	0.37	0.26	0.26
C	0.11	0.41	1	0.31	0.22	0.27	0.33	0.32	0.44	0.42	0.46	0.52	0.55	0.39	0.52	0.28	0.37
D	0.47	0.32	0.31	1	0.33	0.43	0.3	0.46	0.4	0.36	0.4	0.35	0.5	0.4	0.45	0.36	0.4
E	0.27	0.24	0.22	0.33	1	0.37	0.22	0.34	0.29	0.25	0.25	0.21	0.33	0.31	0.3	0.28	0.33
F	0.33	0.34	0.27	0.43	0.37	1	0.4	0.34	0.35	0.34	0.36	0.29	0.37	0.34	0.38	0.32	0.35
G	0.43	0.46	0.33	0.3	0.22	0.4	1	0.25	0.32	0.42	0.46	0.45	0.34	0.32	0.39	0.25	0.26
H	0.38	0.27	0.32	0.46	0.34	0.34	0.25	1	0.39	0.33	0.34	0.3	0.52	0.37	0.44	0.36	0.67
3.5	0.44	0.34	0.44	0.4	0.29	0.35	0.32	0.39	1	0.7	0.5	0.42	0.58	0.52	0.65	0.37	0.42
3.6	0.56	0.36	0.42	0.36	0.25	0.34	0.42	0.33	0.7	1	0.7	0.42	0.47	0.42	0.5	0.32	0.33
3.7	0.6	0.38	0.46	0.4	0.25	0.36	0.46	0.34	0.5	0.7	1	0.44	0.54	0.45	0.53	0.35	0.35
3.10	0.42	0.63	0.52	0.35	0.21	0.29	0.45	0.3	0.42	0.42	0.44	1	0.48	0.37	0.49	0.28	0.31
3.11	0.48	0.4	0.55	0.5	0.33	0.37	0.34	0.52	0.58	0.47	0.54	0.48	1	0.53	0.65	0.38	0.46
3.12	0.43	0.31	0.39	0.4	0.31	0.34	0.32	0.37	0.52	0.42	0.45	0.37	0.53	1	0.57	0.62	0.38
3.13”	0.52	0.37	0.52	0.45	0.3	0.38	0.39	0.44	0.65	0.5	0.53	0.49	0.65	0.57	1	0.38	0.49
3.15	0.33	0.26	0.28	0.36	0.28	0.32	0.25	0.36	0.37	0.32	0.35	0.28	0.38	0.62	0.38	1	0.38
3.19	0.42	0.26	0.37	0.4	0.33	0.35	0.26	0.67	0.42	0.33	0.35	0.31	0.46	0.38	0.49	0.38	1

Figure 3.10

Experimental

Common solvents were purchased from Pharmco and used as is, except for THF, which was refluxed over and distilled from sodium benzophenone ketyl prior to use. Common reagents were purchased from Aldrich and used without additional purification, unless indicated otherwise. NMR spectra were recorded at 25°C on a Bruker Avance III 500 MHz in $CDCl_3$ (unless noted otherwise). X-Ray structures were obtained with a Bruker APEX II instrument. High resolution mass spectra were obtained on the *MDS SCIEX/Applied Biosystems API QSTARTM Pulsar i Hybrid LC/MS/MS System* mass spectrometer from the University of Colorado at Boulder. Flash column chromatography was performed using Teledyne Ultra Pure Silica Gel (230 – 400 mesh) on a Teledyne Isco Combiflash R_f using Hexanes/EtOAc as an eluent.

Synthesis of Photoprecursors and Photoproducts

Compounds **3.3, 3.4** and **13** were synthesized as previously described by our group[14]. **N-hydroxy-benzenecarboximidoyl bromide,**[39] **(1E)-N-phenyl-1-pyridin-2-ylmethanimine,**[52] **N-oxide-N-(phenylmethylene)-methanamine**[50] were prepared according to the existing procedures.

Postphotochemical Modifications

Addition of nitrile oxide, general procedure I: 1 eq of photoproduct was dissolved in EtOAc. To this was added 3 eq of N-hydroxy-benzenecarboximidoyl bromide and 6 eq of $KHCO_3$. An additional 3 eq of N-hydroxy-benzenecarboximidoyl bromide and 6 eq of $KHCO_3$ were added after stirring for 12 h. The reaction was monitored by NMR until the starting photoproduct was consumed. The resulting mixture was diluted with water, extracted with 3x20 ml of EtOAc, washed with brine, dried over Na_2SO_4, and concentrated *in vacuo*. The mixture was then purified by flash chromatography.

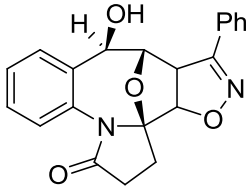

12-hydroxy-15-phenyl-17,19-dioxa-5,16-diazapentacyclo[11.5.1.$0^{1,5}$.$0^{6,11}$.$0^{14,18}$]nonadeca-6,8,10,15-tetraen-4-one (3.6): General procedure **I** was followed. From 0.25 g of **3.3** (1.0 mmol), 1.2 g of **N-hydroxy-benzenecarboximidoyl bromide** (6.2 mmol), and 1.2 g of $KHCO_3$ (12.3 mmol), 0.15 g (61%) of the title compound was obtained. ^{1}H NMR (500 MHz, $CDCl_3$) δ 7.65 (m, 2H), 7.57 (dd, *J* = 8.4, 1.3 Hz, 1H), 7.48 (m, 5H), 7.35 (m, 1H), 4.86 (d, *J* = 8.8 Hz, 1H), 4.78 (m, 2H), 3.87 (dd, *J* = 8.8, 1.0 Hz, 1H), 2.88 (m, 2H), 2.77 (dt, *J* = 14.1, 9.9 Hz, 1H), 2.66 (ddd, *J* = 16.7, 9.5, 0.9 Hz, 1H), 2.46 (ddd, *J* = 14.1, 8.8, 1.0 Hz, 1H). ^{13}C NMR (126 MHz, $CDCl_3$) δ 173.8, 156.3, 133.4, 133.1, 132.6, 130.7, 129.9, 129.2, 128.5, 127.6, 127.5, 126.7, 104.9, 88.1, 82.2, 77.6, 56.3, 29.4, 27.2. HRMS (ESI) calcd for $C_{21}H_{18}N_2O_4Li^+$ $(MLi)^+$ 369.1427 found 369.1405

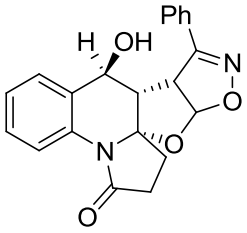

12-hydroxy-15-phenyl-17,19-dioxa-5,16-diazapentacyclo[11.6.0.0^{1,5}.0^{6,11}.0^{14,18}]nonadeca-6(11),7,9,15-tetraen-4-one (3.5): General procedure **I** was followed. From 0.25 g of **3.4** (1.0 mmol), 1.2 g of **N-hydroxy-benzenecarboximidoyl bromide** (6.1 mmol) and 1.2 g of $KHCO_3$ (12.4 mmol), 0.14 g (59%) of the title compound was obtained. ^{1}H NMR (500 MHz, $CDCl_3$) δ 7.98 (d, J = 8.0 Hz, 1H), 7.73 (m, 2H), 7.54 (m, 3H), 7.49 (td, *J* = 7.9, 1.5 Hz, 1H), 7.46 (dd, *J* = 7.5, 1.3 Hz, 1H), 7.27 (td, *J* = 7.5, 1.2 Hz, 1H), 5.81 (d, *J* = 6.2 Hz, 1H), 4.97 (d, *J* = 3.0 Hz, 1H), 3.84 (dd, *J* = 6.2, 3.3 Hz, 1H), 3.29 (t, *J* = 3.1 Hz, 1H), 2.84 (m, 1H), 2.40 (m, 3H).^{13}C NMR (126 MHz, $CDCl_3$) δ 173.3, 158.7, 134.5, 130.8, 130.0, 129.8, 129.2, 128.7, 127.7, 127.1, 125.5, 122.9, 107.0, 101.4, 70.7, 57.1, 55.1, 34.1, 30.1. HRMS (ESI) calcd for $C_{21}H_{18}N_2O_4Li^+$ $(MLi)^+$ 369.1427 found 369.1407

Nitrone Cycloadditions: 1 eq of photoproduct was dissolved in 1 ml of anhyd. toluene along with 4 eq of **N-oxide-N-(phenylmethylene)-methanamine**. The reaction was sealed in a high pressure reaction vessel and heated to completion as shown by ^{1}H NMR. The toluene was removed *in vacuo* and the residue purified by flash chromatography.

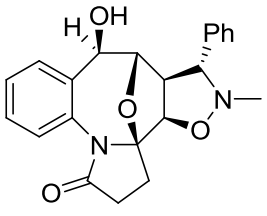

anti-12-hydroxy-16-methyl-15-phenyl-17,19-dioxa-5,16-diazapentacyclo [11.5.1.0^{1,5}.0^{6,11}.0^{14,18}]nonadeca-6,8,10-trien-4-one (3.7): From 100 mg of **3.3** (0.41 mmol) and 0.22 g of **N-oxide-N-(phenylmethylene)-methanamine** (1.6 mmol), 98.0 mg

(63%) of title compound was isolated. ^{1}H NMR (500 MHz, $CDCl_3$) δ 7.50 (d, J = 8.0 Hz, 1H), 7.39 (m, 4H), 7.32 (m, 2H), 7.24 (m, 2H), 4.59 (d, *J* = 4.4 Hz, 1H), 4.38 (m, 2H), 3.32 (d, *J* = 8.6 Hz, 1H), 2.87 (m, 1H), 2.74 (t, *J* = 7.5 Hz, 1H), 2.58 (m, 2H), 2.43 (m, 1H), 2.20 (s, 3H). ^{13}C NMR (126 MHz, $CDCl_3$) δ 173.9, 134.0, 133.6, 132.5, 129.5, 129.1, 128.7, 128.2, 127.8, 127.8, 127.1, 102.6, 84.2, 81.4, 79.5, 77.4, 61.2, 29.6, 27.1. HRMS (ESI) calcd for $C_{22}H_{22}N_2O_4Li^+$ $(MLi)^+$ 385.1740 found 385.1724

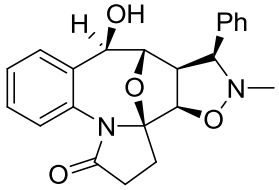

syn-12-hydroxy-16-methyl-15-phenyl-17,19-dioxa-5,16-diazapentacyclo [11.5.1.0^{1,5}.0^{6,11}.0^{14,18}]nonadeca-6,8,10-trien-4-one (3.7'): General procedure **IV** was followed. From 0.10 g of **3.3** (0.41 mmol) and 0.22 g of **N-oxide-N-(phenylmethylene)-methanamine** (1.6 mmol), 33.0 mg (21%) of title compound was isolated. ^{1}H NMR (500 MHz, $CDCl_3$) δ 7.55 (dd, *J* = 8.0, 0.9 Hz, 1H), 7.39 (m, 6H), 7.25 (m, 2H), 4.33 (d, *J* = 7.0 Hz, 1H), 4.19 (m, 2H), 3.61 (d, *J* = 7.7 Hz, 1H), 2.92 (m, 1H), 2.81 (t, *J* = 7.4 Hz, 1H), 2.68 (m, 1H), 2.58 (s, 3H), 2.54 (m, 1H). ^{13}C NMR (126 MHz, $CDCl_3$) δ 173.9, 135.8, 133.9, 133.8, 132.5, 129.4, 128.9, 128.3, 128.2, 128.0, 126.8, 103.6, 83.9, 78.7, 77.7, 75.4, 55.9, 43.6, 29.9, 26.7. HRMS (ESI) calcd for $C_{22}H_{22}N_2O_4Li^+$ $(MLi)^+$ 385.1740 found 385.1724

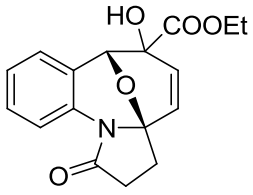

Ethyl 13-chloro-4-oxo-16-oxa-5-azatetracyclo[10.3.1.0^{1,5}.0^{6,11}] hexadeca-6,8,10,14-tetraene-13-carboxylate (3.10): 0.14 g of **3.9** (0.58 mmol) was dissolved in 50 ml of chloroform. To this was added 30 mg of tetrabutylammonium hydrogen sulfate (0.084 mmol) and 10 ml of a 50%

w/w solution of NaOH. The mixture was vigorously stirred at ambient temperature for 20 h, then poured into 200 ml of water and extracted with $CHCl_3$. The organic layer was separated, dried over anh. Na_2SO_4, and concentrated *in vacuo*. The mixture was purified by flash chromatography to yield 0.12 g (66%) of the title compound. ^{1}H NMR (500 MHz, $CDCl_3$) δ 8.42 (dd, *J* = 8.3, 1.0 Hz, 1H), 7.38 (ddd, *J* = 8.7, 7.5, 1.6 Hz, 1H), 7.19 (dd, *J* = 8.0, 1.4 Hz, 1H), 7.09 (td, *J* = 7.7, 1.3 Hz, 1H), 6.38 (dd, *J* = 9.9, 1.2 Hz, 1H), 5.83 (d, *J* = 9.9 Hz, 1H), 5.47 (s, 1H), 4.27 (m, 2H), 2.74 (m, 2H), 2.42 (m, 2H), 1.30 (t, *J* = 7.2 Hz, 3H). ^{13}C NMR (126 MHz, $CDCl_3$) δ 170.8, 167.3, 133.1, 129.7, 126.9, 126.8, 126.4, 123.8, 120.4, 119.9, 85.9, 77.3, 64.2, 62.9, 30.3, 29.9, 13.8. HRMS (ESI) calcd for $C_{17}H_{16}NO_4ClLi^+$ $(MLi)^+$ 340.0928 found 340.0920

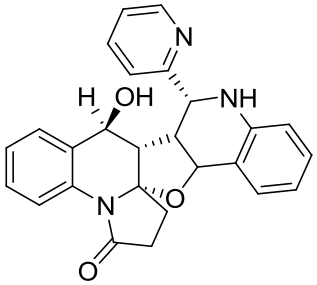

14-hydroxy-11-(pyridin-2-yl)-2-oxa-10,21-diazahexacyclo[11.11.0.0^{1,21}.0^{3,12}.0^{4,9}.0^{15,20}] tetracosa-4(9),5,7,15,17,19-hexaen-22-one (3.11): 0.22 g of **(1E)-N-phenyl-1-pyridin-2-ylmethanimine** (1.2 mmol) and 0.15 g of **3.4** (0.61 mmol) were dissolved in 1.5 ml of 2,2,2-trifluoroethanol and warmed to 40ºC until the reaction was complete as observed by ^{1}H NMR. The resulting mixture was concentrated *in vacuo* and purified by flash chromatography, yielding 80 mg (31%) of the title compound. ^{1}H NMR (500 MHz, $CDCl_3$) δ 8.74 (ddd, *J* = 4.9, 1.8, 0.9 Hz, 1H), 7.88 (td, *J* = 7.7, 1.8 Hz, 1H), 7.85 (d, *J* = 8.1 Hz, 1H), 7.57 (d, *J* = 7.9 Hz, 1H), 7.39 (m, 3H), 7.17 (td, *J* = 7.6, 1.0 Hz, 3H), 7.11 (td, *J* = 7.5, 1.1 Hz, 2H), 6.85 (td, *J* = 7.5, 1.2 Hz, 1H), 6.77 (dd, *J* = 7.4, 1.1 Hz, 2H), 5.25 (d, *J* = 7.7 Hz, 1H), 4.82 (d, *J* = 1.4 Hz, 1H),

4.65 (s, 1H), 3.38 (dd, *J* = 10.4, 2.5 Hz, 1H), 3.10 (d, *J* = 2.5 Hz, 1H), 2.69 (ddd, *J* = 16.3, 10.9, 8.2 Hz, 1H), 2.54 (ddd, *J* = 10.4, 7.9, 2.5 Hz, 1H), 2.18 (dd, *J* = 16.6, 8.6 Hz, 1H), 2.06 (ddd, *J* = 12.4, 10.9, 8.8 Hz, 1H), 1.68 (dd, *J* = 12.6, 8.0 Hz, 1H). ^{13}C NMR (126 MHz, $CDCl_3$) δ 173.7, 159.2, 149.5, 143.4, 137.1, 134.0, 130.6, 130.0, 129.9, 128.9, 128.6, 125.5, 123.8, 123.1, 121.6, 120.8, 119.3, 115.6, 100.2, 77.2, 74.7, 70.2, 56.6, 50.5, 45.9, 36.0, 29.9. HRMS (ESI) calcd for $C_{26}H_{23}N_3O_3Li^+$ $(MLi)^+$ 432.1900 found 432.1889

General Procedure II for oxa-Diels-Alder Reactions: 1 eq of photoproduct and 1 eq of 1,3-dicarbonyl compound were dissolved in 0.7 ml of dry acetonitrile. To this was added 0.08 eq of L-proline and 1.3 eq of 37% aq. formaldehyde solution. The reaction stirred at ambient temperature until full consumption of the photoproduct, as determined by ^{1}H NMR. The reaction was diluted with water and extracted with EtOAc. The organic layer was separated, dried over Na_2SO_4, and concentrated *in vacuo*. The mixture was then purified by flash chromatography.

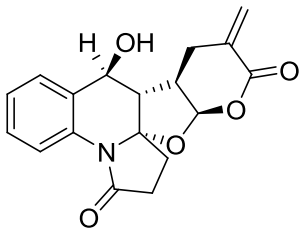

12-hydroxy-16-methylidene-18,20-dioxa-5-azapentacyclo[11.7.0.0^{1,5}.0^{6,11}.0^{14,19}]icosa-6,8,10-triene-4,17-dione (3.13"): General procedure **II** was followed. From 0.10 g of **3.4** (0.41 mmol), 0.06 g of Meldrum's acid (0.41 mmol), 3.8 mg of L-proline (0.033 mmol), and 0.04 ml of 37% w/w formaldehyde solution in water (0.53 mmol), was obtained 52 mg (35%) of the title compound. ^{1}H NMR (500 MHz, $CDCl_3$) δ 7.82 (d, *J* = 8.0 Hz, 1H), 7.42 (td, *J* = 7.7, 1.5 Hz, 1H), 7.33 (d, *J* = 7.3 Hz, 1H),

7.21 (td, *J* = 7.7, 1.2 Hz, 1H), 6.59 (s, 1H), 5.77 (s, 1H), 5.66 (d, *J* = 4.8 Hz, 1H), 4.64 (d, *J* = 2.4 Hz, 1H), 2.89 (dd, *J* = 11.0, 2.5 Hz, 1H), 2.75 (m, 3H), 2.47 (dd, *J* = 12.6, 8.4 Hz, 1H), 2.35 (tdd, *J* = 12.7, 9.8, 1.7 Hz, 1H), 2.23 (dt, *J* = 16.4, 8.1 Hz, 1H), 2.16 (dtd, *J* = 11.3, 4.7, 2.6 Hz, 1H). ^{13}C NMR (126 MHz, $CDCl_3$) δ 173.7, 173.7, 163.5, 133.4, 130.9, 130.0, 130.0, 129.8, 129.3, 125.9, 123.8, 102.9, 102.0, 68.8, 51.7, 40.4, 35.8, 29.6, 27.3. HRMS (ESI) calcd for $C_{18}H_{17}NO_5Li^+$ $(MLi)^+$ 334.1267 found 334.1253

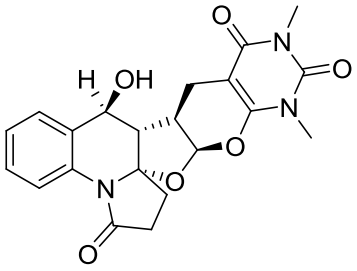

14-hydroxy-6,8-dimethyl-2,4-dioxa-6,8,21-triazahexacyclo[11.11.0.0^{1,21}.0^{3,12}.0^{5,10}.0^{15,20}]tetracosa-5(10),15,17,19-tetraene-7,9,22-trione (3.12): General procedure **II** was followed. From 100 mg of **3.4** (0.41 mmol), 0.064 g of 1,3-dimethylbarbituric acid (0.41 mmol), 3.8 mg of L-proline (0.033 mmol), and 0.04 ml of 37% w/w formaldehyde solution in water (0.53 mmol), was obtained 76 mg (45%) of the title compound. ^{1}H NMR (500 MHz, $CDCl_3$) δ 7.89 (d, *J* = 8.0 Hz, 1H), 7.48 (td, *J* = 7.8, 1.6 Hz, 1H), 7.36 (dd, J = 7.5, 1.5 Hz, 1H), 7.26 (td, *J* = 7.4, 1.2 Hz, 1H), 5.57 (d, *J* = 4.0 Hz, 1H), 4.79 (d, *J* = 2.6 Hz, 1H), 3.42 (s, 3H), 3.39 (s, 3H), 2.90 (m, 1H), 2.85 (dd, *J* = 11.6, 2.6 Hz, 1H), 2.77 (d, *J* = 17.1 Hz, 1H), 2.56 (dd, *J* = 17.1, 6.5, 1H), 2.42 (m, 4H), 2.16 (dddd, *J* = 11.6, 6.5, 4.0, 1.4 Hz, 1H). ^{13}C NMR (126 MHz, $CDCl_3$) δ 173.4, 163.0, 154.0, 151.0, 133.2, 130.3, 129.8, 129.1, 126.1, 124.0, 102.1, 100.0, 82.5, 69.2, 51.6, 39.6, 36.5, 29.6, 28.7, 28.1, 18.1. HRMS (ESI) calcd for $C_{21}H_{21}N_3O_6Li^+$ $(MLi)^+$ 418.1591 found 418.1571

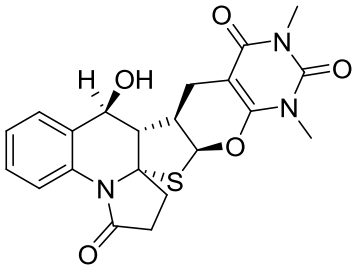

14-hydroxy-6,8-dimethyl-4-oxa-2-thia-6,8,21-triazahexacyclo[11.11.0.0^{1,21}.0^{3,12}.0^{5,10}.0^{15,20}]tetracosa-5(10),15,17,19-tetraene-7,9,22-trione (3.15): General procedure **II** was followed with DMSO as a solvent. From 70.0 mg of **3.14** (0.27 mmol), 0.13 g of 1,3-dimethylbarbituric acid (0.81 mmol), 7.5 mg of L-proline (0.065 mmol, and 0.08 ml of 37% formaldehyde in water (1.1 mmol), was obtained 36 mg (31%) of the title compound. ^{1}H NMR (500 MHz, $CDCl_3$) δ 7.78 (d, *J* = 7.9 Hz, 1H), 7.49 (td, *J* = 7.7, 1.2 Hz, 1H), 7.35 (dd, *J* = 7.5, 1.5 Hz, 1H), 7.27 (dd, *J* = 7.5, 1.0 Hz, 1H), 5.55 (d, *J* = 3.1 Hz, 1H), 4.84 (d, J = 3.1 Hz, 1H), 3.40 (s, 3H), 3.38 (s, 3H), 2.86 (dd, *J* = 12.1, 2.3 Hz, 1H), 2.78 (dd, *J* = 17.0, 0.8 Hz, 1H), 2.65 (m, 2H), 2.60 (dd, *J* = 17.0, 6.5 Hz, 1H), 2.50 (m, 2H), 2.39 (dddd, *J* = 12.05, 6.5, 3.2, 0.8 Hz, 1H), 2.30 (s, 1H). ^{13}C NMR (126 MHz, $CDCl_3$) δ 171.8, 163.1, 154.5, 150.9, 133.5, 130.9, 130.4, 128.9, 126.4, 124.4, 88.8, 85.0, 82.9, 70.4, 56.2, 45.4, 42.4, 30.7, 28.7, 28.1, 20.3. HRMS (ESI) calcd for $C_{21}H_{21}N_3O_5SLi^+$ $(MLi)^+$ 434.1362 found 434.1353

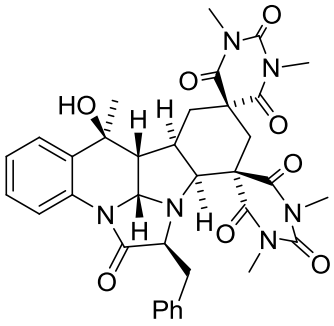

14-benzyl-5-hydroxy-5,21,23,28,30-pentamethyl-17,19-dioxa-12,15,21,23,28,30-hexaazaoctacyclo[16.8.4.1^{4,12}.0^{1,18}.0^{3,16}.0^{6,11}.0^{20,25}.0^{15,31}]hentriaconta-6,8,10,20(25)-tetraene-13,22,24,27,29-pentone (3.19): 0.10 g of **(*S*)-N-(2-acetylphenyl)-3-phenyl-2-(1H-pyrrol-1-yl)propanamide (3.16)** (0.3 mmol) was dissolved in 1.5 ml of DMSO. This was degassed and irradiated in Pyrex reaction vessel in LED-365 until the reaction

was complete, as determined by ^{1}H NMR. The solution was then added directly to 0.05 g of 1,3-dimethylbarbituric acid (0.3 mmol). To this was added 3.0 mg of L-proline (0.024 mmol), and 0.03 ml of 37% w/w formaldehyde solution in water (0.39 mmol). The reaction was heated to 70^{o}C until full consumption of the photoproduct, as determined by ^{1}H NMR. The reaction was diluted with water and extracted with EtOAc. The organic layer was separated, dried over Na_2SO_4, and concentrated *in vacuo*. The mixture was then purified by flash chromatography, yielding 46 mg (23%) of the title compound. ^{1}H NMR (500 MHz, $CDCl_3$) δ 8.63 (dd, *J* = 8.3, 1.2 Hz, 1H), 7.58 (dd, *J* = 7.8, 1.5 Hz, 1H), 7.37 (ddd, *J* = 8.5, 7.3, 1.6 Hz, 1H), 7.19 (m, 6H), 5.04 (d, *J* = 4.5 Hz, 1H), 4.34 (d, *J* = 11.1 Hz, 1H), 3.76 (dd, *J* = 11.2, 3.4 Hz, 1H), 3.40 (s, 3H), 3.27 (s, 3H), 3.22 (s, 3H), 3.17 (dd, *J* = 10.6, 4.5 Hz, 1H), 2.99 (s, 3H), 2.96 (dd, *J* = 13.6, 3.4 Hz, 1H), 2.78 (dd, *J* = 13.5, 11.3 Hz, 1H), 2.75 (dd, *J* = 13.5, 11.3 Hz, 1H), 2.53 (qd, *J* = 11.2, 7.2 Hz, 1H), 2.52, (d, *J* = 14.8 Hz, 1H), 2.45 (dd, *J* = 13.6, 7.1 Hz, 1H), 2.32 (d, *J* = 14.8 Hz, 1H), 2.04 (s, 1H), 1.65 (s, 3H). ^{13}C NMR (126 MHz, $CDCl_3$) δ 173.6, 172.1, 171.3, 170.7, 170.6, 150.7, 150.3, 138.2, 132.4, 130.4, 129.7, 128.8, 127.8, 126.6, 126.1, 124.7, 117.9, 78.3, 71.9, 71.5, 66.7, 56.0, 53.3, 51.4, 39.1, 37.1, 36.5, 36.0, 34.6, 29.4, 29.4, 29.3, 29.1. HRMS (ESI) calcd for $C_{35}H_{36}N_6O_8Li^+$ $(MLi)^+$ 675.2755 found 675.2742

X-Ray Structures

X-Ray structures were obtained with a Bruker APEX II instrument and the structure was refined using XShell software. The goodness of fit "S" is listed after each entry. Structures have been deposited with the CCDC.

1. **anti-12-hydroxy-16-methyl-15-phenyl-17,19-dioxa-5,16-diazapentacyclo [11.5.1.$0^{1,5}$.$0^{6,11}$.$0^{14,18}$]nonadeca-6,8,10-trien-4-one (3.7)** S = 1.049

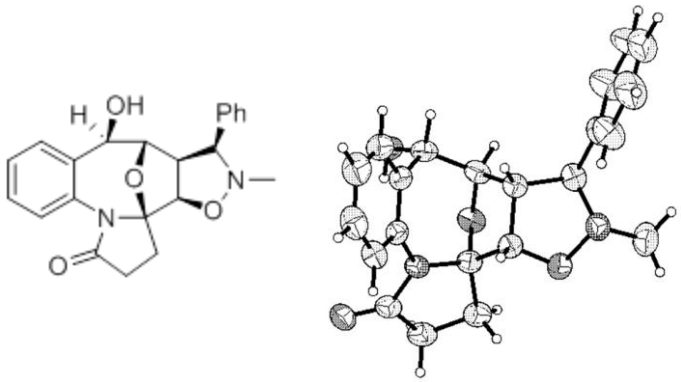

2. **12-hydroxy-16-methylidene-18,20-dioxa-5-azapentacyclo[11.7.0.0^{1,5}.$0^{6,11}$.$0^{14,19}$]icosa-6,8,10-triene-4,17-dione (3.13")** S = 1.031

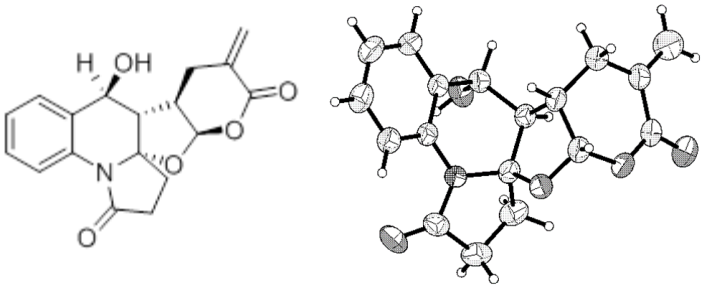

Chapter 4: β-lactams

Although this project was the most frustrating at time, my hope is that the work in this chapter will contribute the most to the chemistry community and to the greater good of society. Applying the post-photochemical modifications from the last chapter to a new scaffold containing a β-lactam, a small library of diverse small molecules, which can serve as potential new drug candidates, has been prepared. The work in this chapter is in preparation for publication.

Introduction

The need for new drug candidates has been discussed thoroughly up to this point, but one area of specific need are antibiotics. The U.S. Center for Disease Control and Prevention (CDC) estimates that there are 2 million infections and 23,000 deaths in the US annually from antibiotic resistant bacteria.[8] It is estimated that this equates to a cost of around 20 billion dollars for treatments and care, and an economic impact of around 35 billion dollars. Several World Health Organization (WHO) countries have even reported that nearly 50% of the documented *E. Coli* related infections are resistant to all current drug treatments.[8] There have been several severe outbreaks in the past decade or so, caused namely by methicillin-resistant Staphylococcus aureus or MRSA, which rapidly became resistant to the current approved treatments.

This is especially startling in light of the amount of research that goes into synthesizing new β-lactam targets annually. **Figure 4.1,** formed from a Web of Science

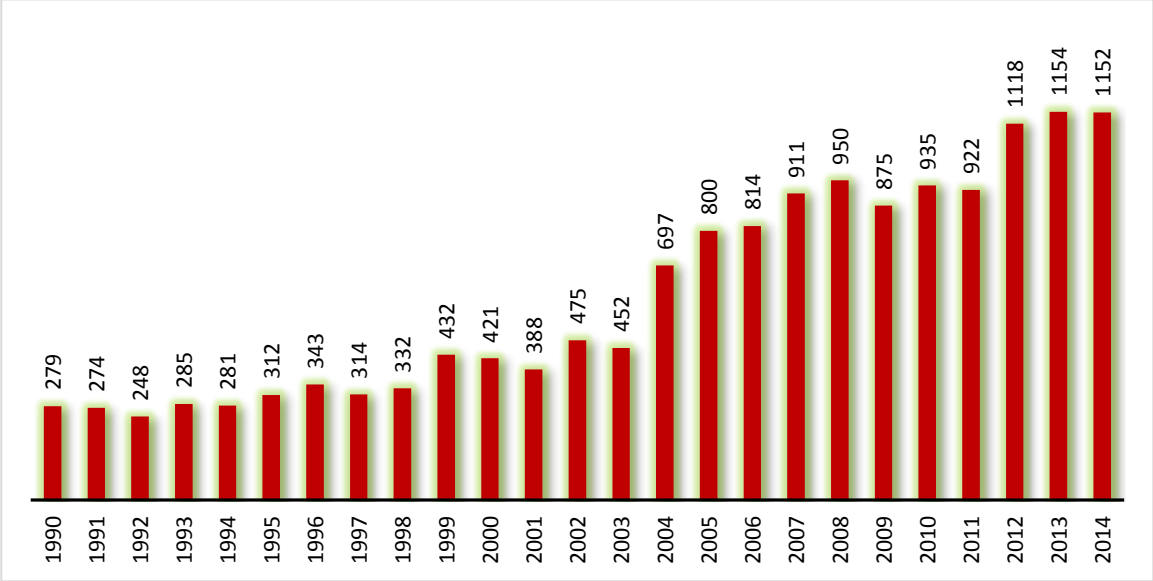

Figure 4.1

search, shows the frequency with which the term β-lactam appears in synthetic chemistry literature. As can be seen, the usage has increased in step with the growing instances of antibiotic resistance of the last decade. But yet we still find ourselves unable to discover new candidates. This is most likely due, again, to the bias of the researchers looking for these scaffolds. Most β-lactam libraries are inspired by already known compounds such as penicillin, cephalosporins, monobactams, and carbapenems.[56] As such, it is important to use the advances in modern computational chemistry, to take advantage of such DOS methods as FBDD, and synthesize better libraries of compounds that probe the chemical space more effectively.

This work sets out to synthesize a small library of chemically diverse compounds to do that. Inspired by the post-photochemical modifications from the last chapter, these

new β-lactams are a departure from the currently approved molecules, as they contain a different substitution pattern of the β-lactam, which will hopefully allow them to serve as better drug candidates.

Results and Discussion – Starting Material

As is the case with most of the azaxylylene photoprecursors discussed so far, the assembly of the β-lactam precursors was very straightforward (**Scheme 4.1**). First, the commercially available 2-amino benzyl alcohol (**4.1**) was protected with trimethylsilyl chloride (TMSCl) yielding the protected 2-amino benzyl alcohol **4.2**. Separately, the commercially available 2-furan acetic acid **4.3** was reacted with carbonyldiimidazole (CDI) forming the activated carbonyl species **4.4**.[57] **4.2** and **4.4** were then coupled, and

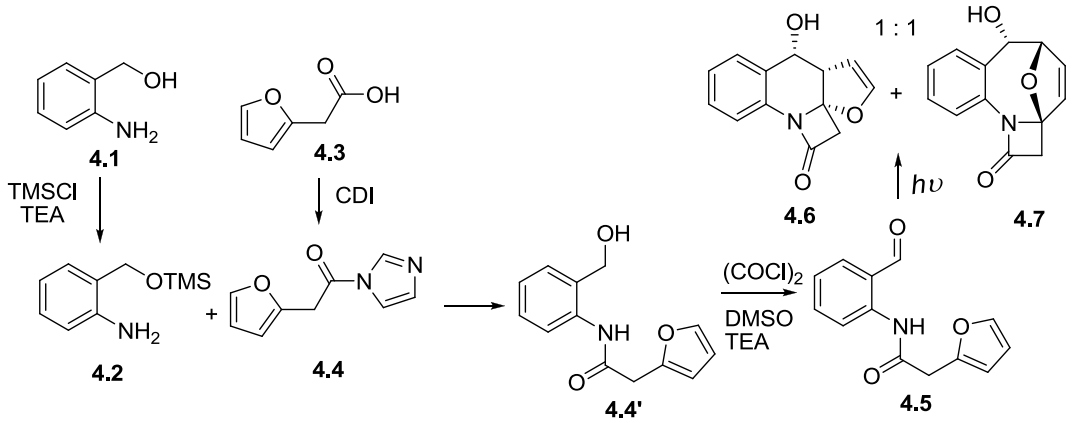

Scheme 4.1

oxidized using Swern oxidation to yield the β-lactam photoprecursor **4.5**. Irradiation conditions were optimized and found to yield clean photoproducts **4.6** and **4.7** in a 3:1 mixture of EtOH/H_2O. Given the usual high reactivity of β-lactams, it is surprising to

note that during purification, and the subsequent post-photochemical reactions, little to no decomposition of the β-lactams is observed.

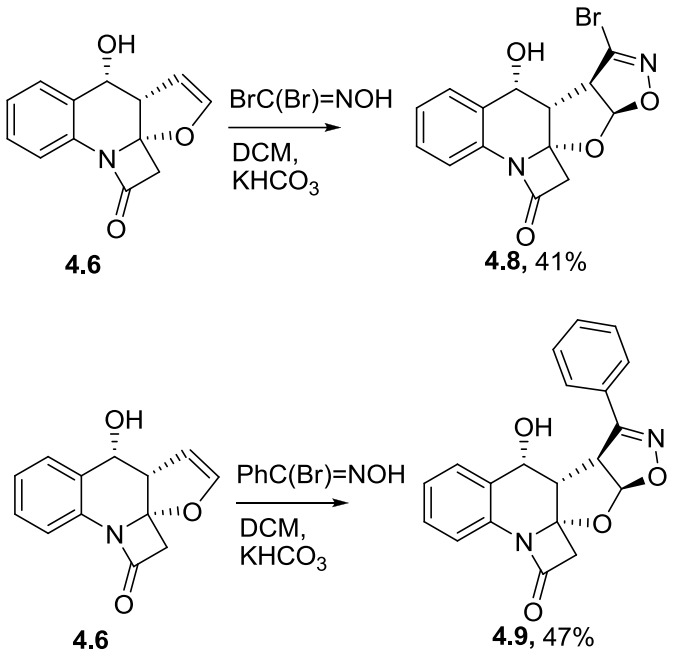

Scheme 4.2

Results and Discussion – [3+2] Cycloadditions

Post-photochemical modifications began with the [3+2] nitrile oxide addition, both with bromine and with phenyl substituents. As was the case previously, the addition of bromo nitrile oxide only yields one regioisomer **4.8**, resulting from the *exo* face addition (**Scheme 4.2**). The addition of phenyl nitrile oxide also only yields one

regioisomer **4.9**. The bromo nitrile oxide addition to the [4+4] scaffold yields two regioisomers **4.10** and **4.10'**, both adding from the *exo* face (**Scheme 4.3**). The ratio of products observed by NMR was 1.5:1, which is drastically different from the previous cases. We reasoned previously that the steric hindrance of the linker determines the ratio. When the heterocycle on the "south" side of the molecule is a five-membered ring, the substituent clashes with the methylene group favoring a "north" facing addition. However with the β-lactams, the methylene group in the four-membered ring is farther away and therefore does not interfere as greatly. This would explain the almost 1 to 1 ratio of

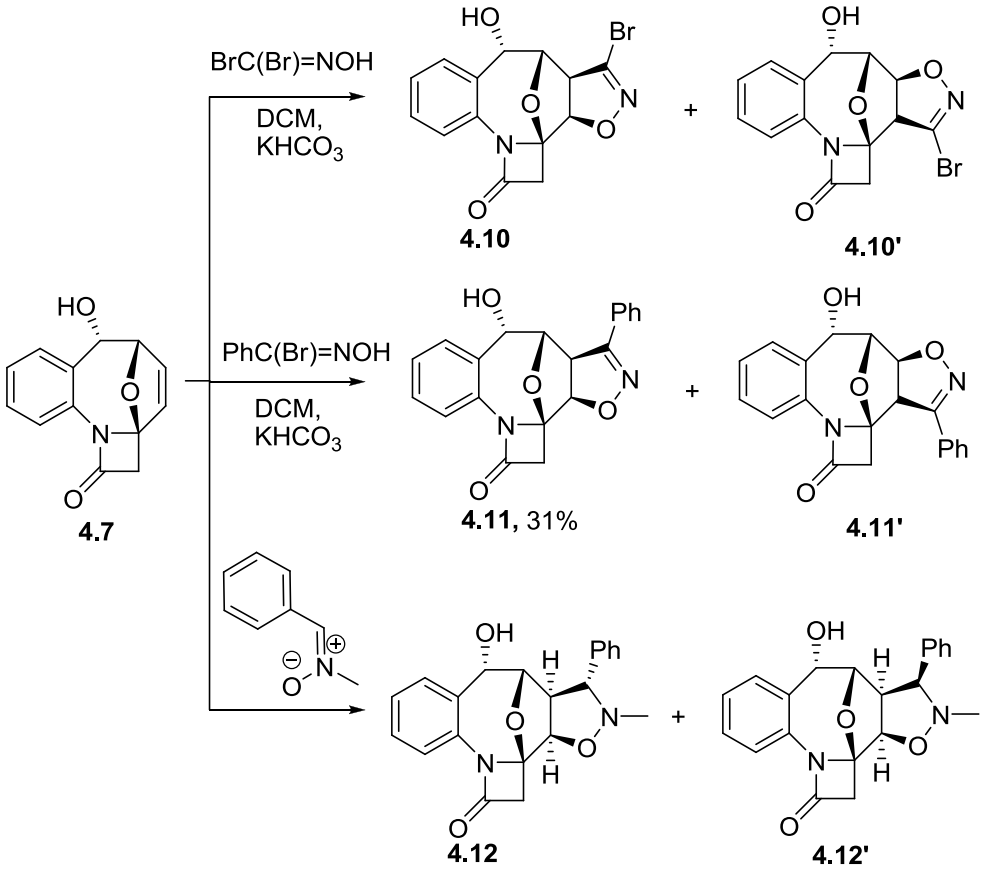

Scheme 4.3

products for the bromo nitrile oxide addition. As of note, the two regioisomers were inseparable by column chromatography.

The phenyl nitrile oxide addition also yields two regioisomers **4.11** and **4.11'**, with **4.11** being the major product, however the ratio is greater than 6:1 in favor of phenyl pointing north (**Scheme 4.3**). Phenyl is certainly a larger substituent than bromine, and since the four-membered ring is quite rigid, there is a large steric clash if phenyl was to face south. The minor isomer **4.11'** was only observed by NMR and not isolated for characterization. The nitrone cycloaddition was again not compatible with the [4+2] scaffold, however [4+4] yielded two isomers **4.12** and **4.12'**, with **4.12** being the major (**Scheme 4.3**). The structure of major isomer **4.12**, was assigned based on NOE experiments (**Figure 4.2**). The signal corresponding to proton H_e is a triplet at 3.03 ppm (**4.12**). Upon irradiating this triplet, a NOE of 11% with H_a is observed, which is indicative of the regiochemistry shown, as well as an NOE of 4% on H_b and 10% on H_c.

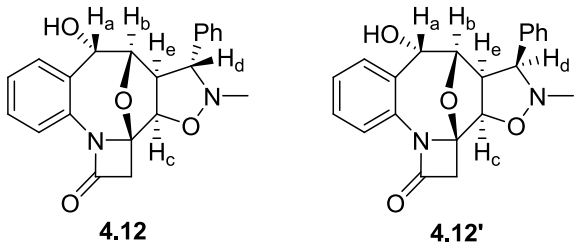

Figure 4.2

No signal from H_d is observed, which implies that protons H_d and H_e reside on the opposite faces of the isoxazoline ring. Comparison of the minor isomer **4.12'** with previously synthesized nitrone compounds shows the constants for all signals matches

very closely, suggesting the regiochemistry shown. The minor isomer **4.12'** could not be isolated cleanly, so a definite set of NOE experiments could not be run.

Results and Discussion – [4+2] Cycloadditions

The Povarov cycloaddition on the [4+2] scaffold yielded cleanly one isomer **4.13**. To show some diversity from the previously synthesized **3.19**, 2-pyridyl imine was substituted by phenyl. The reaction still led to the formation of one isomer with the phenyl group *anti* to the hydroxyl group. The hetero Diels-Alder cycloaddition utilizing 1, 3-dimethylbarbituric acid yielded one clean isomer **4.14**.

The next step in this project should be the testing of the biological activity of this small library. We have shown that even molecular fragments that are usually quite difficult to work with, in this case β-lactams, are amenable to our group's azaxylylene

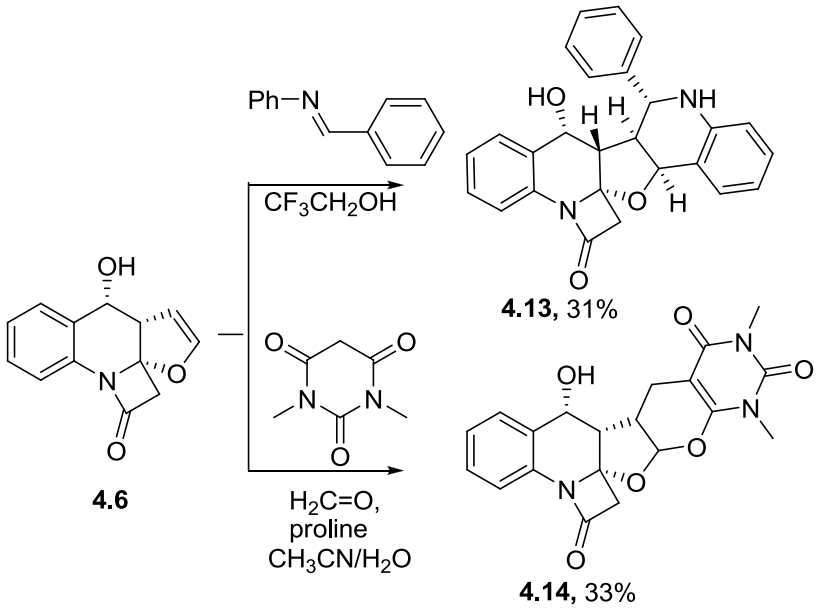

Scheme 4.4

photochemistry as well as the rapid growth in complexity from post-photochemical modifications.

Experimental

Common solvents were purchased from Pharmco and used as is, except for THF, which was refluxed over and distilled from sodium benzophenone ketyl prior to use. Common reagents were purchased from Aldrich and used without additional purification, unless indicated otherwise. NMR spectra were recorded at 25°C on a Bruker Avance III 500 MHz in $CDCl_3$ (unless noted otherwise). X-Ray structures were obtained with a Bruker APEX II instrument. High resolution mass spectra were obtained on the *Waters Synapt G2 ESI-MS* mass spectrometer from the University of Colorado at Boulder. Flash column chromatography was performed using Teledyne Ultra Pure Silica Gel (230 – 400 mesh) on a Teledyne Isco Combiflash R_f using Hexanes/EtOAc as an eluent.

Synthesis of Photoprecursor

Dibromoformaldoxime,[36] **N-hydroxy-benzenecarboximidoyl bromide,**[58] **(1E)-N-phenyl-1-pyridin-2-ylmethanimine,**[52a] **N-oxide-N-phenylmethylene)-methanamine**[50] were prepared according to the existing procedures.

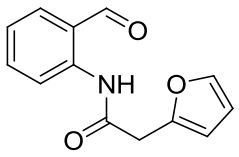

1.0 g of 2-furanacetic acid (8.5 mmol, 1 eq) was dissolved in 10 mL of anhydr. DCM along with 1.6 g of CDI (9.8 mmol, 1.15 eq). This reaction stirred at ambient temperature for 15 mins. The consumption of the starting 2-furanacetic acid was monitored by TLC. Upon full consumption, 1.6 g of **2-{[(trimethylsilyl)oxy]methyl}aniline**[14] (8.5 mmol, 1 eq) was added and the reaction

stirred for an additional 6 hrs, before quenching with 20 mL of water. The organic layer was separated, washed with sat. brine, dried over Na_2SO_4, filtered, and concentrated *in vacuo* to yield 1.6 g of a crude mixture of **2-(furan-2-yl)-N-(2-{[(trimethylsilyl)oxy]methyl}phenyl)acetamide** and **2-(furan-2-yl)-N-[2-(hydroxymethyl)phenyl]acetamide**, which was used in the next step without separation or purification[34].

0.49 mL of oxalyl chloride (5.7 mmol, 1.1 eq) dissolved in 6.4 mL of anhydr. DCM (0.9M solution) was cooled to -78ºC before 0.82 mL of dry DMSO (11.5 mmol, 2.2 eq) was slowly added. Upon complete addition, the mixture stirred for 2 mins while the evolution of gas stopped. Then, 1.6 g of a crude mixture of **2-(furan-2-yl)-N-(2-{[(trimethylsilyl)oxy]methyl}phenyl)acetamide** and **2-(furan-2-yl)-N-[2-(hydroxymethyl)phenyl]acetamide** (5.2 mmol, 1 eq) dissolved in 10.0 mL of anhydrous DCM (0.5M solution) was then slowly added to the activated DMSO solution. Upon complete addition, the mixture stirred for 15 mins. After 15 mins, 3.6 mL of NEt_3 (26.1 mmol, 5 eq) was slowly added. Upon complete addition, the mixture was slowly warmed to RT where it stirred overnight. The reaction was quenched with water and extracted with DCM. The organic layer was separated, washed with sat. brine, dried over Na_2SO_4, filtered, and concentrated in vacuo. The crude product was purified by flash chromatography from hexanes/EtOAc yielding 1.0 g of **N-(2-formylphenyl)-2-(furan-2-yl)acetamide** (57% over two steps). ^{1}H NMR (500 MHz, $CDCl_3$) δ 11.17 (s, 1H), 9.85 (s, 1H), 8.75 (d, J = 8.5 Hz, 1H), 7.64 (dd, J = 7.6, 1.6 Hz, 1H), 7.61 (ddd, J = 8.5, 7.6, 1.6 Hz, 1H), 7.47 (dd, J = 2.0, 0.8 Hz, 1H), 7.23 (td, J = 7.5, 1.0 Hz, 1H), 6.45 (dd, J = 3.3, 2.0 Hz, 1H), 6.39 (dd, J

= 3.3, 0.6 Hz, 1H), 3.85 (s, 2H). ^{13}C NMR (126 MHz, $CDCl_3$) δ 195.2, 168.3, 147.5, 142.9, 140.5, 136.1, 135.9, 123.2, 122.0, 120.0, 110.8, 109.4, 38.1.

Synthesis of Photoproducts

General Procedure **I** for irradiation

A solution with ca. 3.0 mM of N-(2-formylphenyl)-2-(furan-2-yl)acetamide in 3:1 ethanol/H_2O was degassed and irradiated in a Pyrex or borosilicate glass reaction under LED-365 LED Engins (360-370nm UV source with peak emission at 365 nm) until the reaction was complete, as determined by ^{1}H NMR. The solution was concentrated and the mixture was purified by flash chromatography.

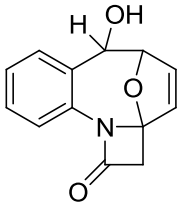

11-hydroxy-15-oxa-4-azatetracyclo[10.2.1.0^{1,4}.0^{5,10}]pentadeca-5,7,9,13-tetraen-3-one: From 1.0 g of N-(2-formylphenyl)-2-(furan-2-yl)acetamide was obtained 0.39 g (39%) of the title compound. ^{1}H NMR (500 MHz, $CDCl_3$) δ 7.79 (dd, J = 8.0, 1.3 Hz, 1H), 7.76 (dt, J = 8.0. 1.2 Hz, 1H), 7.32 (td, J = 7.6, 1.6 Hz, 1H), 7.20 (td, J = 7.7, 1.3 Hz, 1H), 6.71 (dd, J = 5.8, 1.9 Hz, 1H), 6.10 (dd, J = 5.8, 0.9 Hz, 1H), 5.26 (t, J = 4.7 Hz, 1H), 4.99 (dt, J = 3.9, 1.4 Hz, 1H), 3.51 (d, J = 15.5 Hz, 1H), 3.46 (d, J = 15.5 Hz, 1H), 2.33 (d, J = 7.0 Hz, 1H). ^{13}C NMR (126 MHz, $CDCl_3$) δ 160.6, 135.0, 131.2, 129.9, 128.6, 128.4, 128.3, 124.9, 121.3, 94.0, 84.4, 76.2, 45.7. HRMS (ESI) calcd for $C_{13}H_{11}NO_3^+$ $(MH)^+$ 230.0817 found 230.0816

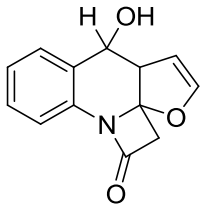

10-hydroxy-6-oxa-2-azatetracyclo[9.4.0.0^{2,5}.0^{5,9}]pentadeca-1(15),7,11,13-tetraen-3-one: From 1.0 g of N-(2-formylphenyl)-2-(furan-2-yl)acetamide was obtained 0.41 g (41%) of the title compound. ^{1}H NMR (500 MHz, $CDCl_3$) δ 7.53 (m, 1H), 7.32 (m, 4H), 6.39 (t, J = 2.8 Hz, 1H), 5.03 (dd, J = 3.0, 2.4 Hz, 1H), 4.95 (d, J = 6.4 Hz, 1H), 4.22 (dt, J = 6.4, 2.4 Hz, 1H), 3.61 (d, J = 15.7 Hz, 1H), 3.46 (d, J = 15.7 Hz, 1H). ^{13}C NMR (126 MHz, $CDCl_3$) δ 164.7, 147.3, 132.4, 132.3, 128.1, 127.2, 124.9, 122.7, 99.3, 91.5, 67.6, 52.0, 50.3. HRMS (ESI) calcd for $C_{13}H_{11}NO_3^+$ $(MH)^+$ 230.0817 found 230.0821

Post-photochemical Modifications

Addition of nitrile oxide, general procedure I:[25] 1 eq of photoproduct was dissolved in EtOAc. To this was added 3 eq of N-hydroxy-benzenecarboximidoyl bromide or dibromoformaldoxime and 6 eq of $KHCO_3$. An additional 3 eq of N-hydroxy-benzenecarboximidoyl bromide or dibromoformaldoxime and 6 eq of $KHCO_3$ were added after stirring for 12 h. The reaction was monitored by NMR until the starting photoproduct was consumed. The resulting mixture was diluted with water, extracted with 3x20 mL of EtOAc, washed with brine, dried over Na_2SO_4, and concentrated *in vacuo*. The mixture was then purified by flash chromatography.

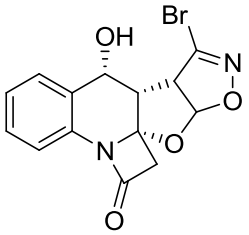

14-bromo-11-hydroxy-16,18-dioxa-4,15-diazapentacyclo[10.6.0.0^{1},^{4}.0^{5},^{10}.0^{13},^{17}]octadeca-5,7,9,14-tetraen-3-one: From 0.14 g of **10-hydroxy-6-oxa-2-azatetracyclo[9.4.0.0^{2,5}.0^{5,9}]pentadeca-1(15),7,11,13-tetraen-3-one**, 0.37 g of dibromoformaldoxime, and 0.36 g of $KHCO_3$, was obtained 85.0 mg (40%) of the title compound. ^{1}H NMR (500 MHz, DMSO) δ 7.44 (dd, J = 7.8, 1.2 Hz, 1H), 7.37 (m, 2H), 7.20 (ddd, J = 8.7, 7.0, 1.9 Hz, 1H), 6.04 (d, J = 6.0 Hz, 1H), 5.81 (d, J = 5.8 Hz, 1H), 4.82 (t, J = 5.4 Hz, 1H), 4.39 (dd, J = 5.9, 0.5 Hz, 1H), 3.28 (d, J = 15.5 Hz, 1H), 3.14 (d, J = 15.5 Hz, 1H). ^{13}C NMR (126 MHz, DMSO) δ 165.5, 142.4, 131.8, 131.0, 129.2, 127.6, 124.9, 118.5, 107.5, 88.5, 63.8, 59.0, 51.9, 43.9. HRMS (ESI) calcd for $C_{14}H_{12}BrN_2O_4^+$ $(MH)^+$ 350.9980 and 352.9960 found 350.9981 and 352.9962

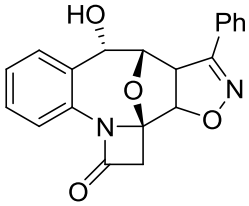

11-hydroxy-14-phenyl-16,18-dioxa-4,15-diazapentacyclo[10.5.1.0^{1},^{4}.0^{5},^{10}.0^{13},^{17}]octadeca-5,7,9,14-tetraen-3-one: From 200 mg of **11-hydroxy-15-oxa-4-azatetracyclo[10.2.1.0^{1,4}.0^{5,10}]pentadeca-5,7,9,13-tetraen-3-one** (1.0 mmol) was obtained 94.0 mg (31%) of the title compound. ^{1}H NMR (500 MHz, CDCl3) δ 7.89 (m, 3H), 7.86 (dt, J = 8.0, 1.4 Hz, 1H), 7.47 (m, 3H), 7.39 (td, J = 7.4, 1.4 Hz, 1H), 7.31 (td, J = 7.9, 1.3 Hz, 1H), 4.99 (m, 1H), 4.94 (d, J = 8.5 Hz, 1H), 4.73 (dd, J = 3.0, 0.8 Hz, 1H), 4.09 (dd, J = 8.6, 1.0 Hz, 1H), 3.68 (d, J = 15.7 Hz, 1H), 3.52 (d, J = 15.7 Hz, 1H), 2.73 (d, J = 5.5 Hz, 1H). ^{13}C NMR (126 MHz, CDCl3) δ 161.1, 157.0, 132.2, 130.6, 129.5, 129.0,

128.9, 128.0, 127.6, 127.2, 125.6, 120.9, 94.1, 87.2, 85.1, 77.2, 73.8, 53.9, 44.0. HRMS (ESI) calcd for $C_{20}H_{16}N_2O_4^+$ $(MH)^+$ 349.1183 found 349.1183

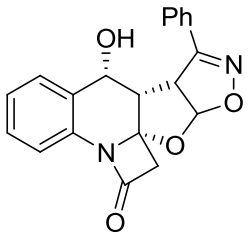

11-hydroxy-14-phenyl-16,18-dioxa-4,15-diazapentacyclo[10.6.0.0^{1},^{4}.0^{5},^{10}.0^{13},^{17}]octadeca-5,7,9,14-tetraen-3-one: From 150 mg of **10-hydroxy-6-oxa-2-azatetracyclo[9.4.0.0^{2,5}.0^{5,9}]pentadeca-1(15),7,11,13-tetraen-3-one** (0.7 mmol) was obtained 0.11 g (47%) of the title compound. ^{1}H NMR (500 MHz, CDCl3) δ 7.75 (m, 2H), 7.56 (dd, J = 8.2, 1.1 Hz, 1H), 7.49 (m, 3H), 7.42 (td, J = 7.7, 1.4 Hz, 1H), 7.22 (td, J = 7.6, 1.2 Hz, 1H), 6.36 (d, J = 6.3 Hz, 1H), 4.97 (dd, J = 8.9, 5.1 Hz, 1H), 4.69 (d, J = 6.3 Hz, 1H), 3.49 (d, J = 16.0 Hz, 1H), 2.96 (d, J = 16.0 Hz, 1H), 2.85 (d, J = 5.2 Hz, 1H), 1.83 (d, J = 8.9 Hz, 1H). ^{13}C NMR (126 MHz, CDCl3) δ 164.5, 131.3, 131.0, 130.5, 130.3, 129.4, 126.9, 125.1, 124.5, 119.2, 107.7, 103.3, 100.0, 87.8, 66.0, 53.8, 52.2, 45.2. HRMS (ESI) calcd for $C_{20}H_{16}N_2O_4^+$ $(MH)^+$ 349.1183 found 349.1179

Nitrone Cycloaddition: 1 eq of photoproduct was dissolved in 1 mL of anhyd. toluene along with 4 eq of nitrone. The reaction was sealed in a high pressure reaction vessel and heated to completion as shown by ^{1}H NMR. The toluene was removed *in vacuo* and the residue purified by flash chromatography.

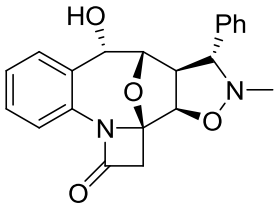

anti-11-hydroxy-15-methyl-14-phenyl-16,18-dioxa-4,15-diazapentacyclo[10.5.1.0^{1},^{4}.0^{5},^{10}.0^{13},^{17}]octadeca-5,7,9-trien-3-one: From 100 mg of **11-hydroxy-15-oxa-4-azatetracyclo[10.2.1.0^{1,4}.0^{5,10}]pentadeca-5,7,9,13-tetraen-3-one** (0.44 mmol) was obtained 51.0 mg (32%) of the title compound. ^{1}H NMR (500 MHz, $CDCl_3$) δ 7.80 (dt, J = 7.8, 1.4 Hz, 1H), 7.67 (d, J = 7.8 Hz, 1H), 7.39 (m, 3H), 7.33 (m, 3H), 7.26 (td, J = 7.6, 1.4 Hz, 1H), 4.92 (dd, J = 5.5, 3.5 Hz, 1H), 4.65 (d, J = 7.0 Hz, 1H), 4.52 (d, J = 3.0 Hz, 1H), 3.44 (d, J = 15.3 Hz, 1H), 3.30 (d, J = 8.5 Hz, 1H), 3.23 (d, J = 15.3 Hz, 1H), 3.03 (t, J = 7.7 Hz, 1H), 2.51 (s, 3H). ^{13}C NMR (126 MHz, $CDCl_3$) δ 160.6, 131.6, 131.0, 129.3, 129.0, 128.6, 128.5, 127.7, 125.6, 121.3, 93.1, 84.9, 81.5, 72.4, 61.9, 43.3, 42.3. HRMS (ESI) calcd for $C_{21}H_{21}N_2O_4^+$ $(MH)^+$ 365.1496 found 365.1502

Povarov Cycloaddition:[52b] A solution was prepared with 2 eq of the corresponding imine and 1 eq of corresponding photoproduct in 1.5 mL of 2,2,2-trifluoroethanol. This was warmed to 40^{o}C until the reaction was complete as observed by ^{1}H NMR. The resulting mixture was concentrated *in vacuo* and purified by flash chromatography.

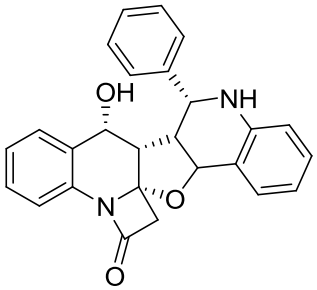

(1S,11S,13S,14S)-14-hydroxy-11-(phenyl)-2-oxa-10,21-diazahexacyclo[11.10.0.0^{1},^{21}.0^{3},^{12}.0^{4},^{9}.0^{15},^{20}]tricosa-4(9),5,7,15,17,19-hexaen-22-one: From 50.0 mg of **10-hydroxy-6-oxa-2-azatetracyclo[9.4.0.0^{2,5}.0^{5,9}]pentadeca-1(15),7,11,13-tetraen-3-one** *Results are ongoing*

Hetero Diels-Alder Cycloaddition:[59] 1 eq of photoproduct and 1 eq of 1,3-dicarbonyl compound were dissolved in 0.7 mL of dry acetonitrile. To this was added 0.08 eq of L-proline and 1.3 eq of 37% aq. formaldehyde solution. The reaction stirred at ambient temperature until full consumption of the photoproduct, as determined by ^{1}H NMR. The reaction was diluted with water and extracted with EtOAc. The organic layer was separated, dried over Na_2SO_4, and concentrated *in vacuo*. The mixture was then purified by flash chromatography.

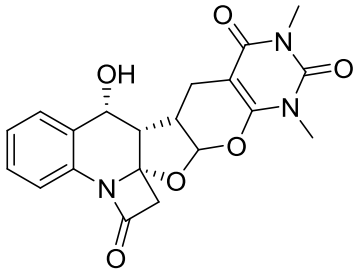

(1S,13S,14S)-14-hydroxy-6,8-dimethyl-2,4-dioxa-6,8,21-triazahexacyclo[11.10.0.0^{1},^{21}.0^{3},^{12}.0^{5},^{10}.0^{15},^{20}]tricosa-5(10),15,17,19-tetraene-7,9,22-trione: From 100.0 mg of **10-hydroxy-6-oxa-2-azatetracyclo[9.4.0.0^{2,5}.0^{5,9}]pentadeca-1(15),7,11,13-tetraen-3-one** (0.42 mmol) and 65 mg of 1,3-dimethyl barbituric acid (0.42 mmol) was obtained 55.2 mg (33%) of the title compound. ^{1}H NMR (500 MHz, DMSO) δ 7.65 (dt, *J*=7.4, 1.4 Hz 1H), 7.40 (td, *J* = 7.5, 1.3 Hz, 1H), 7.36 (tq, *J*= 7.5, 1.7, 0.80 Hz, 2H), 7.19 (dd, *J* = 7.5, 1.2 Hz, 1H), 6.14 (d, *J* = 5.3 Hz, 1H), 5.80 (d, *J* = 4.0 Hz, 1H), 4.93 (t, *J* = 5.8 Hz, 1H), 3.74 (d, *J* = 15.8 Hz, 1H), 3.42 (d, *J* = 15.8 Hz, 1H), 3.24 (s, 3H), 3.18 (s, 3H), 2.97 (d, *J* = 15.9 Hz, 1H), 2.40 (d, *J* = 15.9 Hz, 1H). ^{13}C NMR (126 MHz, DMSO) δ 19.5, 28.0, 28.8, 38.3, 39.5, 39.6, 39.8, 40.0, 40.1, 40.1, 40.2, 40.3, 40.4, 40.5, 40.6, 46.8, 51.2, 66.7, 82.9, 93.2, 103.6, 123.1, 126.5, 127.6, 128.2, 132.2, 134.7, 151.0, 154.4, 162.7, 165.5. HRMS (ESI) calcd for $C_{20}H_{20}N_3O_6^+$ $(MH)^+$ 398.1347 found 398.1342

Chapter 5: LED Irradiator Design

Photochemistry has often been stereotyped as being “messy”, resulting in reactions that are difficult to predict or control. Additionally, there is a misconception that photochemistry is expensive and requires specific light conditioning apparatus such as water cooling jackets and filters. These factors have prevented many chemists from utilizing this powerful synthetic tool. This section is intended to dispel these myths, and to demonstrate that photochemistry powered by LEDs is actually quite inexpensive, and that the equipment is easy to build and maintain. This will also serve as an instructional

Figure 5.1

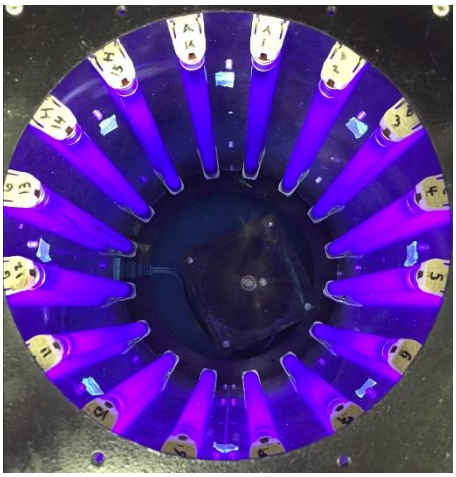

Figure 5.2

on how to build the LED irradiators utilized by the Kutateladze group for its photochemistry.

Rayonet Photo-Reactors (RPR)

In the work by Mukhina et al., it was discovered that azaxylylene photochemistry could be initiated at wavelengths above 300 nm, with most azaxylylene precursor's absorption maximum ranging from 330 nm to 380 nm. The original generation of Rayonet Photo-Reactors (RPR) from The Southern New England Ultraviolet Co. (**Figure 5.1**) contained broad UV source lamps that emitted light from 300-420 nm, with an emission maximum at 350 nm, thus they are called RPR-3500 (**Figure 5.2**). This irradiator consists of 16 individual UV lamps that output 8 W each, or a combined 128 W of power. A particular drawback to this apparatus is the amount of energy waste, as not all 128 W is going to produce the desired wavelengths of irradiation. Integration of the area under the power output curve shows the irradiator is only producing around 20 W at the emission maximum. One of the major focuses in engineering a new generation of irradiators should be to improve upon this wastefulness. Additionally, the average cost for one of these units ranges from 3000 to 4000 dollars depending upon the specifications of the desired unit, not including the lamps. For a group attempting to start a photochemistry project, this could present too large of a barrier for entry. New generations of irradiators should seek to improve on this price point.

Power and Photon Flux

Before building a new irradiator, it is important to understand the relationship between power and the number of photons being emitted, or photon flux. For *o*-azaxylylene photochemistry, the desired outcome of a perfect system would be every one photon captured by the sample leads to one azaxylylene formation event. This is never the case, as many other side processes lead to a return to ground state without productive photochemistry. However, the more photons that are produced and captured by the sample, the faster the reaction will be. The photon flux of a light source can be calculated using the power and the wavelength of the light. This calculation is not completely accurate for many light sources as this is assuming the light being emitted is only a single wavelength. In reality, many UV sources emit over a range, such as is the case for the RPR-3500. However, the newest generation of LEDs that will be described later, have an emission band of 360 to 370 nm, with a maximum emission at 365 nm. They are rated to produce exactly 2.9 W at this 365 nm, so in this case the calculation is accurate. The energy of this wavelength of light can be calculated using the energy equation (**Figure 5.3**). Photon flux is then calculated by the photons/sec equation (**Figure 5.3**), and if

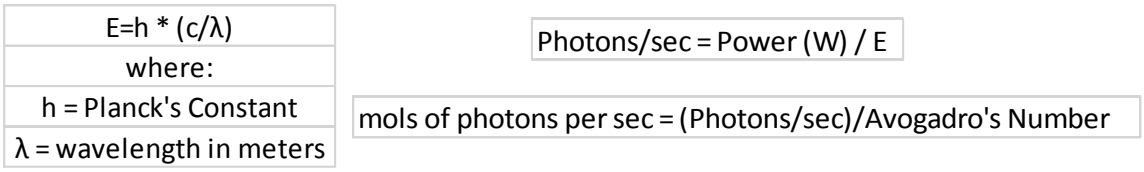

Figure 5.3

desired, photon flux can be converted into mols of photons per sec by dividing photon flux by Avogadro's number (**Figure 5.3)**. For the LEDs in focus, the photon flux is

calculated at 5.3*10^18 photons/sec or 8.0 µmol photons/sec. So, if the setups had a 100% absolute quantum yield, theoretically 1 mol of starting material could be irradiated in 124,378 secs or 34.5 hrs. using one of these LEDs.

Light Emitting Diodes (LEDs) and UV LED Irradiators with λ > 350 nm

With the recent drop in the price of manufacturing LEDs, it is now more advantageous for the Kutateladze group to make its own irradiators. Supplies were easily purchased online from either Newegg or Mouser Electronics. Mouser offers a wide range of LEDs from visible to UV, as well as a wide range of power supplies depending on the application. The first generation of LED irradiators built in the Kutateladze group ranged from 0.5 W to 1.25 W. While these were powerful enough for NMR scale experiments and some smaller scale reactions, large scale reactions simply took too long. Therefore a more powerful LED irradiator needed to be built, one that matched the power of the RPR-3500 (~20 W). This new setup consisted of seven 2.9 W LED Engin LZ4-44UV00 LED Emitters (**Figure 5.4**). When purchased in bulk, these LEDs cost 58 dollars. Each

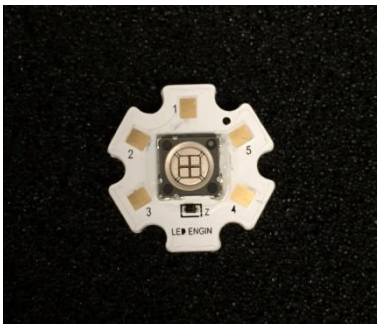

Figure 5.4

LED requires a current of 700 mA and an input voltage of 18 V, so proper power supply selection is crucial. Voltage runs in series with the circuit, while current does not, so the

power supply has to have a combined voltage higher than the sum of the LEDs, and a current at the maximum rating of one LED. Since this irradiator was to contain seven LEDs, the power supply needed to provide at least 126 V (18 V * 7) for proper function. The power supply that was chosen (**Figure 5.5**) was rated for 142 V and 700 mA. The

Figure 5.5

power supply can supply more voltage than the whole array needs, however higher voltage power supplies cost more money, so it is better to only buy what is needed. This particular power supply cost 78 dollars from Mouser. Work begun with the selection of a proper heatsink that would accommodate all seven LEDs (**Figure 5.6**). The heat sink serves to aid in the dissipation of the heat generated by the LEDs. Every heat sink is rated

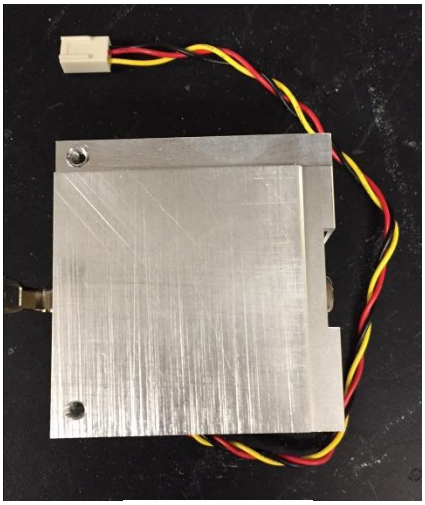

Figure 5.6

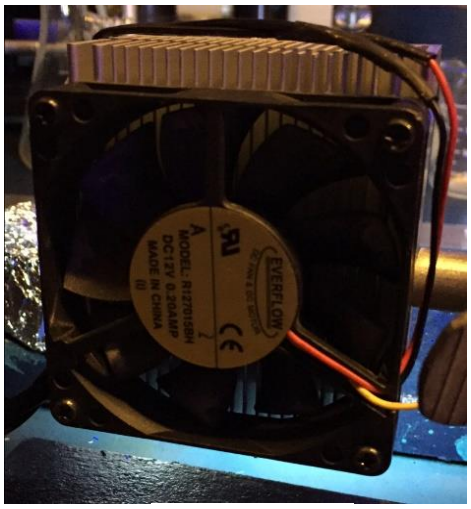

Figure 5.7

based on how much power in the form of heat it can dissipate. Since each LED requires

18 V, but the actual output is only 4 V (2.9 W), about 14 V is lost to heat formation. The heat sink needs to be able to dissipate this heat effectively. As the heat sink gets larger, it dissipates more heat, so larger arrays are cooled more efficiently on the necessarily larger heat sinks. It is also beneficial to have a fan attached to the back side of the setup to provide additional forced cooling (**Figure 5.7**). The heat sink/CPU fan assembly in **Figure 5.6** and **5.7** was purchased from Newegg for under 5 dollars and came preassembled. Every fan has a different set of criteria for power, but most CPU fans are rated for around 12 V and 500 mA. A regular AC adaptor for common household electronics can be used, as long as it meets the criteria. The desired LED pattern was then decided, and holes marked for drilling (examples shown in **Figure 5.6**). Several holes were drilled using a 7/64" bit fitted to a drill press. The resulting holes were threaded using a 6-32 NC tap and some cutting oil to prevent stripping the hole. Small #6 button head screws were then used to attach the LED array. On the backside of each LED was added some thermal compound, which helps in the transfer of heat from the LED to the heat sink. Each LED has 5 pads for creating a circuit (**Figure 5.8**). A schematic provided by the manufacturer shows that pads 1, 2, and 3 are the cathodes (+) of the LED; pads 4 and 5 are the anodes (-) (**Figure 5.8**). Every LED is set up differently, so double check the manufacturer specifications, but electrons always flow from the anode (-) to the cathode (+). Each pad should be cleaned with flux to remove any oils or dirt from the manufacturing and handling process. Each pad was "tinned" with a little solder to establish a strong connection, followed by the attachment of the wires. Once the circuit was complete, the array was attached to the power supply to check for continuity. This

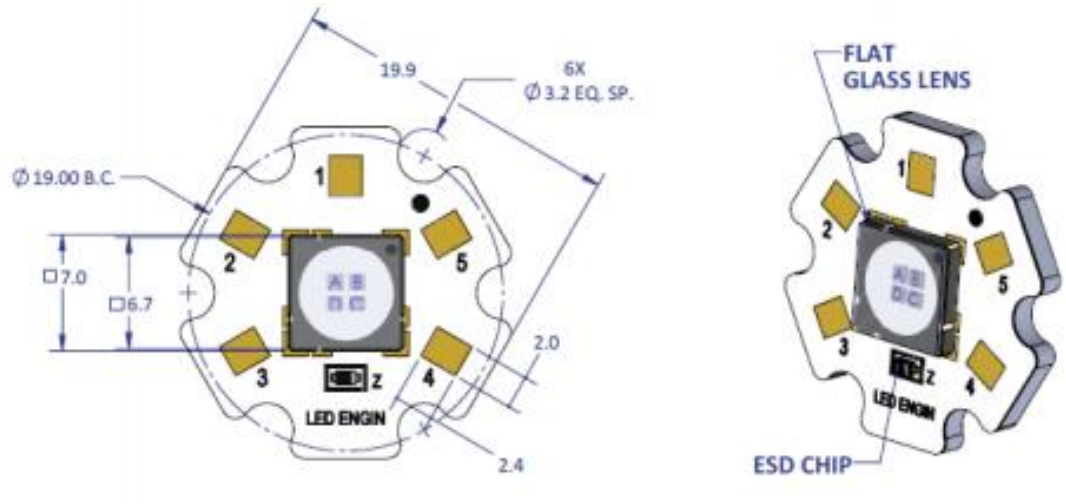

Figure 5.8

new array matched the power of the RPR-3500, without the extra waste (**Figure 5.9**). The calculated photon flux was 3.7 *10^19 photons/sec or 56 µmol photons/sec. At 100%

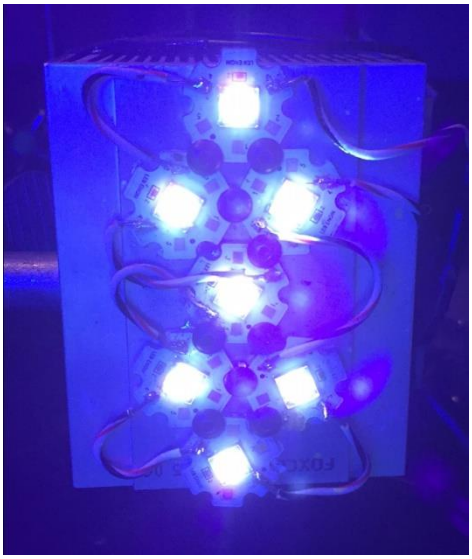

Figure 5.9

efficiency, this irradiator could convert 1 mol of starting material in 4.9 hrs. It has been extremely useful in large scale irradiations, allowing for the irradiations of 1.2 g of **3.2** (**Scheme 3.2**) in only 30 mins. Total cost to build this array was about 500 dollars, a nearly 3500 dollar savings over the Rayonet photoreactor.

The newest generation of LED irradiators were designed to be housing in a sealable enclosure, just like the RPR-3500. They each contain two 2.9 W LED Engin LZ4-44UV00 LED Emitters, a heat sink and fan, as well as a power supply. Each LED still required 18 V and 700 mA, so the power supply needed to supply at least 36 V. The power supply chosen supplied a variable 10-43 V and 700 mA, and cost 28 dollars (**Figure 5.10**). Assembly of the irradiator was identical to the previously described 20.3

Figure 5.10

W setup (**Figure 5.11**). Additional holes on the corners of the heat sink were drilled to allow for attachment to the irradiation container (**Figure 5.12**). The housing for these

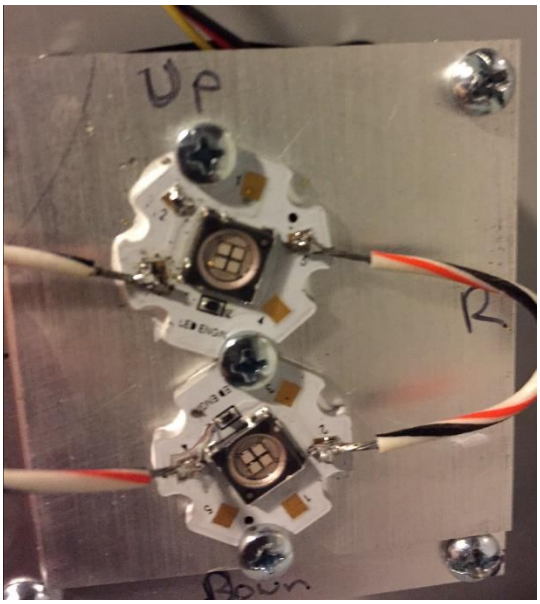

Figure 5.11

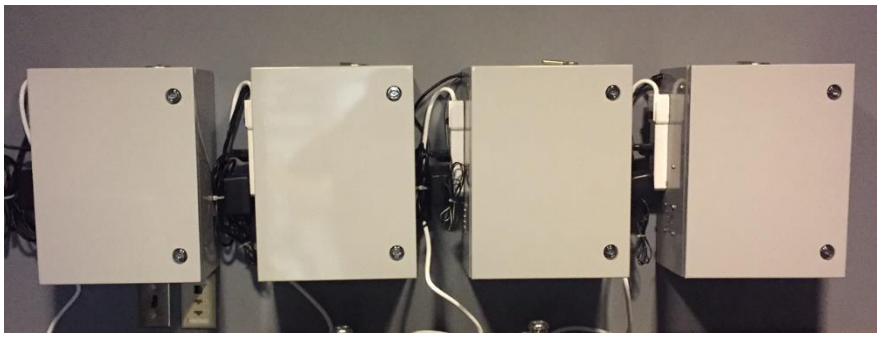

Figure 5.12

units was a steel electrical junction box, purchased on Amazon for $70. A series of holes were drilled in the side to allow for air flow, for feeding the power cords through, and for fastening the power supply and irradiator to the inside. Once drilled and tapped, the unit was connected to power and checked for continuity (**Figure 5.13**). To increase the

Figure 5.13

ascetics and functionality, a power strip was added to the outside of the box (**Figure 5.14**). The power strip also allows for the user to place their reaction inside and turn the

unit on without having to look at the LEDs. A ring stand and magnetic stirrer were also added, the stirrer to allow for proper mixing during irradiation, and the ring stand for extra stability. These new irradiators have a combined 5.8 W of power, or 1.0 * 10^19 photons/sec or 16.0 μmol photons/sec. The reaction times are therefore on the order of 5

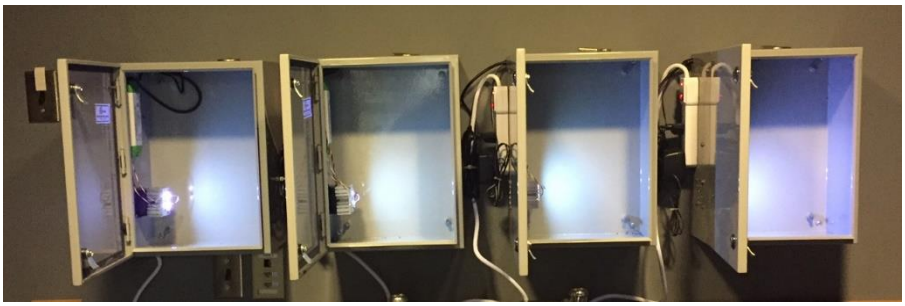

Figure 5.14

to 23 times faster than the original 1.25 W and 0.5 W irradiators respectively. The cost to build all four of these irradiators was only 900 dollars from easily purchased materials.

Further work for these UV irradiators will include experimenting with different shapes of arrays, including but not limited to bowls and rings. For now, these new irradiator setups represent a huge improvement over previous setups. They are powerful and focused, allowing for more efficient photochemistry. The new 20.3 W irradiator allows the group to irradiate large quantities of starting materials quickly, or to irradiate at low temperatures without a large increase in reaction time. The new 5.8 W enclosed irradiators allow for quicker small scale reactions on the order of 23 times faster than previous generations, with the added ascetics and protection from the UV sources. Most importantly, the dramatic drop in cost has removed a huge barrier for new groups starting photochemistry projects that utilize this powerful chemistry.

Chapter Six: Conclusions

As the global population continues to age, more effective pharmaceutical treatments are always needed to combat the new issues that arise. Despite the large number of new small organic molecules, new drug approvals have been extremely slow, due in part to the lack of diversity in these compounds. The complexity and diversity that has been unlocked thanks to the photogeneration of *o*-azaxylylenes will hopefully be an important step towards solving these problems.

This work has demonstrated that the pre-photochemical modification of o-azaxylylenes is straightforward, allowing for the addition of heteroatoms to the linker that tethers the photoactive pendant to the *o*-azaxylylene. Irradiation at 350 nm yields new, complex N, O, S polyheterocycles, not easily synthesized by conventional benchtop methods.

This work has also demonstrated that the modular assembly of post-photochemical modifications can lead to the synthesis of a small, diverse library as recognized by analysis of Tanimoto coefficients. These post-photochemical modifications allow for additional diversification of the photoproducts, ultimately covering more area in the chemical space.

Additionally, a new set of β-lactam scaffolds was shown to be amenable to these post-photochemical modifications. As more bacteria build up a resistance to current treatments, these new β-lactams could serve as better alternatives to combat these needs.

And finally, the misconception has been dispelled that photochemistry is expensive. Given the decrease in raw material cost, it is now easier than ever to build in-house reactors as powerful, if not more powerful than, commercially available units. This allows for the user to tailor-make an array that fits the needs of the group.

References

(1) (a) Kirkpatrick, P.; Ellis, C. *Nature*, **2004**, *432*, 823 (b) Dobson, C. M. *Nature*, **2004**, *432*, 824

(2) Administration for Community Living – United States Department of Health and Human Services. http://www.aoa.acl.gov/aging_statistics/index.aspx (accessed April 15th, 2016)

(3) Skarnulis, L. "7 Health Challenges of Aging." WedMD. Web

(4) United States Center for Disease Control and Prevention – The State of Aging and Health in America 2013. http://www.cdc.gov/aging/pdf/state-aging-health-in-america-2013.pdf (accessed April 15th, 2016)

(5) " Orphans' No More: Renaissance in New Drugs for Rare Diseases." American Chemical Society. ACS, **13 May 2013**. Web.

(6) "Rare Diseases Act of 2002" 107th Cong., U.S. G.P.O. (2002) (enacted). Print

(7) (a) Aronson, J. *British Journal of Clinical Pharmacology*, **2006**, *333*, 127 (b) PHRMA – Rare Diseases: A Report on Orphan Drugs in the Pipeline. http://phrma.org/sites/default/files/pdf/Rare_Diseases_2013.pdf (accessed April 15th, 2016)

(8) Center for Disease Dynamics, Economics & *Policy State of the World's Antibiotics, 2015*. CDDEP: Washington, D.C, **2015**

(9) United States Center for Disease Control and Prevention: Antibiotic Resistance Threats in the United States, 2013 http://www.cdc.gov/drugresistance/threat-report-2013/ (accessed April 15th, 2016)

(10) Cronk, W. C. "Photo-generated O-Azaxylyenes: Mechanistic Studies and Synthetic Applications." Diss. U of Denver, **2015**.

(11) Steinhagen, H.; Corey, E. J. *Angew. Chem. Int. Ed*. **1999**, *38*, 1928

(12) Omura, S.; Nakagawa, A. *Tetrahedron Lett*. **1981**, *22*, 2199-2202.

(13) Borak J.; Diller W. F. *Journal of Occupational and Environmental Medicine* **2001**, *43*, 110–9

(14) Mukhina, O. A.; Kumar, N. N.; Arisco, T. M.; Valiulin, R. A.; Metzel, G. A.; Kutateladze, A. G. *Angew. Chem. Int. Ed*. **2011**, *50*, 9423.

(15) (a) Schreiber, S. L. *Science*, **2000**, *287*, 1964-969 (b) Schreiber, S.L. *Chemical and Engineering News*, **2003**, *81*, 51-61

(16) Trabocchi, A. "Diversity-oriented Synthesis: Basics and Applications in Organic Synthesis, Drug Discovery, and Chemical Biology"

(17) Lipinski, C. A.; Feeney, P. J. *Advanced Drug Delivery Reviews*, **1997**, *23*, 3-25.

(18) (a) Szychowski, J.; Truchon, J. F.; Bennani, Y. L. *J. Med. Chem*. **2014**, *57*, 9292–9308. (b) Ertl, P.; Schuffenhauer, A. *Prog. Drug Res*. **2008**, *66*, 217–235.

(19) Lipkus, A. H.; Trippe, A. J. *J. Org. Chem*., **2008**, *73*, 4443-451.

(20) (a) Bemis, G. W.; Murcko, M. A. *J. Med. Chem*. **1996**, *39*, 2887–2893. (b) Bemis, G. W.; Murcko, M. A. *J. Med. Chem*. **1999**, *42*, 5095–5099. (c) Wang, J; Hou, T. *J. Chem. Inf. Model*. **2010**, *50*, 55–67.

(21) Oprea, T. I.; Davis, A. M.; Teague, S. J.; Leeson, P. D. *J. Chem. Inf. Comput. Sci.*, **2001**, *41*, 1308 -1315

(22) Holliday, J. D.; Willett. P. *J. Chem. Inf. Comput. Sci*., **2003**, *43*, 819-28

(23) Schuffenhauer, A.; Jacoby. E. *J. Chem. Inf. Model*., **2006**, *46*, 525-35.

(24) Combinatorial Chemistry." Merriam-Webster, Web

(25) Umstead, W.J.; Mukhina, O.A.; Kumar, N.N.B.; Kutateladze, A.G. *Aust. J. Chem*., **2015**, *68*, 1672-1681

(26) Kumar, N.N.B.; Mukhina, O.A.; Kutateladze, A.G. *J. Am. Chem. Soc*., **2013**, *135*, 9608-9611

(27) Cronk, W.C.; Mukhina, O.A.; Kutateladze, A.G. *J. Org. Chem*., **2014**, *79*, 1235-1246.

(28) Oprea, T. I. "Chapter 1: Introduction to Chemoinformatics in Drug Discovery – A Personal View." *Chemoinformatics in Drug Discovery*. Weinheim: Wiley-VCH, **2005**. 1-22

(29) Jencks, W, P. *Proc Nat Acad Sci USA*, **1981**, *78*, 4046–4050

(30) Shuker, S. B.; Hajduk, P. J.; Meadows, R. P. *Science*, **1996**, *274*, 1531–1534

(31) Roberts, G. C. K. Encyclopedia of Biophysics. **2013**, 2279-2280. Print.

(32) Congreve, M.; Carr, R.; Murray, C. *Drug Discov Today*, **2003**, *8*, 876–877

(33) Erlanson, D. A. *Top. Curr. Chem.,* **2011**, *317*, 1-32

(34) Bollag, G.; Nolop, K. *Nature*, **2010**, *467*, 596-99

(35) Queirolo, P.; Spagnolo, F. *Cancer Treatment Reviews*, **2015**, *41*, 519-26

(36) Umstead, W.J.; Mukhina, O.A.; Kutateladze, A.G. *Eur. J. Org. Chem*., **2015**, *10*, 2205-2213.

(37) CAS: A Division of the American Chemical Society. https://www.cas.org/content/chemical-substances (accessed April 15th, 2016)

(38) FDA: United States Food and Drug Administration. http://www.fda.gov/AboutFDA/WhatWeDo/History/ProductRegulation/SummaryofNDAApprovalsReceipts1938tothepresent/default.htm. (accessed April 15th, 2016)

(39) Deng, M. Z.; Caubere, P.; Senet, J. P.; Lecolier, S. *Tetrahedron*, **1988**, *44*, 6079–6086.

(40) Mukhina, O. A.; Kumar, N. N. B.; Cowger, T. M.; Kutateladze, A. G. *J. Org. Chem*. **2014**, *79*, 10956–10971.

(41) Nandurkar, N.S.; Kumar, N.N.B.; Mukhina, O.A.; Kutateladze, A.G. *ACS Combinatorial Sci*., **2013**, *15*, 73-76.

(42) Queirolo, P.; Spagnolo, F. *Cancer Treatment Reviews*, **2015**, *41*, 519-26

(43) Brown, N. *CSUR ACM Comput. Surv.,* **2009**, *41*, 1-38.

(44) Ertl, P.; Selzer, P. *J. Med. Chem.*, **2006**, *49*, 4568-573.

(45) Vyas, D. M.; Chiang, Y.; Doyle, T. W. *Tetrahedron Lett*. **1984**, *25*, 487–90

(46) "Phenytoin - Drugs.com." Phenytoin - Drugs.com. *Drugs.com,*. Web. 30 Mar. **2016**.

(47) Pitkänen, A.; Moshé, S. L. *Models of Seizures and Epilepsy*. Amsterdam: Elsevier Academic, **2006**. 539

(48) FAO SPECIFICATIONS AND EVALUATIONS FOR AGRICULTURAL PESTICIDES : IPRODIONE.: Food and Agricultural Organization of the United Nations, **2006**. Pdf

(49) Lovering, F.; Bikker, H.; Humblet, C. *J. Med. Chem*. **2009**, *52*, 6752.

(50) Canterbury, D. P.; Herrick, I. R.; Um, J.; Houk, K. N.; Frontier, A. J. *Tetrahedron* **2009**, *65*, 3165.

(51) Snowden, T. S *ARKIVOC 2012*, **2012**, *24*

(52) (a) Borrione, E.; Prato, M.; Scorrano, G.; Stivanello, M.; Lucchini, V. *J. Heterocycl. Chem*. **1988**, *25*, 1831 (b) Spanedda, M. V.; Hoang, V. D.; Croisse, B.; Bonnet-Delpon, D.; Be´gue´, J. P. *Tetrahedron Lett*. **2003**, *44*, 217

(53) Kutateladze, A. G.; Mukhina, O. A. *J. Org. Chem*. **2015**, *80*, 5218

(54) Kumar, N.N.B.; Mukhina, O.A.; Kutateladze, A.G. *J. Am. Chem. Soc*., **2013**, *135*, 9608-9611

(55) Kuan, H. H.; Chien, C. H.; Chen, K. *Org. Lett*. **2013**, *15*, 2880.

(56) Holten, K. B.; Onusko, E. M. *American Family Physician* **2000**, *62*, 611–20

(57) Padwa, A.; Reger, T. S. *Can. J. Chem*. **2000**, *78*: 749–756

(58) Liu, Y. *TIANJIN INST PHARM RESEARCH*, assignee. Patent CN101402641. **8 Apr. 2009**. Print

(59) Stevenson, R. *Heterocycles*. **1988**, *27*, 1929-1933

Appendix A: Further Acknowledgements

I want to thank my parents, Ronald and Julie Umstead, who, regardless of the cost, always found a way to make sure I was educated and provided for. Their valuable lessons in life have shaped me into the man I am today, and their support and confidence has always carried me through the difficult times. I love you both tremendously!

I'd like to thank Pastor Charlie and Jackie Clark, for being great friends. Five years ago, I would have never imagined myself in Denver, let alone finding an amazing church family. Wednesday night and Sunday morning services were always a highlight of my week, and our fun back and forth was always uplifting. We are members of the same body!

Now for my group members, thank you for your companionship through my stay in the Kgroup. Teresa, Bhuvan, Cole, Dima, and Olga, you have all played an important part in my development as a chemist. Olga, thank you especially for always giving your time to ensure I knew what I was doing, and for making me look good for group meetings and presentations. As a postdoc, you did not need to help as much as you did, so for that, I am grateful. And Cole, I always knew I could come to your room and chat for a bit, and occasionally win some money from you on your awful bets. But in all seriousness, you were a great friend through the whole process; I cannot thank you enough.

Dr. K, I cannot begin to thank you enough for the opportunity you gave me to join your group. The experience has been rewarding on many levels, and I will never forget it. Thank you for the work you put into seeking funding that paid my salary, for the time

spent editing and writing papers, and for the patience and understanding throughout this, at times, crazy ride.

And finally, I would like to fully explain the dedication of this dissertation. We lost my grandfather, Robert Loomis, on August 26th, 2015, just a few days short of his 80th birthday. He foundationally shaped me in countless ways, and was one of my biggest supporters heading into graduate school. Pop-Pop, you were always proud of me for what I was doing, and this work is a crowning achievement of that. I know you were disappointed you would not be able to see this in person, but I pray God is letting you take a glimpse down to see everything. I love you and miss you more than words can adequately describe!

Appendix B: List of Abbreviations

Δ	heat
Ac	acetyl
ACN	acetonitrile
anhydr.	anhydrous
aq.	aqueous
Ar	aryl
ca.	circa
calcd	calculated
cat.	catalyst (or catalytic amount)
CDI	1, 1'-Carbonyldiimidazole
$CHCl_3$	chloroform
$(COCl)_2$	oxayl chloride
d	doublet
dd	doublet of doublets
ddd	doublet of doublet of doublets
dddd	doublet of doublet of doublet of doublets
dt	doublet of triplets
DCM	dichloromethane
DFT	density functional theory
DIPEA	N,N-diisopropylethylamine
DMF	dimethylformamide

DMSO	dimethyl sulfoxide
DOS	diversity oriented synthesis
ESI	electro-spray ionization
ESIPT	excited state intramolecular proton transfer
Et	ethyl
EtOAc	ethyl acetate
EtOH	ethanol
eq	equivalent
FVT	flash vacuum thermolysis
g	gram(s)
h	hour(s)
hex	hexane
HPLC	high-performance liquid chromatography
HRMS	high-resolution mass spectrum
hν	light (irradiation)
$KHCO_3$	potassium bicarbonate
LED	light emitting diode
LC	liquid chromatography
mA	milli amperes
Me	methyl
mg	milligram(s)

min	minute(s)
MS	mass spectroscopy
NaOH	sodium hydroxide
Na_2SO_4	sodium sulfate
NMR	nuclear magnetic resonance
PCC	pyridinium chlorochromate
Ph	phenyl
Py	pyridine
q	quartet
RPR	Rayonet Photo Reactor
r.t.	room temperature
s	singlet
S	goodness of fit
sat.	saturated
SOC	spin orbit coupling
td	triplet of doublets
TEA	triethylamine
THF	tetrahydrofuran
TMS	trimethylsilane
TMSCl	trimethylsilyl chloride
TOS	target-oriented synthesis
UV	ultraviolet

V	volt(s)
W	watt(s)